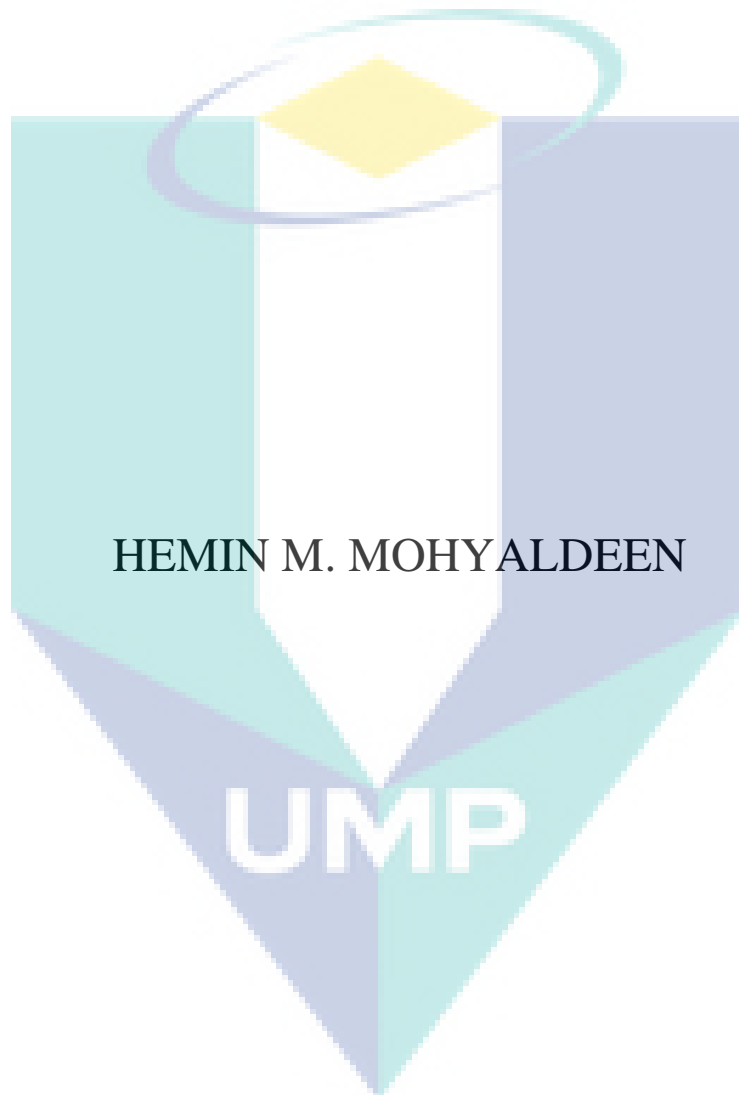
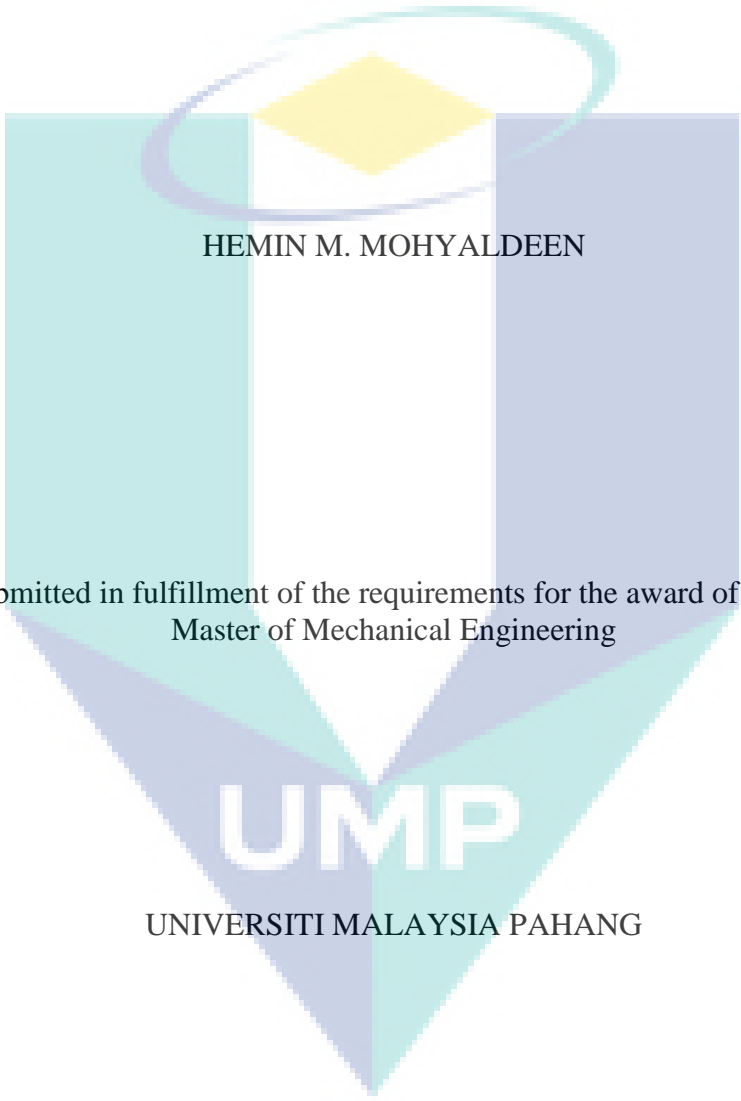


ANALYSIS OF AN AUTOMOBILE SUSPENSION  
ARM USING THE ROBUST DESIGN METHOD



Faculty of Mechanical Engineering  
UNIVERSITI MALAYSIA PAHANG

# ANALYSIS OF AN AUTOMOBILE SUSPENSION ARM USING THE ROBUST DESIGN METHOD

The logo of the University of Malaysia Pahang (UMP) is a shield-shaped emblem. It features a central white diamond shape. Above the diamond is a yellow diamond, and above that is a teal oval with a white center. The shield is divided into four quadrants: top-left is teal, top-right is light blue, bottom-left is light blue, and bottom-right is teal. The text 'HEMIN M. MOHYALDEEN' is centered within the white diamond.

HEMIN M. MOHYALDEEN

Thesis submitted in fulfillment of the requirements for the award of the degree of  
Master of Mechanical Engineering

**UMP**

UNIVERSITI MALAYSIA PAHANG

2011

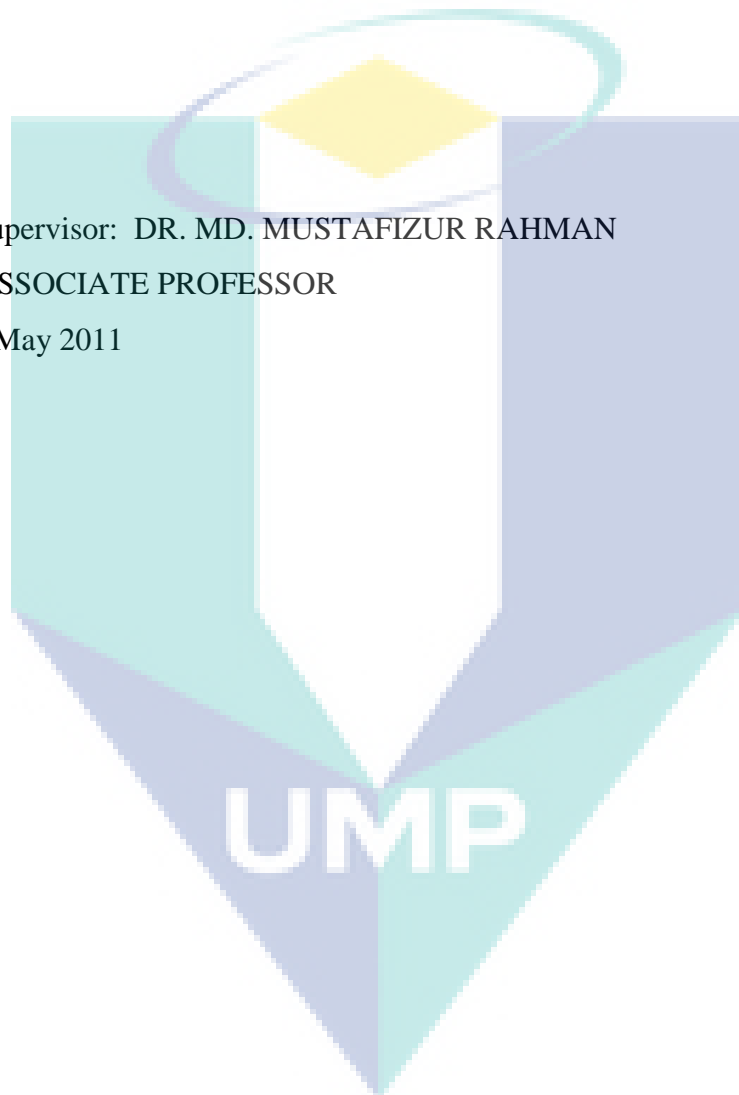
## SUPERVISOR'S DECLARATION

I hereby declare that I have checked this thesis and in my opinion this thesis is satisfactory in terms of scope and quality for the award of the degree of Master of Mechanical Engineering.

Name of Supervisor: DR. MD. MUSTAFIZUR RAHMAN

Position: ASSOCIATE PROFESSOR

Date: 10 May 2011



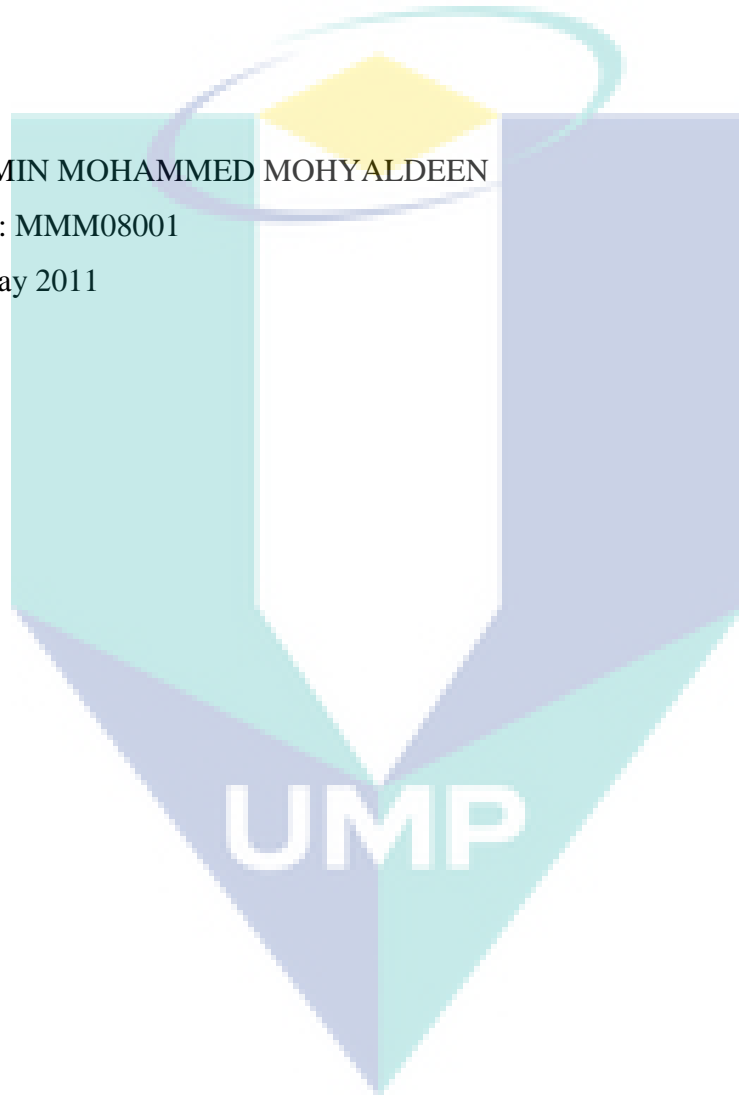
## STUDENT'S DECLARATION

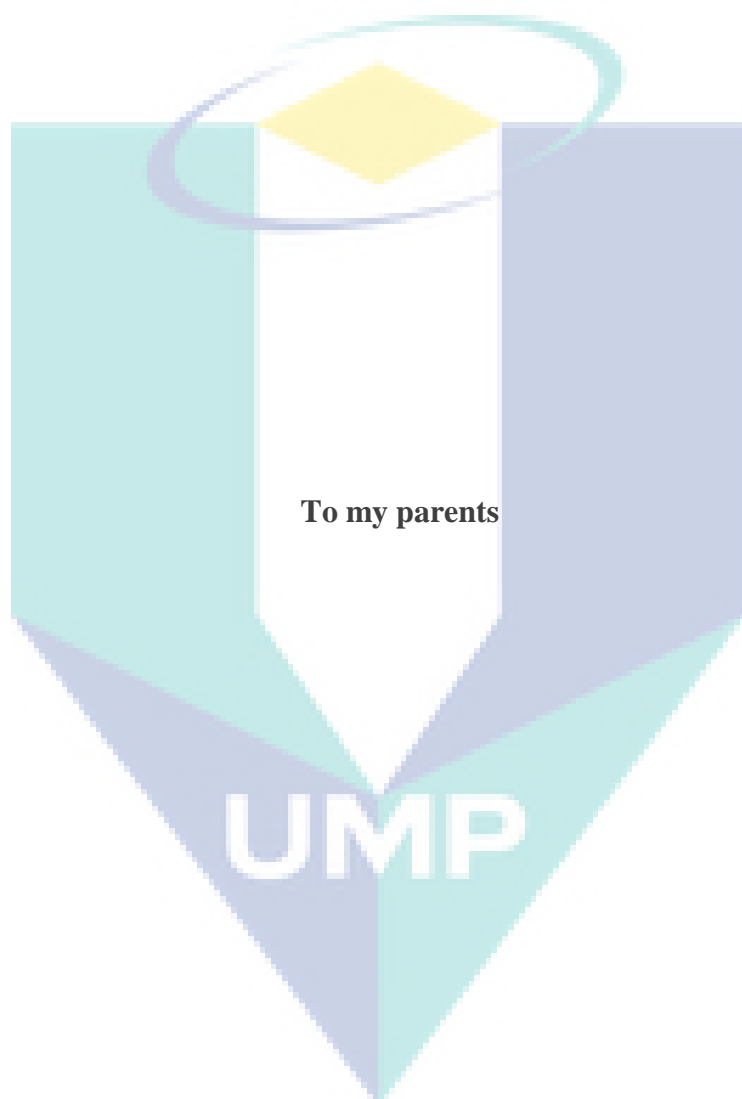
I hereby declare that the work in this thesis is my own except for quotations and summaries which have been duly acknowledged. The thesis has not been accepted for any degree and is not concurrently submitted for award of other degree.

Name: HEMIN MOHAMMED MOHYALDEEN

ID Number: MMM08001

Date: 10 May 2011





## ACKNOWLEDGEMENTS

In the name of Allah, the Most Benevolent, the most Merciful. First of all, I wish to record immeasurable gratitude and thankful fullness to the One and The Almighty Creator, the Lord and Sustainer of the universe, and the Mankind, in particular. It is only through His mercy and help that this work could be completed, and it is ardently desired that this little effort be accepted by Him to be of some service to the cause of humanity.

I would like to take this opportunity to express my gratitude to my supervisor Dr. Md. Mustafizur Rahman for his constant guidance and encouragement.

A special thank to Universiti Malaysia Pahang (UMP) for the real support and laboratory facilities. I don't forget to thank Dr. Ahmad Syahrizan Bin Sulaiman; for his encouraging, supporting, advice me and care about my work as it's his work. Special thank to Dr. Ahmed N. Abd. Alla for his help, who was not only a friend gives me his time and the knowledge that I need, what make me work in confidence, but he was also a brother. To all my friends in the hostel and lab, for the support and give me a suitable environment to study, and for the nice and useful moments I spend with them specially Brother Waleed K. Abduljabbar, Brother Ali Asghar Jumah and Brother Riaz Ulhaq.

Finally, but most importantly of all, my father, mother and brother Hiwa, should receive my greatest appreciation for their enormous love. They always respect what I want to do and give me their full support. Encouragement over the years

## ABSTRACT

This thesis describes the analysis of lower automobile suspension arm using stochastic design improvement technique. The suspension system is one of the most important components of vehicle, which directly affects the safety, performance, noise level and style of it. The objectives of this study are to characterise the dynamic behavior, to investigate the influencing factors of lower suspension arm using FEM incorporating design of experiment (DOE) and artificial neural network (ANN) approach and to analysis the lower suspension arm using robust design method. The structural three-dimensional solid modeling of lower arm was developed using the Solidworks computer-aided drawing software. The three-dimensional solid model then imported to the MSC.PATRAN software and employed to generate meshes and defined material properties for the finite element modeling. The linear elastic analysis was performed using NASTRAN codes. The optimization of lower suspension arm were carried out using stochastic design improvement based on Monte Carlo approach, Response surface methodology (RSM) based on central composite design (CCD) and artificial intelligent technique based on radial basis function neural network (RBFNN). Tetrahedral element with 10 nodes (TET10) and tetrahedral element with 4 nodes (TET4) mesh were used in the stress analysis. The modal analysis was performed with using Lanczos method to investigate the eigenvalue and mode shape. The highest von Mises stresses of TET10 were selected for the robust design parameter. The development from the Stochastic Design Improvement (SDI), RSM and ANN are obtained. The design capability to endure highest load with lower predicted stress is identified through the SDI process. CCD used to predict and assess linear response Von Mises and Displacement on Lower arm systems models. On the other hand, RBFNN used to investigate linear response of lower arm. It can be seen that the robust design was capable to optimize the lower vehicle arm by using stochastic optimization and artificial intelligent techniques. The developed linear model based on SDI and CCD is statistically adequate and can be used to navigate the design space. A new parameter of material can be reconsidered in order to optimize the design. The results can significantly reduce the cost and time to market, improve product reliability and customer confidence. These results can be use as guideline before developing the prototype.

## ABSTRAK

Kajian thesis ini adalah untuk menganalisa suspensi lengan bawah sesebuah kenderaan menggunakan teknik rekabentuk stokastik. Sistem suspensi ini merupakan salah satu komponen terpenting bagi sebuah kenderaan, yang secara langsung mempengaruhi keselamatan, prestasi, tahap kebisingan dan gaya sesebuah kenderaan. Kajian ini bertujuan untuk mengklasifikasikan perilaku dinamik, untuk mengetahui faktor yang mempengaruhi suspensi lengan bawah sesebuah kenderaan dengan menggunakan teknik FEM dan menggabungkannya dengan teknik DOE dan ANN serta menganalisa menggunakan kaedah rekabentuk tahan lasak. Struktur tiga-dimensi untuk suspensi lengan bawah dibangunkan dengan menggunakan perisian Solidworks. Model ini kemudiannya dimasukkan ke perisian MSC.PATRAN dan digunakan untuk menghasilkan jaringan serta menetapkan jenis bahan untuk pemodelan elemen terhingga. Kod Nastran di gunakan untuk menanalisa elastik linier. Proses pengoptimum suspensi lengan bawah dilakukan dengan menggunakan kaedah rekabentuk perbaikan berdasarkan pendekatan Monte Carlo, RSM, rekabentuk komposit berpusat (CCD) dan teknik RBFNN. Elemen tetrahedral dengan 10 titik (TET10) dan 4 titik (TET4) yang digunakan dalam menganalisa tegangan. Kaedah Analisa “modal” dilakukan dengan menggunakan kaedah Lanczos untuk mengetahui nilai eigen dan bentuk mod. Nilai tertinggi untuk tegangan von Mises TET10 dipilih untuk parameter kaedah rekabentuk tahan lasak. Keputusan dari SDI, RSM dan ANN diperolehi dan kemampuan rekabentuk untuk menanggung beban tertinggi dengan tekanan dianggarkan lebih rendah dikenalpasti melalui proses SDI. CCD digunakan untuk menjangka dan menilai tindakbalas linier Von Mises dan perpindahan pada model yg digunakan. Manakala kaedah RBFNN digunakan untuk menganalisa tandakbalas linear suspensi tersebut. Rumusan dapat di buat bahawa rekabentuk tahan lasak mampu untuk mengoptimumkan suspensi lengan bawah kenderaan dengan menggunakan kaedah optimasi stokastik dan teknik kebijaksanaan tiruan. Model linier yang dibangunkan berdasarkan SDI dan CCD secara statistik adalah mencukupi dan boleh digunakan untuk menavigasi ruangan rekabentuk. Satu parameter baru untuk bahan boleh dipertimbangkan untuk mengoptimumkan rekabentuk. Keputusan yang diperolehi dari kajian ini secara berkesan boleh mengurangkan kos dan masa ke pasaran dan meningkatkan kebolehpercayaan produk dan kepercayaan pelanggan. Keputusan ini boleh digunakan sebagai rujukan sebelum sesebuah prototaip dibina.

## TABLE OF CONTENTS

	<b>Page</b>
<b>SUPERVISOR'S DECLARATION</b>	ii
<b>STUDENT'S DECLARATION</b>	iii
<b>DEDICATION</b>	iv
<b>ACKNOWLEDGEMENTS</b>	v
<b>ABSTRACT</b>	vi
<b>ABSTRAK</b>	vii
<b>TABLE OF CONTENTS</b>	viii
<b>LIST OF TABLES</b>	xi
<b>LIST OF FIGURES</b>	xii
<b>LIST OF NOMENCLATURES</b>	xiv
<b>LIST OF ABBREVIATIONS</b>	xvii
<b>CHAPTER 1 INTRODUCTION</b>	
1.1 Background	1
1.2 Problem Statement	3
1.3 Objectives of Study	4
1.4 Scopes of Research	5
1.5 Organization of Thesis	5
<b>CHAPTER 2 LITERATURE REVIEW</b>	
2.1 Introduction	6
2.2 History of Vehicle Suspension Systems	6
2.3 Types of Vehicle Suspension System	7
2.3.1 Front suspensions	8
2.3.2 Rear suspensions	10
2.4 Aluminium Alloy in Automotive Design	11
2.5 Finite Element and Analysis	12
2.6 Optimization Techniques	17
2.6.1 Design of experimental technique	19

2.6.2	Artificial intelligent	21
2.6.3	Stochastic design improvement	23
2.7	Conclusion	25

### **CHAPTER 3      METHODOLOGY**

3.1	Introduction	26
3.2	Structural Model Description	26
3.3	Material Properties	28
3.4	Finite Element Modeling	28
3.5	Dynamic Model of Suspension Arm	29
3.6	Optimization Techniques	33
3.6.1	Response surface methods	34
3.6.2	Radial basis function neural network technique	35
3.6.3	Robust design	40
3.7	Conclusion	44

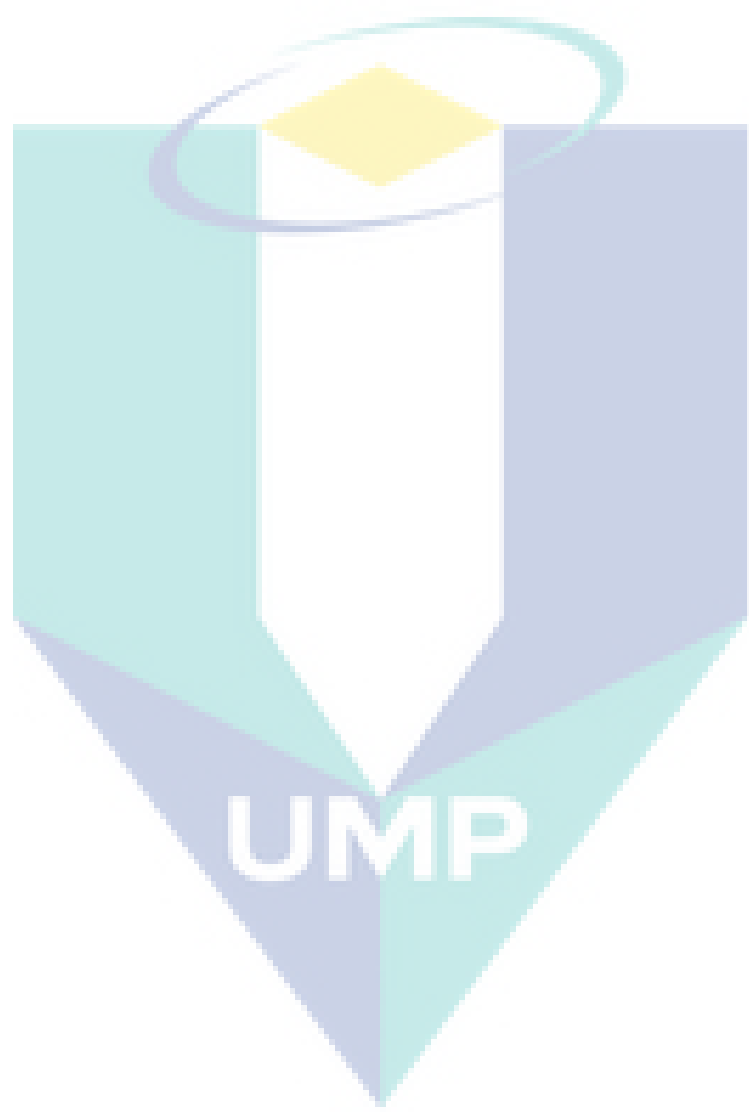
### **CHAPTER 4      RESULTS AND DISCUSSION**

4.1	Introduction	45
4.2	Finite Element Modeling and Analysis	45
4.2.1	Meshing technique	47
4.2.2	Identification of mesh convergence	51
4.2.3	Linear static analysis	52
4.2.4	Dynamic analysis of lower suspension arm	52
4.3	Optimization Techniques	56
4.3.1	Response surface methodology	56
4.3.2	Artificial neural network	68
4.3.3	Robust design using SDI	77
4.4	Conclusion	84

### **CHAPTER 5      CONCLUSION AND RECOMMENDATIONS**

5.1	Introduction	85
5.2	Summary of Findings	85

5.3	Contribution of the Study	87
5.4	Recommendation for future research	87
	<b>REFERENCES</b>	88
	<b>LIST OF PUBLICATION</b>	96



## LIST OF TABLES

Table No.	Title	Page
3.1	Mechanical properties of aluminum alloy 7079-T6	28
4.1	Natural frequency of lower arm	53
4.2	Maximum displacement from modal analysis	55
4.3	Load conditions of lower am	58
4.4	Coded levels of variable and actual values for CCD	58
4.5	Analysis of variance ANOVA results	59
4.6	R <sup>2</sup> analysis results	61
4.7	Comparison between predicted versus FEA results	62
4.8	Output from FEM and RBFNN techniques	70
4.9	Error RBFNN	70
4.10	Output from dynamic analysis and RBFNN techniques	72
4.11	RSM and RBFNN techniques prediction stress-strain for suspension arm	73
4.12	Design parameter before and after SDI	82

## LIST OF FIGURES

<b>Figure No.</b>	<b>Title</b>	<b>Page</b>
1.1	Suspension system	4
2.1	Overall car	7
2.2	McPherson suspension strut	9
2.3	Double wishbone suspension arm	9
2.4	Multi link suspension arm	10
2.5	Suspension lower arm	11
2.6	Dynamic analysis process	16
2.7	Suspension system based on CCD	21
2.8	Robust concept	24
3.1	Structural model and overall dimensions of suspension arm	27
3.2	Quarter car passive suspension arm	31
3.3	Suspension system	32
3.4	General guidelines for conducting DOE	35
3.5	Radial basis function neural networks	37
3.6	Schematic diagram of the SDI	43
3.7	Flow chart of steps in SDI	43
4.1	Three-dimensional FE model and (loading and constraints)	46
4.2	Finite element model was using TET4 and TET10 elements	48
4.3	von Mises stresses contours	49
4.4	Variation of maximum principal stress for different element types	50
4.5	Variation of maximum displacement for different element type	50
4.6	Maximum stresses versus mesh size at critical location for TET10 of lower suspension arm to check mesh convergence	51

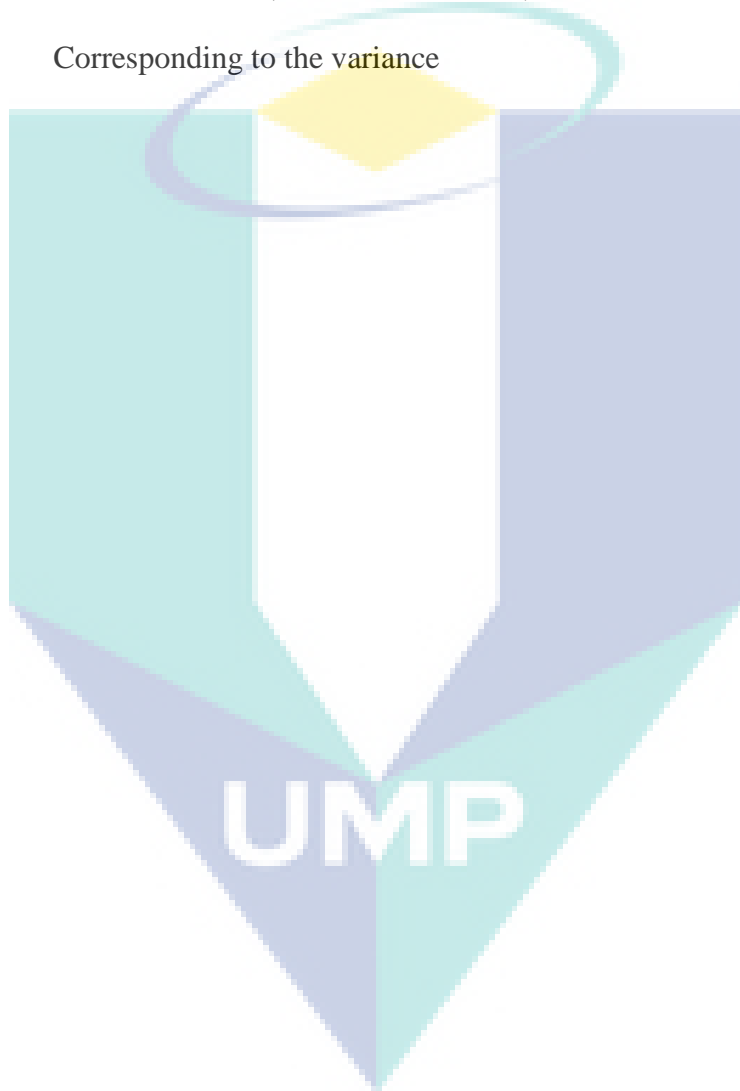
4.7	Stresses versus mesh size at critical location for TET10 to check mesh convergence	52
4.8	Mode contour and mode shape	54
4.9	XY-directional strain distribution for various cases.	57
4.10	3D Surface plots for the response of von Mises against load and mesh size	63
4.11	3D Surface plots for the response of displacement against load and mesh size	64
4.12	Normal probability plot of residuals	65
4.13	The best fit line plot	66
4.14	Predicted versus actual simulation	66
4.15	Residuals versus Run	67
4.16	Percentage deviation of FEA results	67
4.17	Model of RBFNN approach for stress analysis	68
4.18	FEM and RBFNN displacement	69
4.19	FEM and RBFNN maximum principal stress	69
4.20	Model of RBFNN approach for suspension arm	71
4.21	Comparison of RSM models and RBFNN against experimental values (FEA)	74
4.22	Percentage deviation by neural network and response surface method	75
4.23	Residual by neural network and response surface method	76
4.24	Decision map	78
4.25	Influence factors to the stress value	79
4.26	Ant hill scatter plot for stress versus material	79
4.27	Ant hill scatter plot for stress versus load scale factor	80
4.28	Ant hill scatter plot for stress versus load scale factor using SDI	83

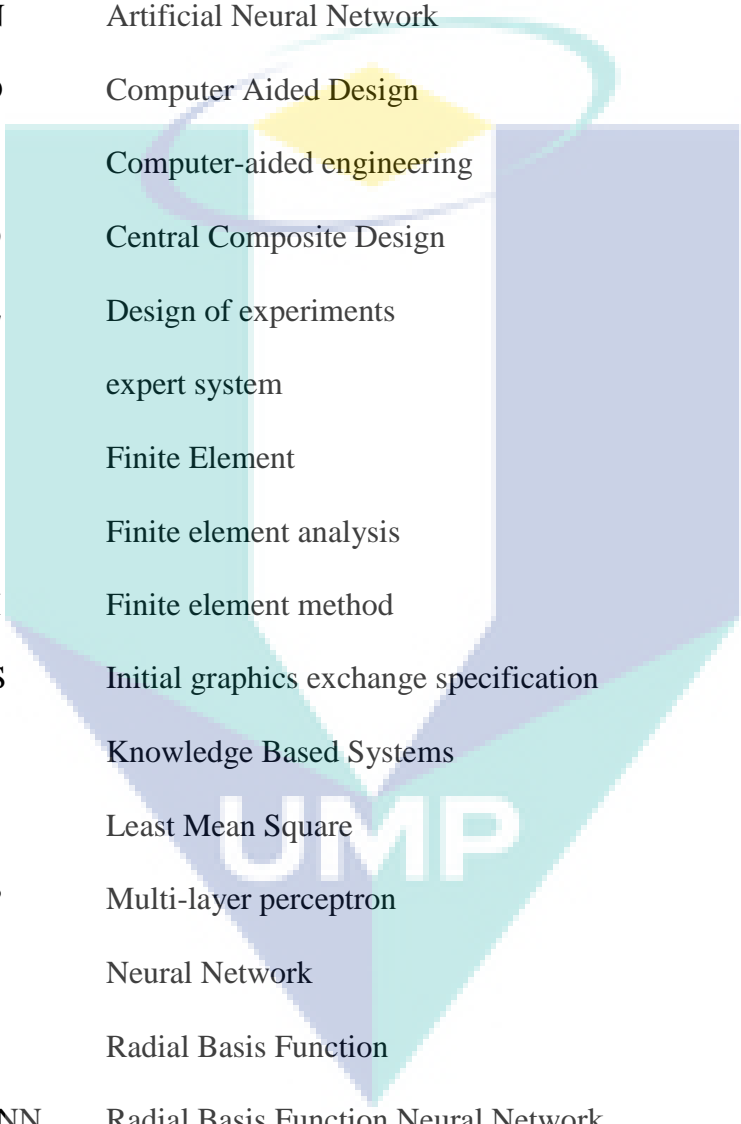
## LIST OF NOMENCLATURES

$A$	Mesh size
$B$	Load in $X$ direction
$C$	Load in $Y$ direction
$c$	Center of the basis function
$[C]$	Coefficient matrix
$Cc$	Damping coefficient
$D$	Load in $Z$ direction
$d$	Radial distance
$E$	Young modulus
$E_r$	Error RBF
$exp$	Exponential
$F$	Scale factor
$f(x)$	Function
$g$	Acceleration of gravity
$G$	Basis function
$GPa$	Giga Pascal
$h$	Hidden layer
$H$	$\parallel$ Matrix
$Hz$	Hertz
$K$	Stiffness of the suspension arm material
$[K]$	Stiffness matrix
$Kg$	Kilogram
$K_s$	Suspension stiffness

$K_t$	Tire deflection stiffness
$M$	Mass of suspension arm
$mm$	Millimeter
$[M]$	Mass matrix
$\mu m$	Micrometer
$M_c$	The mass of the vehicle
$MPa$	Mega Pascal
$m_w$	Unsprung mass
$Nu$	Poisson's ratio
$q$	Road disturbance
$r$	Linear correlation coefficient
$\rho$	Density
$T$	Dynamic displacement
$t$	Constant vector
$u$	Mean value
$u$	Input vector
$W$	Weight matrix
$\omega_n$	Natural frequency
$x$	N-Dimensional vector of input signal
$x, y$	stochastic variables
$Y$	Desired output
$\hat{y}$	Desired output
$Z_l$	Unsprung mass displacement
$\dot{Z}_l$	Unsprung mass velocity

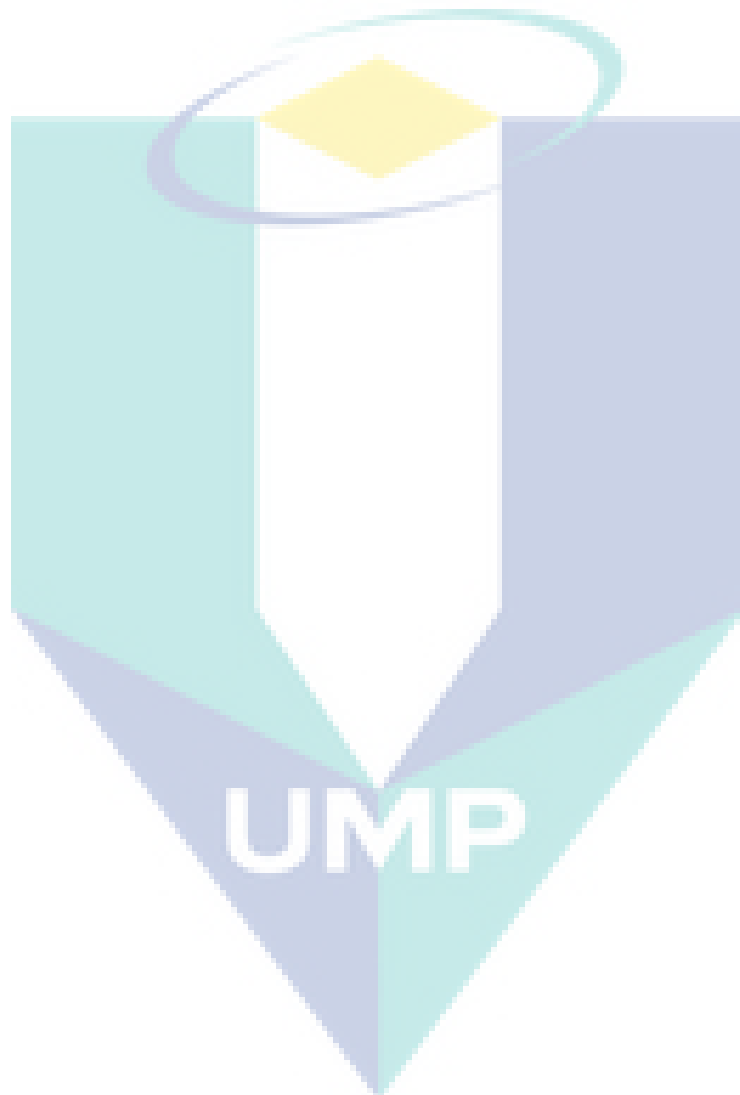
$\ddot{z}_1$	Unsprung mass acceleration
$Z_2$	Sprung mass displacement
$\dot{Z}_2$	Sprung mass velocity
$\ddot{z}_2$	Sprung mass acceleration
$\ $	Euclidean norm ( Euclidean distance)
$\sigma_i$	Corresponding to the variance



**LIST OF ABBREVIATIONS**

AA	Aluminum Alloy
AI	Artificial Intelligent
AL	Aluminum
ANN	Artificial Neural Network
CAD	Computer Aided Design
CAE	Computer-aided engineering
CCD	Central Composite Design
DOE	Design of experiments
ES	expert system
FE	Finite Element
FEA	Finite element analysis
FEM	Finite element method
IGES	Initial graphics exchange specification
KBS	Knowledge Based Systems
LMS	Least Mean Square
MLP	Multi-layer perceptron
NN	Neural Network
RBF	Radial Basis Function
RBFNN	Radial Basis Function Neural Network
RSM	Response surface method
SDI	Stochastic Design Improvement
SED	Statistical experimental design
SPC	Statistical process control

STEP	Standard for the exchange of product model data
SVM	Support vector machine
TET	Tetrahedral element



## CHAPTER 1

### INTRODUCTION

#### 1.1 BACKGROUND

The vehicle suspension system is responsible for driving comfort and safety as the suspension carries the vehicle-body and transmits all forces between body and road. Positively, in order influence these properties, semi-active or active components are introduced, which enable the suspension system to adapt to various driving conditions. From a design point of view, there are two main categories of disturbances on a vehicle namely the road and load disturbances. Road disturbances have the characteristics of large magnitude in low frequency (such as hills) and small magnitude in high frequency (such as road roughness). Load disturbances include the variation of loads induced by accelerating, braking and cornering. Therefore, a good suspension design is concerned with disturbance rejection from these disturbances to the outputs. A conventional suspension needs to be “soft” to insulate against road disturbances and “hard” to insulate against load disturbances. Consequently, the suspension design is an art of compromise between these two goals (Wang, 2001).

There is an increasing interest within the automotive industry in the ability to produce models that are strong, reliable and safe whilst also light in weight, economic and easy to produce. In automotive industry, aluminum alloy (AA) has limited usage due to their higher cost and less developed manufacturing process compared to steels. However, AA has the advantage of lower weight and therefore, has been used increasingly in automotive industries for the last 30 years, mainly as engine block, engine parts, brake components, steering components and suspension arms (Rahman et al., 2009). The increasing use of AA is due to the safety, environmental and

performance benefits that aluminum offers, as well as the improved fuel consumption because of light weight. That is why aluminum is the fastest growing material in the automobile industry. Recently commercial finite element packages have been readily available and their utility has increased with the development of super computers. The finite element method (FEM) provides a relatively easy way to model the system. For this feature, the FEM has become an indispensable engineering tool in design processes of components for automotive industry (Bath, 1996). Design of a robust suspension lower arm is crucial to the success of manufacturing the car and requires that suspension components have to be well in aspects of both compactness and crashworthiness, which is defined as a measure of the whole vehicle. Its components structural ability to plastically deform and yet maintain a sufficient survival space for its occupants in crashes involving reasonable deceleration loads (Praya and Jamel, 2004).

Stochastic design improvement (SDI) is a fast and efficient method for improving the performance of a system. It can be specifying the desired target behavior for a system and get multiple alternative solutions that satisfy the target. The suspension arm gets more attention by many researches like study dynamic analyses of the motor-vehicle suspension system using the point-joint coordinate's formulation (Kim et al., 2002 and Zang et al., 2004). The mechanical system is replaced by an equivalent constrained system of particles and then the laws of particle dynamics are used to derive the equations of motion. Modeling and simulation are indispensable when dealing with complex engineering systems. It makes it possible to do an essential assessment before systems are developed. It can alleviate the need for expensive experiments and provide support in all stages of a project from conceptual design, through commissioning and operation.

The most effective way to improve product quality and reliability is to integrate them in the design and manufacturing process. Response surface methodology (RSM) is a useful technique that can be integrated into the early stages of the development cycle. RSM is used to estimate the transfer functions at the optimal region. Hence Central Composite Design (CCD) approach was selected for the present study (Montgomery, 2005 and Wu and Hamad, 2000). Statistical design of experiments refers

to the process of planning the experiment so that the appropriate data can be analysed by statistical methods, resulting in valid and objective conclusions (Montgomery, 2005).

Neural networks have been used in mechanical engineering problems since the early 1990's. The main areas of concentration have been control, identification, and damage detection. Radial basis function neural network (RBFNN) has increasingly attracted interest for engineering applications due to their advantages over traditional multilayer perceptions, namely faster convergence, smaller extrapolation errors, and higher reliability. In particular, RBFNN has proven to be very useful for many systems and applications (Erdman et al., 2001).

## 1.2 PROBLEM STATEMENT

The suspension arms are the essential elements in the vehicle as shown in Figure 1.1 (Milliken, 2002) conventionally these parts made of steel, which is a heavy metal then today try to use aluminum, a lighter metal, economic and easy to produce. Uncertainty propagation and quantification are a challenging problem in engineering. Indeed, the analyst often makes use of complex models in order to assess the reliability or to perform a robust design of industrial structures. The stochastic nature of the optimization arises from incorporating uncertainty into the procedure. The goal of stochastic optimization is to minimize the expectation of the sample performance as a function of the design parameters and the randomness in the system and concept stochastic optimization consists in combining deterministic optimization methods with uncertainty quantification techniques to measure the sensitivity and the variability of the response. Most applications of robust design have been concerned with static performance in mechanical engineering and process systems (Zang et al., 2004) whereas the objective of robust design is to optimize the mean and minimize the variability that results from uncertainty represented by noise factors and to test the effect of the variability in different experimental factors using statistical tools. A stochastic process is a probabilistic model of a system that evolves randomly in time and space. Another objective concerns the reliability-based optimization, i.e. the computation of the probability of a risk of failure (Lucor et al., 2007). In addition the main statement of the problem of this research expressed by bringing reality of simulation, improving the

design and essential to the move towards virtual product development using stochastic design technique and ANN because there is an increasing interest within the automotive industry in the ability to produce models that are strong, reliable and safe.

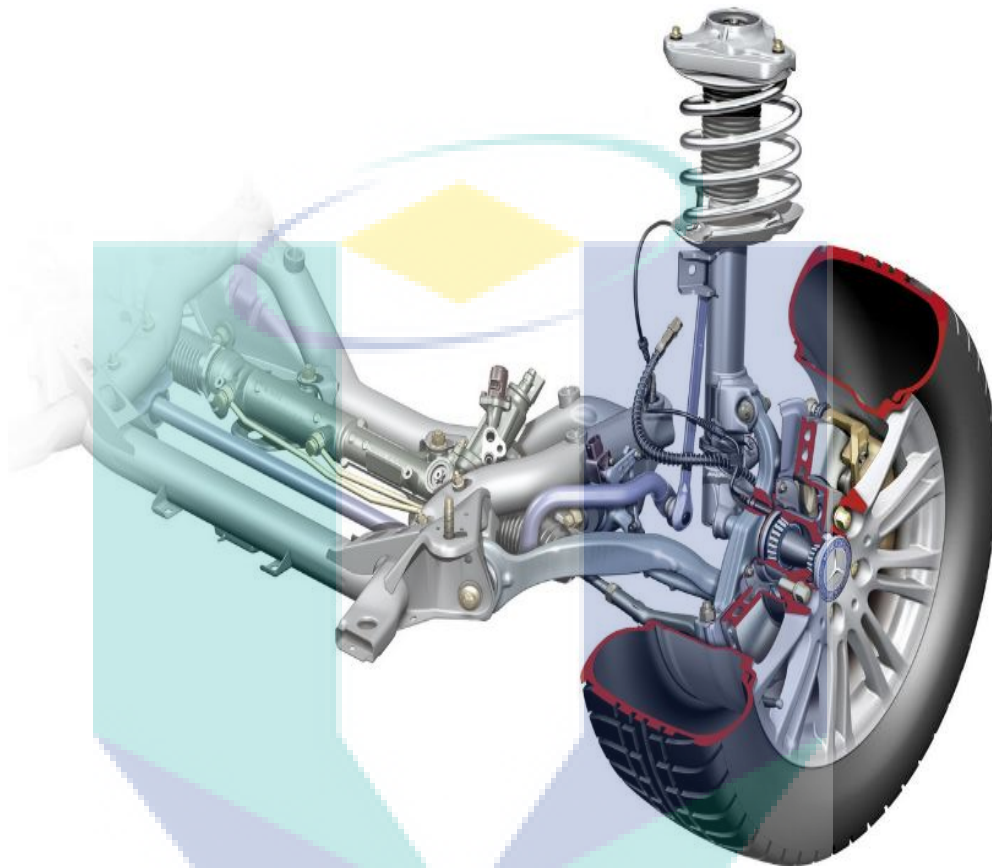


**Figure 1.1:** Suspension system (Milliken, 2002)

### **1.3 OBJECTIVES OF STUDY**

The objectives of this study are as follows:

- i. To assess the dynamic behavior of suspension arm.
- ii. To investigate the influencing factors of the lower suspension arm integrating finite element analysis results with RSM and ANN approach.
- iii. To analysis of the suspension arm using stochastic optimization.

## 1.4 SCOPES OF RESEARCH

The scopes of this research are as follows:

- i. Structural modeling develops utilizing computer aided design codes.
- ii. Finite element modeling and analysis utilizing PATRAN/NASTRAN commercial software.
- iii. Dynamic analyses perform using modal analysis.
- iv. Develop the stochastic optimization model using stochastic design improvement based on modified Monte Carlo optimization.
- v. Investigate the influencing factors of the lower suspension arm utilize response surface methodology based on central composite design.
- vi. Investigate linear response by artificial intelligence technique using radial basis function neural network.

## 1.5 ORGANIZATION OF THESIS

This thesis has been prepared to give details on the facts, observations, arguments, and procedures in order to meet its objectives. Chapter 1 gives the brief background of a vehicle suspension, the problem statement, objectives and scope of the research. Chapter 2 presents the literature review of vehicle suspension arm, aluminum alloy, finite element method, and dynamic analysis. The most representative optimization methods are also discussed. Chapter 3 discusses the mechanical model description and introduced the methods of real eigenvalue extraction. The three techniques, stochastic design improvement, response surface methodology and radial basis function neural network are presented. Chapter 4 addresses the geometry of control lower arm used for the FEA. The mesh generation and its convergence are also discussed. In addition, the validation of the finite element model is presented in this chapter. Linear static stress analysis, dynamic analysis, artificial intelligent method RBFNN has been presented. The conclusions of the present research are summarized and presented in Chapter 5. Suggestions and recommendations for the future work are also presented in this chapter.

## CHAPTER 2

### LITERATURE REVIEW

#### 2.1 INTRODUCTION

This chapter will provide information of past research efforts related to a vehicle suspension system. Carry out a brief introduction on the types of suspensions and Background on important performance characteristics for suspensions will be presented. Introduced the finite element analysis and dynamic analysis, stochastic optimization, including stochastic design improvement, response surface methodology and artificial neural network are reviewed in this chapter with great details. A review of other relevant research studies is also provided.

#### 2.2 HISTORY OF VEHICLE SUSPENSION SYSTEMS

Pioneering vehicle manufacturers were faced early on with the challenges of enhancing driver control and passenger comfort. The early 1900's, cars still rode on carriage springs as shown in Figure 2.1. Early drivers had bigger things to worry about than the quality of their ride like keeping their cars rolling over the rocks and ruts that often passed for roads. These early suspension designs found the front wheels attached to the axle using steering spindles and kingpins. This allowed the wheels to pivot while the axle remained stationary. Suspension systems have been widely applied to vehicles from the horse-drawn carriage with flexible leaf springs fixed in the four corners, to the modern automobile with complex control algorithms. The vehicle design typically represents a trade-off between performance and safety since durability especially of safety components is important. This means that the design of the components must be adapted as accurately as possible to the operating conditions (AA, 2004).

The suspension systems basically consist of all the elements that provide the connection between the tires and vehicle body and are designed to meet the following requirements: (i) ride comfort, (ii) road-holding, and (iii) handling. As the tire revolves, the suspension system is in a dynamic state of balance, continuously compensating and adjusting for changing driving conditions. Today's suspension system is automotive engineering at its best. The components of the suspension system perform the following basic functions (SCC, 2011):

- i. Maintain correct vehicle ride height.
- ii. Reduce the effect of shock forces.
- iii. Maintain correct wheel alignment.
- iv. Support vehicle weight.
- v. Keep the tires in contact with the road.
- vi. Control the vehicle's direction of travel.



**Figure 2.1:** Overall car (Church, 1995)

### **2.3 TYPES OF VEHICLE SUSPENSIONS SYSTEM**

Suspension systems form one key subsystem of an automobile that are used to isolate the occupants from shocks and vibrations induced due to road surface irregularities. It is also used as a wheel locating and guiding mechanism when the vehicle is in motion.

### 2.3.1 Front Suspensions

Front suspensions are classified as dependent and independent suspensions. The most common dependent front suspension is the beam axle, which is used less and less in recent vehicles because of numerous disadvantages like large unsprung mass, packaging space, and considerable caster change. However, some off-road application vehicles tend use still to the beam axle dependent front suspension as they offer high articulation and high ground clearance.

The most common types of front independent suspensions are the double wishbone suspension and the Macpherson strut. The double wishbone suspension also known as the double A-arm suspension has parallel lower and upper lateral control arms. The main advantage of the double wishbone is that the camber can be adjusted easily by varying the length of the lateral upper control arm such that it has a negative camber in jounce. The coil spring and the shock absorber are combined into a single unit extending vertically making it more compact. Over the years, many types of independent front suspension have been tried. Many of them have been discarded for a variety of reasons, with only two basic concepts, the double wishbone and the McPherson strut, finding widespread success in many varying forms.

The McPherson strut type suspension consists of a single lower wishbone arm which controls the lateral and longitudinal location of the wheel Figure 2.2. The McPherson suspension providing the suspension can be combined into one assembly and the disadvantage set as less favorable kinematic characteristics. The friction between piston rod and guide impairs the springing effect. Much space needed above the wheel for spring and strut, connection between the upper strut mount and frame unstiff and expensive, clamping of a strut to steering knuckle very difficult for the axle loads of truck and expensive spare part (Fleuren, 2009).

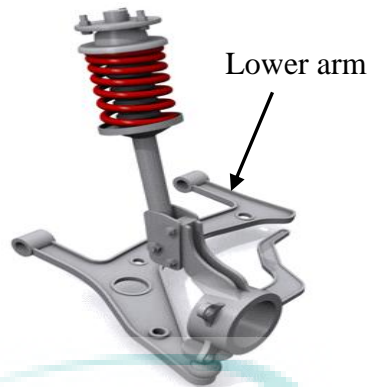


**Figure 2.2:** McPherson suspension strut

Double wishbone suspension type suspension consists of pairs of parallel arms can be arranged to control suspension geometry (Figure 2.3). Giancarlo and Lorenzo (2009) sighted of the initial design double wishbone suspension and concluded the independent double wishbone front suspension adopted in the automobile manufactures. Most advantages for double wishbone suspensions are space saving, attenuate of road noise, decreasing steering vibration and good kinematic possibilities. The disadvantage set as more space needed besides the frame in a lateral direction, king pin inclination high, and less favorable ratio of spring rate and damper rate. A few disadvantages of this type of suspension are that it requires sufficient vertical space and a strong top mount (Jack, 2005).

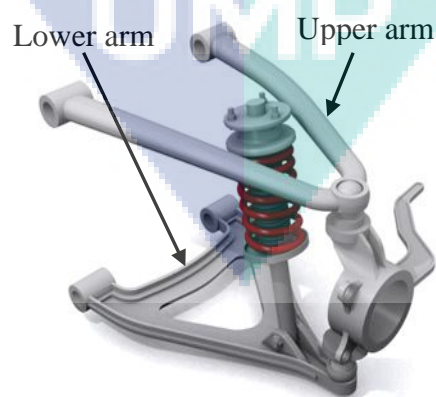


**Figure 2.3:** Double wishbone suspension arm

A multi link front suspension, a short upper link is attached to the chassis with a bracket, and the outer end of the upper link is connected to the third link (Figure 2.4).

High-performance suspension systems are usually installed on sport cars. In this case, the driver expects good kinematic possibilities, good ride and handling comfort, and small space needed in the vertical direction in wheel housing (Knowles, 2010). Disadvantage of this type are much space needed beside a frame in the lateral direction (especially for control rod), higher number of ball joints, bearings and links, increased unsprung masses, and expensive.

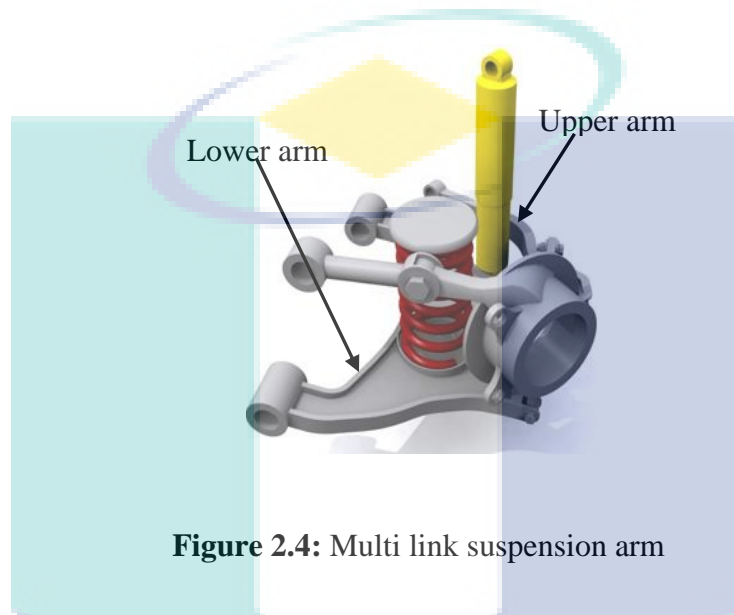


**Figure 2.4:** Multi link suspension arm

### 2.3.2 Rear Suspensions

Similar to the front suspensions, rear suspensions too are of dependent and independent suspension types. Some of the commonly used dependent rear suspensions are the twist beam, leaf springs, live and dead axles. The main advantage of a twist beam is that it is inexpensive, compact and is suitable for small cars where package space is limited. Live rear axles use longitudinal leaf spring to attach the axle to the vehicle chassis. Live rear axles are not used in small cars due to their high unsprung mass and are used mainly only on pickup trucks and SUV's. Some of the independent type rear suspensions are the swing axles, semi trailing arms, wishbones, multi-link suspensions. Wishbones suspensions are similar to front wishbone suspensions. Multi-link suspension is the most commonly used type of rear independent type suspension. Multi-link suspension has 3 or more lateral arms arranged in space. They have the greatest flexibility in modifying any suspension parameter to suit the required vehicle application.

## 2.4 ALUMINIUM ALLOYS IN AUTOMOTIVE DESIGN

Using aluminium alloys in vehicles is not a new idea for instance featured an aluminium body. Since, the aluminium alloys have been limited in use due to their higher cost and less developed manufacturing processes compared to steel. Aluminium offers the advantage of lower weight. Therefore, Aluminum alloy used in high performance vehicles where the higher cost can be justified (Figure 2.5). Vehicle weight reduction becomes increasingly important in the past decades. The world has imposed some of the strictest standards on fuel efficiency and exhaust emissions (Homeister, 2001). The mounting problems of air pollution in larger cities during this period promoted emission legislations. The immediate response from the automotive industry was to reduce the size of passenger vehicles and discontinue the larger engine options (Johnson, 1997).



**Figure 2.5:** Suspension lower arm (Sigmund, 2006)

Weight reduction influences the fuel economy directly, since less energy is needed for acceleration and indirectly, since a smaller engine is required in a lighter

vehicle. In order to reduce the vehicle weight, the automotive industry has seen a continuous increase in aluminium usage in the last 30 years mainly as cast engine blocks, engine parts and transmissions where significant weight savings can be achieved (Miller et al., 2000 and Dwigth, 1999). In the last decade, aluminium has also found use in structural applications in mass market vehicles, such as brake components, steering components and suspension control arms where safety is of great concern and traditional steel solutions used to dominate. Vehicles with an extensive use of aluminium such as in body structures and panels are still mainly found in the high-end market. It is paradoxical that the increased use of lightweight chassis designs. The average weight of cars has increased steadily since the mid 1980s. This is especially pronounced in USA, where the average weight for all 2006 models was 1878 kg, up from 1406 kg in 1987 and exceeding the 1975 average by 37 kg (LDA, 2009).

Suspension components along with wheel rims and brake components are unsprung masses which make weight reduction important for ride quality and response as well as for reducing the total vehicle weight. The suspension arm material is typically used a 7079 aluminium alloy, which has good formability and corrosion resistance as well as high impact and fatigue strength. Good formability is important since it is produced by forging although stronger aluminium alloys exist. These are less suitable for forging operations and may also lack adequate corrosion resistance (Staley and Lege, 1993). The 6061 alloy has been used for similar applications due to its better formability, albeit lower strength (Dwigth, 1999). Advances in manufacturing technologies have in the past decades established less formable, higher strength alloys as viable and light weight alternatives to steel in vehicle bodies and safety critical components (Carle and Blount, 1999 and Jensrud et al., 2006).

## **2.5 FINITE ELEMENT AND ANALYSIS**

The finite element analysis (FEA) is a computational technique which is used to obtain approximate solutions of boundary value problems in engineering. In simple, a boundary value problem is a mathematical problem in which one or more dependent variables must satisfy a differential equation everywhere within a known domain of independent variables and satisfy specific conditions on the boundary of domain

(Hutton, 2004). FEM technology has been widely used in solving structural, mechanical, heat transfer, and fluid dynamics problems as well as problems of other disciplines. The advancement in computer technology enables us to solve an even larger system of equations, to formulate and assemble the discrete approximation and to display the results quickly and conveniently. The FEM provides a relatively easy way to model the system. In FEM, a complex region defining a continuum is discrete into simple geometric shapes called finite elements. The material properties and the governing relationships are considering over these elements and express in terms of unknown values at the nodes. An assembly process, duly considering the loading and constraints results in a set of equations. Solution of these equations gives us approximate behaviour of the continuum (Chandrupatla and Belegundu, 1997). Since that time, FEM has spread to all engineering disciplines and is now used to determine the engineering response of complex systems such as vehicle occupant safety, fluid flow and magnetic fields.

Conle and Mousseau (1991) used vehicle simulation and the finite element results for the chassis components using automotive proving ground load history results combined with the computational techniques. They concluded that the combination of the vehicle dynamics modeling and finite element analysis are the viable techniques for the design of the automotive components.

A stress analysis activity depends on the function and maturity of the phase, an important benefit of performing stress analyses is the ability to determine design sensitivities and to conduct trade studies. Thus, effective optimization of the structure can be achieved, enhancing reliability while reducing cost and weight. Stress analysis is a very important step to find out suitable material and the best shape for part design. The stress analysis result gets the data of the strength and life of the part that have been design. Asadi et al. (2009) were carried out an experimental study for Tractor MF-285 connecting rod by using finite element analysis. The maximum stresses in different parts of MF-285 connecting rod were determined. From the analysis, three parts were being considered of the stress distributions which are pinning end, rod and crank end. Finally, authors show good agreement between finite element analysis and the experimental equation method.

Afzal and Fatemi (2004) were used finite element to predict stresses and hotspots experienced by the connecting rod. From the resulting of stress contours, the state of stress as well as stress concentration factors can be obtained.

Seo et al. (2007) were studied numerical integration design process to development of suspension parts by semi-solid die casting process. Authors predicted stress distribution for the lower suspension control arms from the strength analysis. The strength analyses were presented von Mises stress distributions and the strain distributions by using five ultimate load conditions and dynamic strength analyses were distributed. ADAMS/NASTRAN and ADAMS/FLEX are used to provide solutions to the stress loading equations for the shovel components (Frimpong and Li, 2007). It contains computationally efficient numerical simulation routines for executing realistic full-motion behavior of complex mechanical systems and provides quick analysis for multiple design variations toward an optimal design (Erdman et al., 2001).

Srikantan et al. (2000) were discussed the vehicle durability and stress analysis using data from proving ground testing. The authors were discussed the differences between yield strength based durability analysis. The authors concentrated on the design of truck body structure and the loads from proving ground tests of similar vehicles are used in simulations to determine the stresses of the vehicle. The simulation used to calculate stress is MSC.NASTRAN. The results from a correlation study showed the analytical strains from FE analysis and proving ground tests correlated very well.

Medepalli and Rao (2000) were discussed the prediction of road loads. The authors here used of computer simulations to predict road loads early in the design process, before a prototype vehicle is developed. The authors outline and validated a process for the prediction of road loads. The computer simulation used was created using ADAMS. The results obtained from the simulations were correlated to measured road loads. The results showed that the flexible body models correlated more closely to the measured road loads. The authors find out and measured loads were correlated very well.

One of the basic tasks in the dynamic analysis of the various constructions is to evaluate the displacements of the construction as the time dependent functions when the time varying loads are given. Before the equations of motion are defined one should assume that the system for which those equations are to be defined is linear or nonlinear. It is important to define the goal of the analysis prior to the formulation of the finite element model. The dynamic analysis process is shown in Figure 2.6. The natural frequencies and mode shapes of a structure provide enough information to make design decisions. Forced response is the next step in the dynamic evaluation process. The solution process reflects the nature of the applied dynamic loading.

Dynamic behaviour is determined by the forces imposed on the vehicle from the tires, gravity and aerodynamics. In a real vehicle, the wheel loads are constantly changing. These loads may be in the longitudinal direction such as acceleration and braking forces in the lateral direction such as cornering forces and in the vertical direction. Dynamic response play a key role in automotive industries under different operating conditions for determining whether engine frequencies or tire excitations from the road surface adversely affect responses at other areas of a vehicle such as at the steering column or in the seats and to evaluate the effect of vibrations on the performance of consumer products and other high-tech electronic devices.

Baek et al. (1993) were proposed an integrated computational durability analysis methodology. The multi-body dynamic simulation software (DADS) was used to calculate dynamic loads of a mechanical component that is modeled as a rigid body in the multi-body mechanical system. Finite element analysis with substructure techniques was used to produce accurate stress fields. The superposition principle was used to obtain the dynamic stress histories at the critical location.

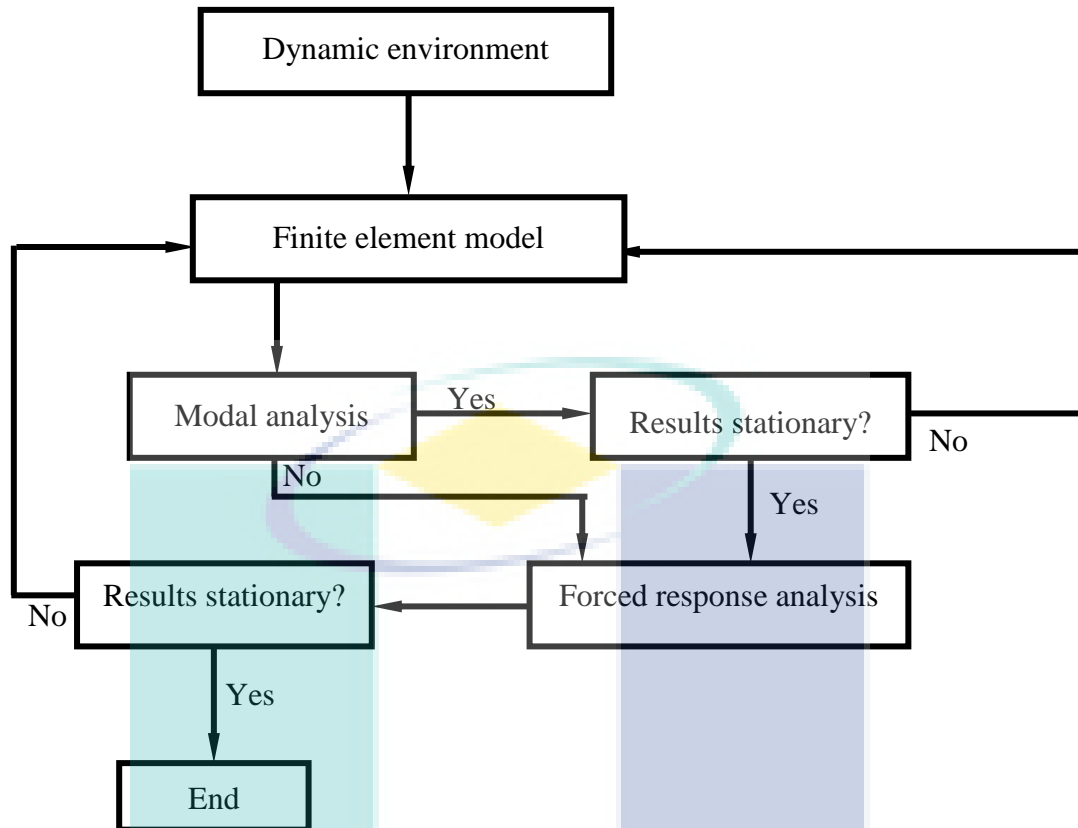


**Figure 2.6:** Dynamic analysis process (Rahman, 2007)

Kim et al. (2002) were studied a method for simulating vehicle dynamics loads however they include the durability estimation. For their multibody dynamic analysis, they use DADS and a flexible body model. For their dynamic stress analysis MSC NASTRAN was used. This study showed that the actual service environment could be simulated instead of using an accelerated testing environment. Since the durability results for the actual service environment can be obtained using a simulation, they can be determined early in the design process. Recently, the suspension arm get more attention by much research such as Attia (2002) study dynamic analysis of the double wishbone motor-vehicle suspension system using the point-joint coordinate's formulation the mechanical system is replaced by an equivalent constrained system of particles and then the laws of particle dynamics are used to derive the equations of motion.

Yuan (2004) was investigated an active and robust vibration control technique based on identified models. The technique was suitable for applications where modal

parameters, such as eigenfunctions or mass/stiffness coefficients are not available analytically. This optimization strategy moves the fundamental natural frequencies of a dynamically loaded component away from the maximum frequency of its forcing functions so that there is no resonance problem (Krishna, 1998; Krishna and Carifo, 2000 and Ma et al., 1995). The inputs into such programs must include a complete description of the forces acting on the components through the dynamic modeling (Frimpong et al., 2005).

Yim and Lee (1996) were proposed an integrated system for the dynamic stress of the vehicle components by developing a data structure that defines the vehicle system and interface programs which support multidisciplinary computer-aided simulation and design activities. They concluded that the combination of the dynamics modeling and finite element analysis is the practical techniques for the fatigue design of the automotive component.

Gopalakrishnan and Agrawal (1993) carried out the durability analysis of full automotive body structures using an integrated procedure in which the dynamic simulation software ADAMS was used to generate loading histories. The inertia relief analysis of MSC NASTRAN was used to analyze the model and to obtain the displacements and stresses. Then, the Fatigue Life Analysis Procedure (FLAP) was used to analyze the durability for selected critical areas from the full model.

The solution of the natural frequencies and normal modes requires a special reduced form of the equation of motion. The methods of eigenvalue extraction including transformation methods and tracking methods. In the transformation method, the eigenvalue equation is first transformed into a special form which eigenvalues may easily be extracted. In the tracking method, the eigenvalues are extracted one at a time using an iterative procedure.

## **2.6 OPTIMIZATION TECHNIQUES**

In engineering design, the knowledge about a planned system is not at all complete. Often, a probabilistic quantification of the uncertainty arising from the

missing information is warranted in order to incorporate efficiently the partial knowledge about the system and its environment into their respective models. In this framework, the design objective is typically related to the expected value of a system performance measure. This system design process is called stochastic system design and the associated design optimization problem is stochastic optimization. Firstly, it is in a design lead to the best system performance in terms of a specified metric. It is therefore, desirable to optimize the performance measure over the space of design variables that define the set of acceptable designs. Secondly, the modeling uncertainty arises because no mathematical model can capture perfectly the behavior of a real system and its environment. In practice, the designer chooses a model that adequately represents the behavior of the built system as well as its future excitation. However, there is always uncertainty about which values of the model parameters give the best representation of the constructed system and its environment. Thus the uncertainty parameter should be quantified. Furthermore, whatever model is chosen, there always be an uncertain prediction error between the model and system responses. For an efficient engineering design, all these uncertainties associated with the future excitation events as well as the modeling of the system must be explicitly accounted.

Stochastic programming was introduced by Dantzig (1955) and many researchers (Ermoliev and Wets, 1988 and Mulvey et al., 1995). Extensions to stochastic integer programming appear in Schultz et al. (1998) and Takriti and Birge (2000). Applications of similar design approaches considering uncertainties have been presented in many areas including transportation engineering (Sakawa et al., 2002); chemical engineering (Acevedo and Pitsikopoulos, 1988 and Gupta and Maranas, 2000); telecommunications (Laguna, 1998); energy scheduling (Morton, 1996); control design (Wang and Stengel, 2002); and finances (Kouwenberg and Zenios, 2001). The state-of-the-art review by Sahinidis (2004) provides details about the optimization methods that have been suggested for identifying the optimal design configuration in such design applications. Most of these methods take advantage of some special characteristics of the class of problems addressed. This feature often limits their applicability to other types of robust-to-uncertainties design problems.

It should be noted that even though the theoretical ideas for design considering modeling uncertainties were introduced many decades ago. The computational cost associated with this design methodology has reduced the range of applications considered because of the complex coupling between system modeling, stochastic analysis, and optimization. Often the formulation of stochastic design improvement is restricted by the available computational resources and the ability to perform the associated design optimization. Complex systems have eventually dictated (i) use of mathematical models that do not adequately consider all characteristics of the true system behavior, (ii) adaptation of approximate techniques for evaluating their performance in a probabilistic setting. Recent advances in software and hardware computer technology have contributed to overcome many of these restrictions and the general concept of stochastic system design is rapidly spreading to new types of applications.

In the current study, the focus is primarily on the design of structural and components. For this part, stochastic design improvement is usually related to the expected reliability of the components design, material, quantified in terms of the probability typically expressed in one of the following three forms: (i) optimization of the system reliability given deterministic constraints (May and Beck, 1998 and Au, 2005); (ii) optimization of the cost of the structure given reliability constraints (Enevoldsen and Sorensen, 1994 and Vietor, 1997); or (iii) optimization of the expected life-cycle cost of the structure (Ang and Lee, 2001). Approaches have been suggested for transforming the latter problem to one of the former two. This is established by approximating the cost related to future damages to the structure in terms of its failure probability (Kong and Frangopol, 2003).

### **2.6.1 Design of Experimental Technique**

Design of experiments (DOE) is a useful tool that used for exploring new processes gaining increased knowledge of the exiting processes and optimizing these processes to achieving a better performance (Rowlands and Antony, 2003). The DOE was developed in the early 1920s by Sir Ronald Fisher and his co-worker focus on agricultural science. Design of experiment is not a favorite technique for many

engineers and manager in an organization due to the number of crunching involve a statistical number until they know the true potential of DOE for achieving breakthrough improvement in product quality and process efficiency in 1951 to late 1970.

The most effective way to improve product quality and reliability is to integrate them in the design and manufacturing process. The DOE is a useful tool that can be integrated into the early stages of the development cycle. It has been successfully adopted by many industries including automotive, semiconductor, medical devices, chemical products, etc. The RSM is an important methodology used in developing new processes, optimizing their performance, improving the design and formulation of new products. It is often an important concurrent engineering tool in which product design, process development, quality, manufacturing engineering and the operations personnel often work together in a team environment to apply RSM. The dynamic and foremost important tools are design of experiment, wherein the relationship between responses of a process with its input decision variables is mapped to achieve the objective of maximization or minimization of the response properties (Raymond and Douglas, 2002). Central composite design is far more efficient than running 3K factorial design with quantitative factors (Montgomery, 2005).

In order understand properly a design of experiment, it is essential to have a good understanding of the whole process. A process is the transformation of inputs to outputs. In the context of manufacturing, input are factoring of process variable such as a people, material, method, environment, machine, procedure, etc. and output can be performance characteristic of the product. Sometimes, an output can also be referring to as a response. Suspension system can moreover, be treated like a system based on RSM technique. Figure 2.7 shows the outputs are performance characteristic, which is measuring to assess the process performance. The controlled and uncontrolled variables are responsible to variability in product performance. This is the fundamental strategy of robust design (Anthony, 2003). Different designs have been used for different experiment purposes.

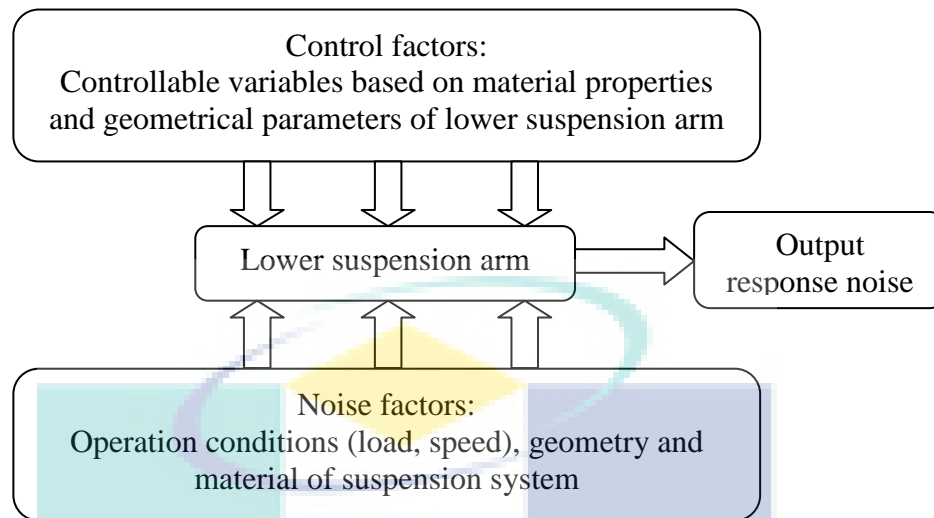


**Figure 2.7:** Suspension system based on CCD

### 2.6.2 Artificial Intelligent

The purpose of artificial intelligent (AI) is to develop a robot that lives in the world with a computer for brain. Knowledge based systems (KBS) are different from traditional computer applications in multiple aspects. First, a KBS represents knowledge explicitly as a set of declarations which is referred to as the knowledge base. Traditional applications implement knowledge implicitly as procedures and therefore, can only apply it in a predetermined way. Furthermore, they are hard to maintain as an update of the information is reflected by the modification of a procedure. A KBS provides problem solving capability which is performed by an inferential engine. It is also able to justify its behavior by expressing the inferential steps that have led to a certain conclusion. An expert system (ES) has an intelligent behavior and is capable of performing tasks for which a specific competence or expertise is usually required. Most expert systems implement the model of a KBS with additional tools that enables it to solve specific tasks such as a medical diagnose. A completely general and flexible expert system has not yet been developed. Neural networks have been partly successfully used integrated into expert systems to automate common sense functions such as the identification of forms. A neural network implements the opposite of the intellectual model of a KBS. It is constructed with units called neurons, whose behavior

is defined by mathematical and statistical functions. There are “input units”, “output units” and “hidden units” which are all connected to each other, building the network. They interact by sending and receiving signals over the connections which are assigned weights. Neural networks can and must be trained by practicing learning patterns. If the network’s output is incorrect, signals are sent back into the network until it “learned” the right answer. If a completely new input is fed into the network, it will try to find an already learned input pattern that is similar and will produce the learned output. This means that the neural network is capable of reasoning by analogy without having been programmed in a traditional way.

One of the used artificial neural networks models is the well-known Multi-layer perceptron (MLP) (Haykin, 1998). The training process of MLP for pattern classification problems consists of two tasks. The first one is the selection of an appropriate architecture for the problem and the second is the adjustment of the connection weights of the network. The other technique RBFNN is defined in the literature as a kind of ANN that has radial activation functions on its intermediary layer. The function approximation problem has been tackled many times in the literature by using RBFNN. It is a robust and versatile computational method that can simulate the physical behaviour of suspension arm. The growth of neural networks has been heavily influenced by the RBFNN. The application of the RBF network can be found in pattern recognition (Musavi et al., 1992). The two most important parameters of RBFNN, the center and the covariance matrix, have been researched thoroughly. RBFNN models are the popular network architectures used in most of the research applications in medicine, engineering, mathematical modelling, etc. (De Alcantara et al., 2002 and Coccorese et al., 1994). The main areas of concentration have been control, identification and damage detection. The majority of research in this area uses the neural network and the results are mostly limited to computer simulations. A few successful experimental results in the area of vibration control have been published by Chen et al. (1992). Szewczyk and Hajela (1993) used a neural network to solve a problem similar to the model updating problem. However, the finite element modeling is useful to analyze and optimize these structures (Gass et al., 1993).

Many researchers focus on linear and nonlinear response application, the most important work in terms of FEM program and integrating with artificial intelligence techniques. Abdullah, (2009) was developed RBFNN model for prediction of nonlinear response for paddle cantilever. The stress distributions and the vertical displacements of the designed cantilevers were simulated through ANSYS a nonlinear finite element program and the regression between the result of FEM and prediction by RBFNN model has shown the least error. Two intelligent techniques had been used by (Wannas, 2008 and Wannas and Abd, 2008). RBFNN and Support Vector Machine (SVM) on the uniformly loaded paddle, the simulation has been shows that SVM modeling better than RBFNN and the both techniques is fast, saving time and quite feasible.

The primary goal of AI research is to increase the understanding of perceptual, reasoning, learning, linguistic and creative processes. This understanding is helpful in the design and construction of useful new tools in science, industry and culture, Just as the invention of the internal combustion engine and the development of machines result in unprecedented enhancement of the mobility of our species, the tools resulting from artificial intelligent research are already beginning to extend human intellectual and creative capabilities in ways that our predecessors could only dream about. Sophisticated understanding of the underlying mechanisms and the potential and limits of human as well as other forms of intelligence are also likely to shed new lights on the social, environmental and cultural problems of our time and aid the search for solutions.

### **2.6.3 Stochastic Design Improvement**

Most applications of robust design have been concerned with static performance in mechanical engineering and process systems (Zang et al., 2004). Whereas the objective of robust design is to optimize the mean and minimize the variability that results from uncertainty represented by noise factors and to test the effect of the variability in different experimental factors using statistical tools. Bharatendra et al. (2004) were studied the robust design of an interior hard trim to improve occupant safety in a vehicle crash. They used orthogonal arrays and compound noise factors to cut down on the number of experimental runs originally needed to address all the control and noise factors of interest. To achieve a robust interior hard trim design, the

study used separate analyses to identify control factors affecting mean and variability. From a technical standpoint, the statistical process control (SPC) and statistical experimental design (SED) are two methods have been used as a robust design to improve quality and productivity (Sreeram, 1994). Figure 2.8 presents the goal of robust design to evaluate and find a suitable design of any modal. Robust design is a tool to evaluate and understand the behaviour of systems in the presence of uncertainty. The types of uncertainties that can be treated are: engineering tolerances (e.g. on thickness, stiffness, etc.), the material property scatter (e.g. yield stress), the load scatter (environmental forces, e.g. gusts, temperature, etc.) and scatter in boundary conditions.

Stochastic design improvement technique is a very fast and efficient method for improving the performance of a system simulated with stochastic approach. The cost of SDI is independent of the number of stochastic variables. SDI does not optimize –it tries to take a system (the corresponding cloud of points) to a user-specified target location. This location represents acceptable (not optimal) performance and may be specified for as many outputs as desired. Target performance should not be specified for outputs that are correlated (dependent). Information on which outputs are independent (i.e. that can be used as targets in SDI) could be obtained from a previous stochastic simulation.

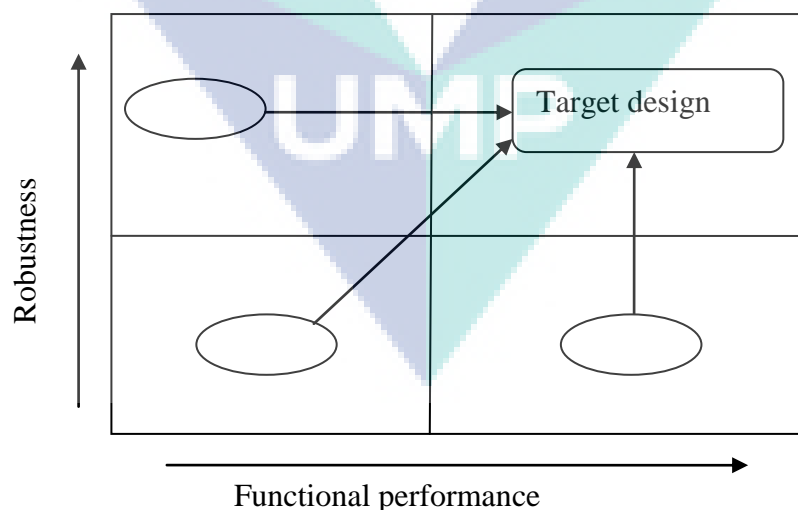


**Figure 2.8:** Robust concept

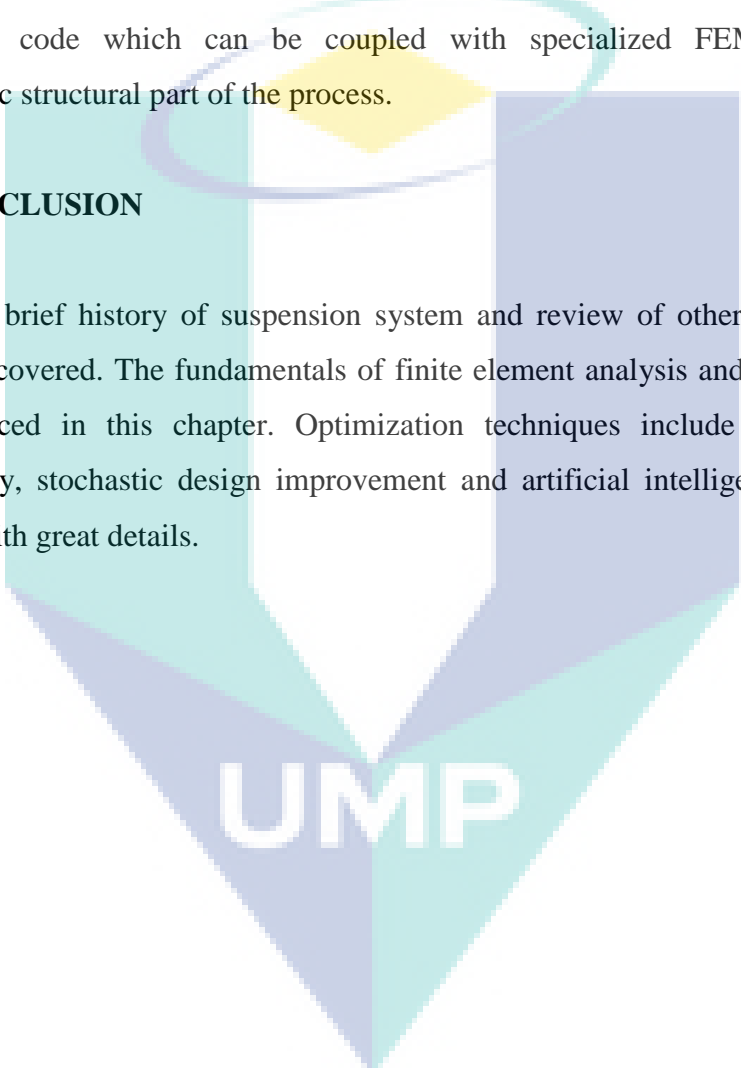
The relevance of this methodology is that it allows finding the design variables which bring the output objective variables as nearest to a chosen target. Fundamentally,

it is based on an iterative Monte Carlo simulation procedure. Therefore the substructure approach enables to speed up the analysis of a large amount of cases and at the same time to generate enough data for an evaluation of the new methodology.

In the present work, the deals with the linear response of the dynamic behavior of lower arm located in the suspension part of a vehicle and which makes use of a new stochastic methodology, stochastic design improvement as implemented in the commercial code which can be coupled with specialized FEM codes for the deterministic structural part of the process.

## **2.7 CONCLUSION**

The brief history of suspension system and review of other relevant research studies are covered. The fundamentals of finite element analysis and dynamic analysis are introduced in this chapter. Optimization techniques include response surface methodology, stochastic design improvement and artificial intelligent techniques are reviewed with great details.

The logo of UMP (Université de Metz) is a large, downward-pointing arrow shape. It is composed of several colored segments: a light blue segment on the left, a light green segment on the right, and a central white segment. The letters 'UMP' are written in white, bold, sans-serif font across the bottom of the arrow.

**UMP**

## CHAPTER 3

### METHODOLOGY

#### 3.1 INTRODUCTION

This chapter presents the mechanical model description and introduced the methods of real eigenvalue extraction. Detailed insight on the finite element analysis techniques is also presented. Propose the robustness analysis is explained. Finally, the potential neural network technique and the response surface methodology are also presented.

#### 3.2 STRUCTURAL MODEL DESCRIPTION

Structural model vehicle suspension is a mechanism locating between the sprung mass (vehicle body) and the unsprung masses (wheels) of the vehicle. The suspension provides forces between these two masses of the vehicle according to certain state variables of the vehicle. A good car suspension system should have satisfactory road holding ability while still providing comfort when riding over bumps and holes in the road. When the vehicle is experiencing any road disturbance the vehicle body should not have large oscillations and the oscillations should dissipate quickly.

The advantage of good kinematic possibilities, the low unsprung mass at moderate costs is a reason to select the double wishbone system as concept for an independent front suspension on a vehicle. The double wishbone suspension shows a spring made by the torsion bar, applied to the lower arm. This allows a limited upper arm and introduces limited values of stress in the upper parts. Therefore, the lower arm alone adopts most of the load. Different front suspension types exist on the market.



### 3.3 MATERIAL PROPERTIES

A material property plays an important role in the result of finite element (FE) method. The material properties are one of the major inputs. The materials parameters required depend on the analysis methodology being used. The mechanical properties of 7079-T6 aluminum alloy are shown in Table 3.1. AA7079-T6 has been chosen for the lower suspension arm due to their good workability, high resistance to corrosion and lightweight, economic and easy to produce (KM, 2011).

**Table 3.1:** Mechanical properties of aluminum alloy 7079-T6

<b>Material</b>	<b>Young's Modulus (GPa)</b>	<b>Poisson's ratio</b>	<b>Tensile strength (MPa)</b>	<b>Yield strength (MPa)</b>
Aluminum alloy AA7079-T6	70	0.33	540	450

### 3.4 FINITE ELEMENT MODELING

Finite element analysis (FEA) has been conducted both on individual components and on assemblies of connected components. Using the finite element models to predict the stress-strain results of the structures becomes more and more important in the modern mechanical industries, such as the aerospace and vehicle suspension arm. The traditional method for evaluating the structural properties of a product is to perform a series of dynamic tests on the prototypes of the product. The objective of the stress/strain analysis is to obtain the complete three dimensional stress and strain distributions at a potential failure site. Linear elastic analysis is the most common type of stress analysis pursued in automotive design and analysis. FE analysis used to calculate the stress distribution for an entire lower arm structure and provides an ideal predict to durability analysis.

The modeling process is made up of four important steps: importing 3D representations in to FE Tools, Assigning Material Properties, Constraining the Model, and Loading the Model. The combined approach of modeling using Computer Aided

Design (CAD) and FE is found to be statistically adequate. The MSC.Nastran suite for finite element analysis is known for high performance, quality and ability to solve all kinds of challenging simulation.

The stress histories calculated using the linear static analysis method and usually the most accurate used by members of the finite element community as a reference to evaluate the accuracy of the design. MSC.Nastran performs static and dynamic analysis and simulation on structure. Generate the mesh for the components and free meshing feature of the software employed since it has no geometry restrictions and it defined on complicated volumes. Tetrahedral meshing produce high quality meshing for boundary representation most of solids model imported from CAD systems.

### 3.5 DYNAMIC MODEL OF SUSPENSION ARM

Automotive suspension is a vibration system and always the mechanical vibration associated with the fluctuation of mechanical loads. The suspension system can offer both the reliability and versatility including passenger ride comfort with less power demand. Vibration can affect comfort, performance and the safety of people. These facts make it imperative that engineers understand the vibration behaviour of every mechanical component, machine, structure, and system. Natural frequency is the rate of energy interchange between the kinetic and the potential energies of a system during motion. As the mass pass through the static equilibrium position, the potential energy is zero (Dimarogonas, 1996). The natural frequency is expressed as Eq. (3.1) and Eq. (3.2).

$$\omega_n = \sqrt{\frac{K}{M}} \quad (3.1)$$

where:  $\omega_n$  is natural frequency  
 $K$  is the stiffness of the suspension arm material.  
 $M$  is mass of suspension arm

$$\omega_n = \sqrt{\frac{K_s}{M_c}} \quad (3.2)$$

where:  $K_s$  is the suspension stiffness  
 $M_c$  is the mass of the vehicle

For the wheel natural frequency  $\omega_n$ , it is necessary to take into account  $K_s$  and  $K_t$  because of the wheel oscillates the suspension and tire springs. Although these two springs are on opposite side of the wheel mass, the mass would feel the same force when the two springs were in parallel on one side of the mass. In the other words, the two springs  $K_s$  and  $K_t$  are in parallel and their equivalent rate is their sum as Eq. (3.3).

$$\omega_n = \sqrt{\frac{K_s + K_t}{m_w}} \quad (3.3)$$

where:  $K_t$  is tire deflection stiffness  
 $m_w$  is the unsprung mass

The role of the vehicle suspension system is to support and isolate the vehicle body and payload from road disturbances, maintain the traction force between tires and road surface. Automobile suspension arm is two-degree of freedom system. The two-degree of freedom suspension model is illustrated in Figure 3.2. Typical whole suspension system is also shown in Figure 3.3 (Milliken, 2002 and Milliken and Milliken, 2002). The suspension model can be defined by Eq. (3.4) and (3.5). In order to observe the suspension status, Eq. (3.4) and (3.5) can be re-written as a state-space in Eq. (3.6).

$$m_w \ddot{z}_1 = -C_c(\dot{z}_1 - \dot{z}_2) - K_s(z_1 - z_2) - K_t(z_1 - q) + m_w g \quad (3.4)$$

$$M_c \ddot{z}_2 = -C_c(\dot{z}_2 - \dot{z}_1) - K_s(z_2 - z_1) - K_t(z_1 - q) + M_c g \quad (3.5)$$

$$[M]\{\ddot{Z}\} + [C]\{\dot{Z}\} + [K]\{Z\} = \{Q\} \quad (3.6)$$

where

- $z_1$  is the unsprung mass displacement
- $z_2$  is the sprung mass displacement
- $\dot{z}_1$  is the unsprung mass velocity
- $\dot{z}_2$  is the sprung mass velocity
- $g$  is the acceleration of gravity
- $q$  is the road disturbance
- $\ddot{z}_1$  is the unsprung mass acceleration
- $\ddot{z}_2$  is the sprung mass acceleration
- $[M]$  is the mass matrix
- $[K]$  is the stiffness matrix
- $[C]$  is the coefficient matrix

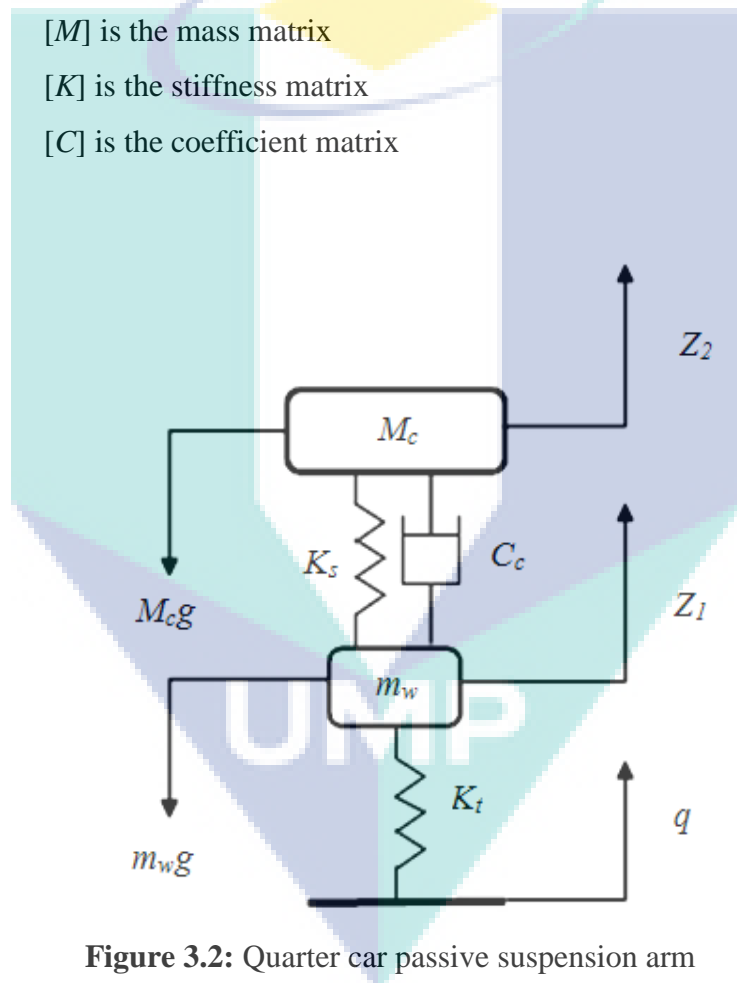


**Figure 3.2:** Quarter car passive suspension arm

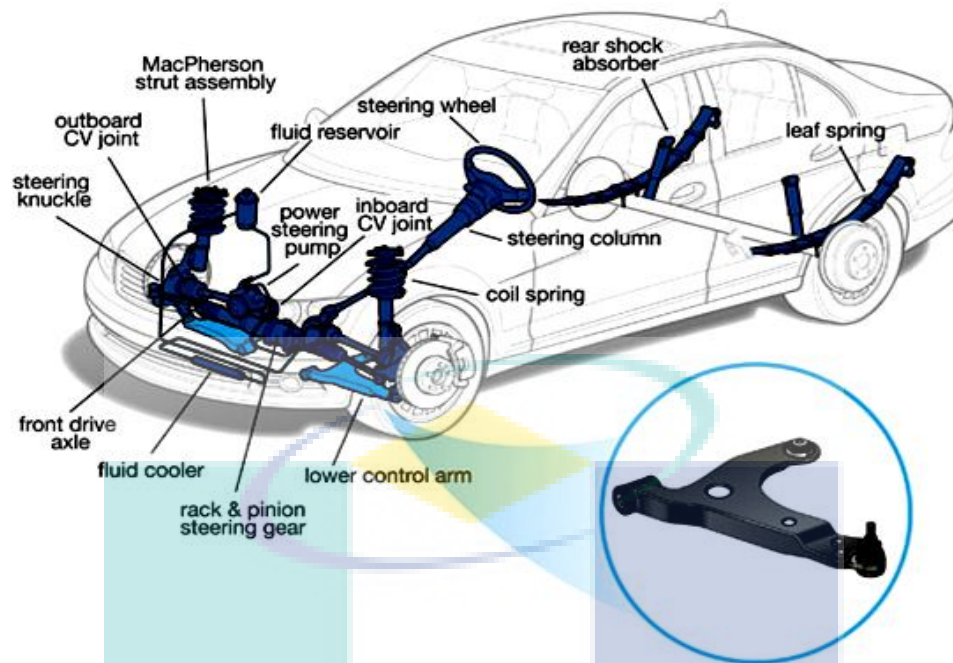


**Figure 3.3:** Suspension system

The Lanczos method combines the best characteristics of both the tracking and transformation methods. Due to this the Lanczos method is the best method to use for most models. The Lanczos method overcomes the limitation and combines the best features of the other methods. It requires that the mass matrix be positive semi-definite and the stiffness be symmetric. It does not miss roots but has an efficiency of the tracking methods due to it only makes the calculations necessary to find the roots. This method computes accurate eigenvalues and eigenvectors. This method is the preferred method for most medium-to large-sized problems since it has a performance advantage over the other methods. The basic Lanczos recurrence is a transformation process to tridiagonal form (Lanczos, 1950). However, the Lanczos algorithm truncates the tridiagonalization process and provides approximations to the eigenpairs (eigenvalues and eigenvectors) of the original matrix. The block representation increases performance in general and reliability on problems with multiple roots. The matrices used in the Lanczos method are specially selected to allow the best possible formulation of the Lanczos iteration.

### 3.6 OPTIMIZATION TECHNIQUES

Optimization has been applied to problems in finance for at least the last half century. An important distinguishing feature of problems in financial markets is that they are generally separable and well defined. The objective is usually to maximize profit or minimize risk, and the relevant variables are amenable to quantification, most of the times in monetary term. Stochastic optimization delivers new nominal values in the design variables that satisfy the targets. A stochastic process is a probabilistic model of a system that evolves randomly in time and space. Stochastic optimization consists in combining the deterministic optimization methods with uncertainty quantification techniques to measure the sensitivity and variability of the response. Optimization today is a basic research tool in all areas of engineering, medicine and sciences. The decision making tools based on optimization procedures are successfully applied in a manufacturing of practical problems.

Optimization has been expanding in all directions at an astonishing rate during the last few decades. New algorithmic and theoretical techniques have been developed, the diffusion into other disciplines has proceeded at a rapid pace and the knowledge of all aspects of the field has grown even more profound (Floudas and Pardalos, 2002 and Abello et al., 2001).

A slightly different strategy for robust design optimization is based on stochastic optimization. The stochastic nature of the optimization arises from incorporating uncertainty into the procedure, either as the parameter uncertainty through the noise factors. The earliest work on stochastic optimization can be traced back to the 1950s (Beale, 1955) and detailed information may be obtained from Birge and Louveaux (1997) and Kall and Wallace (1994). The objective of stochastic optimization is to minimize the expectation of the sample performance as a function of the design parameters and the randomness in the system.

### 3.6.1 Response Surface Methods

Response surface methods are used to estimate the transfer functions at the optimal region. The estimated function is then used to optimize the responses. The quadratic model is the model used in RSM. Similar to the factorial design, linear regression and analysis of variance (ANOVA) are the tools for data analysis in RSM. Hence, central composite design (CCD) approach was selected for the present study. In light of this phase, two variables out of the four variables were selected for this phase. DOE is not only a collection of statistical techniques that enable an engineer to conduct better experiments and analyze data efficiently. In this section, general guidelines for planning efficient experiments are given. The seven-steps of procedure are presented in Figure 3.4 (Montgomery, 2005 and Wu and Hamad, 2000). The objectives of the experiment are clearly stated. It is helpful to prepare a list of specific problems that are to be addressed by the experiment. Responses are the experimental outcomes. An experiment may have multiple responses based on the stated objectives. The responses that have been chosen should be measurable. A factor is a variable that is going to be studied through the experiment in order to understand its effect on the responses. Once a factor has been selected, the value range of the factor that will be used in the experiment should be determined. Two or more values within the range need to be used. These values are referred to as levels or settings. Practical constraints of treatments are considered, especially when safety is involved. A cause and effect diagram capable utilized to help identify factors and determine factor levels. According to the objective of the experiments, the analysts select the number of factors, the number of level of factors and an appropriate design type. A design matrix used as a guide for the experiment. This matrix describes the experiment in terms of the actual values of factors and the test sequence of factor combinations. Engineering knowledge integrated into the analysis process. Once the data have been analyzed, practical conclusions and recommendations made. Graphical methods are often useful, particularly in presenting the results to others. Confirmation testing performed to validate the conclusion and recommendations.

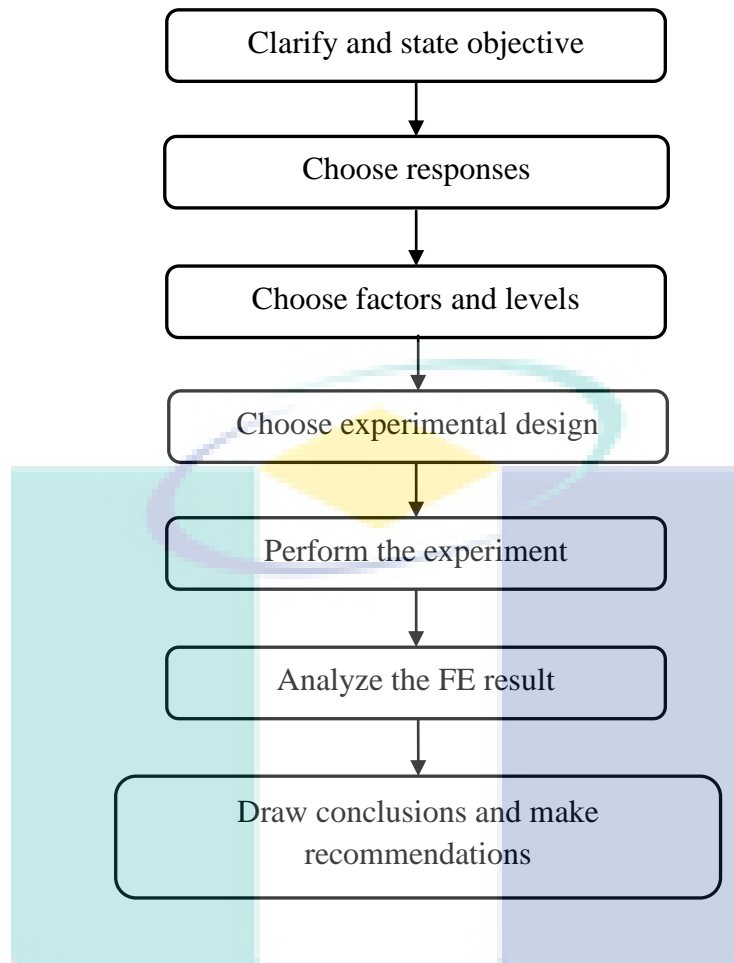


**Figure 3.4:** General guidelines for conducting DOE

The above describe steps are the general guidelines for performing an experiment. A successful experiment requires knowledge of the factors, the ranges of these factors and the appropriate number of levels to be used. Generally, this information is not perfectly known before the experiment. Therefore, it is suggested to perform experiments iteratively and sequentially. It is usually a major mistake to design a single, large, comprehensive experiment at the start of a study.

### **3.6.2 Radial Basis Function Neural Network Technique**

Radial basis function neural network have increasingly attracted interest for engineering applications due to their advantages over traditional multilayer perceptrons namely faster convergence, smaller extrapolation errors and higher reliability. Over the last few years, more sophisticated types of neurons and activation functions have been

introduced in order to solve different sorts of practical problems (Kumar, 2005). In particular, RBFNN have proved very useful for many systems and applications. One of the used artificial neural networks models is the well-known MLP. The training process of MLP for pattern classification problems consists of two tasks, the first one is the selection of an appropriate architecture for the problem and the second is the adjustment of the connection weights of the network. The major difference between RBF networks and back propagation networks (that is, multi layer perceptron trained by back propagation algorithm) is the behavior of the single hidden layer. Rather than using the sigmoidal or S-shaped activation function as in back propagation, the hidden units in RBF networks use a Gaussian or some other basis kernel function. Each hidden unit acts as a locally tuned processor that computes a score for the match between the input vector and its connection weights or centers. In effect, the basis units are highly specialized pattern detectors. The weights connecting the basis units to the outputs are used to take linear combinations of the hidden units to product the final classification. The idea of RBFNN derives from the theory of function approximation are as follows:

- i. The hidden nodes implement a set of radial basis functions
- ii. The training is very fast.
- iii. The networks are very good at interpolation.

### ***Structure of RBF Networks***

RBFNN was used in the context of neural networks as linear and nonlinear function estimators and indicated their interpolation capabilities by Broomhead and Lowe (1988). Hartman et al. (1990); Park and Sandberg (1991, 1993) were proved that RBFNN are capable of approximating any function with arbitrary accuracy. As a popular model in the community of artificial neural networks, RBFNN has attracted intense researching interests (Sandro, 2006). The neural network is a mapping between its inputs and outputs based on a number of known sample input-output pairs. In general, the more samples available to train the network, the more accurate the representation of the real mapping will be. These samples are obtained by solving the direct problem. The structure of an RBFNN networks in its most basic form involves three entirely different layers as shown in Figure 3.5. The first input layer feeds data to a

hidden intermediate layer. The hidden layer processes the data and transports it to the output layer.

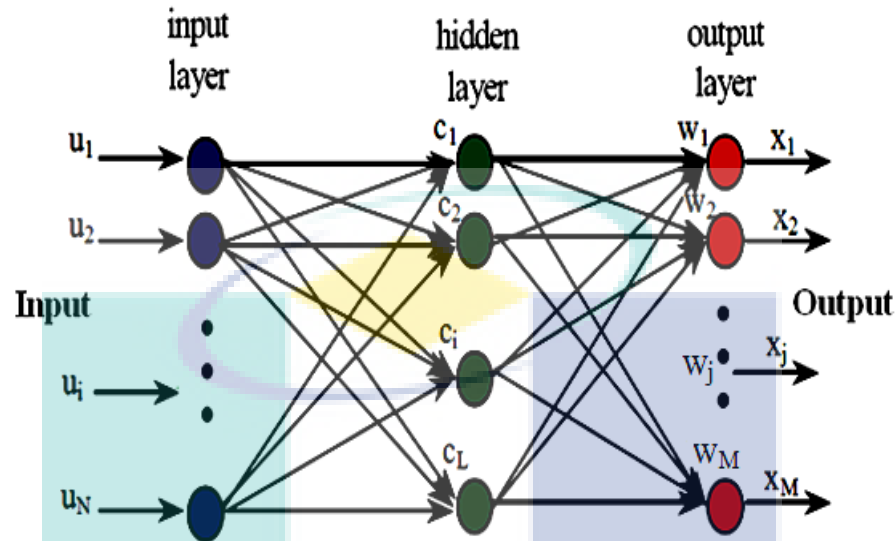


**Figure 3.5:** Radial basis function neural networks

Only the tap weights between the hidden layer and the output layer are modified during training. Each hidden layer neuron represents a basis function of the output space with respect to a particular center in the input space. The activation function chosen is commonly a Gaussian kernel. This kernel is centered at the point in the input space specified by the weight vector. Radial basis function networks are used commonly in function approximation and series prediction (Pandya, 1995). The input layer is made up of source nodes (sensory units) whose number is equal to the dimension of the input vector ( $u$ )

### ***Network Training***

One of the advantages in the RBFNN use is the training speed, taking into account that this process involves, usually, two distinct stages: an unsupervised training and a supervised training. In the unsupervised training, the centers are created for the intermediary layer. Commonly, this stage employs means algorithm (Sandro, 2006). In supervised training, a linear method is employed to minimize the established error measure. However, it is important to note that the RBFNN performance measure is

intrinsically linked to the intermediary layer determination. A characteristic feature of radial function is that its response decreases or increases monotonically with distance from a central point named as center of the radial function (Simon, 2002). These neurons are so called radial basis activation function. Various methods have been used to train RBF networks (Kumar, 2005; Kurban and Besdok, 2009). Approach first uses  $K$ -means clustering to find cluster centers which are then used as the centers for the RBF functions. However,  $K$ -means clustering is a computationally intensive procedure and it often does not generate the optimal number of centers. Another approach is to use a random subset of the training points as the centers. Training of the RBFNN in general can be divided into two stages that are training in the hidden layer followed by training in the output layer. Training in the hidden layer is unsupervised and it involves determination of the centers and spread of the Gaussian functions of the hidden nodes utilizing an appropriate clustering algorithm. On the other hand, training in the output layer uses a supervised method like the least mean square (LMS) algorithm. The centers of the Gaussian functions are determined with the  $K$ -means clustering algorithm and the spreads are calculated using the second order nearest neighbor heuristic. The weights between the hidden and output layers are determined by minimizing the square error of the network output with the LMS algorithm

### ***Hidden layer***

The second layer is the hidden layer which is composed of nonlinear units that are connected directly to all of the nodes in the input layer. It is of high enough dimensions which serves a different purpose from that in a multilayer perceptron. Each hidden unit takes its input from all the nodes at the components of the input layer and the hidden units contain a basis function, which has the parameters center and width. The center of the basis function for a node  $i$  at the hidden layer is a vector  $c_i$  whose size is the as the input vector  $u$  and there is normally a different center for each unit in the network.

First, the radial distance  $d_i$ , between the input vector ( $u$ ) and the center of the basis function ( $c_i$ ) is computed for each unit  $i$  in the hidden layer as Eq. (3.7)

$$d_i = \|u - c_i\| \quad (3.7)$$

where  $d_i$  is the radial distance  
 $u$  is the input vector  
 $c_i$  is the center of the basis function  
 $\|$  is Euclidean norm

The output ( $h_i$ ) of each hidden unit  $i$  is then computed by applying the basis function  $G$  to this distance as Eq. (3.8)

$$h_i = G(d_i, \sigma_i) \quad (3.8)$$

where  $\sigma_i$  is corresponding to the variance  
 $h$  is hidden layer  
 $G$  is the basis function

**Output layer**

The transformation from the input space to the hidden unit space is nonlinear, whereas the transformation to the hidden unit space to the output space is linear. The  $j^{\text{th}}$  output is computed as Eq. (3.9)

$$x_j = f_j(u) = w_{0j} + \sum_{i=1}^L w_{ij} h_i \quad j = 1, 2 \dots M \quad (3.9)$$

where  $w$  is weight matrix

Let  $y = x_j$  be a given function of  $u$ . The function can be written in terms of the given basis functions as Eq. (3.10)

$$y = w_{0j} + \sum_{i=1}^L w_{ij} G(\|u - c_i\|) \quad j=1, 2 \dots M \quad (3.10)$$

$u$  is the  $n$ -dimensional vector of input signal,  $c$  is a constant vector in the same direction while  $\|$  is Euclidean norm in the  $n$ -dimensional space and Practically  $x_j$  shows how close vector  $u$  is to vector  $c$  in  $n$ -dimensional space. The choice of  $\|$  and  $c$  plays a critical role in the training algorithm and stability of the neural network system. There are no theoretical guidelines found for choosing these constants so they are chosen on heuristic grounds by experimental or trial and error techniques. In the summary the mathematical model of the RBF network can be expressed as Eq. (3.11) (Chiang et al., 2009).

$$\hat{y} = \begin{bmatrix} W_{11} & \cdots & W_{1j} \\ \vdots & \ddots & \vdots \\ W_{i1} & \cdots & W_{ij} \end{bmatrix} \begin{bmatrix} 1 \\ \sigma(-\|u - c_1\|^2) \\ \sigma(-\|u - c_i\|^2) \end{bmatrix} \quad (3.11)$$

RBF can be optimized with adjusting the weights and center vectors by iteratively computing the partials and performing the following updates (Kurban and Beşdok, 2009), the algorithm can be implemented to minimize the error after defining the error function has been written as Eq. (3.12).

$$E_r = \sum (y - \hat{y})^2 \quad (3.12)$$

where  $E_r$  is the error RBF  
 $\hat{y}$  is the desired output

### 3.6.3 Robust Design

The robust design technique is very important to develop a better product for the automotive industry such as lower suspension arm. Rakesh et al. (2002) were using robust design method for developing and minimizing variability of products and processes in order to improve their quality and reliability for the spindle motor. The method of robust design using to make sure that a light weight, low cost and better safety component can be made at the final give us a better performance and market value in the automotive industry. Robust design performs stochastic simulation using modified Monte Carlo method that provides approximate solutions to problems expressed mathematically. Using random numbers and trial and error, it repeatedly

calculates the equations to arrive at a solution. Robust design provides the means to quickly sort through indicate the variables that have the most significant correlations, and therefore most impact the product's performance. Correlation is a concept different from of sensitivity in that collective changes in variable values are considered. Correlation between two variables expresses the strength of the relationship between these variables by taking into account the scatter in all the other variables in a system. It is possible to compute correlations between any pair of variables (input-output, output-output, etc.). Knowledge of the correlations in a system is equivalent to the understanding of how that system works.

The general approach of robust optimization is to optimize against the worst instance that might arise due to data uncertainty by using a minimum-maximum objective. The resulting solution from the robust counterpart problem is insensitive to the data uncertainty as it is the one that minimizes the worst case and therefore is “immunized” against this uncertainty. The robust optimization methodology assumes the uncertain parameters belong to a bounded uncertainty set. Clearly the size of the uncertainty set influences the deviation from optimality of the robust solution (Diaz, 2010). Robust Design uses two metrics for measuring the correlation between variables:

- i. Pearson's correlation coefficient (or linear correlation coefficient)
- ii. The Spearman rank coefficient (or non-linear correlation coefficient)

Pearson's correlation coefficient measures the linear correlation between variables. For two stochastic variables,  $x$  and  $y$ , their Pearson, or linear correlation is expressed as Eq. (3.13)

$$r = \frac{\sum_i (x_i - u_x)(y_i - u_y)}{\sqrt{\sum_i (x_i - u_x)^2} \sqrt{\sum_i (y_i - u_y)^2}} \quad (3.13)$$

where  $r$  is linear correlation coefficient  
 $u$  mean value  
 $x, y$  is stochastic variables

The values of the Pearson correlation range from  $-1$  to  $1$ . A value close to either  $1$  or  $-1$  indicates a strong linear correlation. Values close to zero indicate the variables are uncorrelated. The Spearman rank correlation compensates for this, and is a more reliable means for determining if a significant relationship exists between stochastic variables. The computation of the Spearman's rank correlation is done by ranking the variables from highest to lowest assigning ranks from  $1$  to  $N$ . The variable value is then replaced with its corresponding rank. The Spearman rank correlation coefficient ( $r_s$ ), is then computed as the linear correlation coefficient between the ranks ( $R_i$ ) of the  $x_i$ s and the ranks ( $S_i$ ) of the  $y_i$ s, the ( $r_s$ ) is expressed as Eq. (3.14).

$$r_s = \frac{\sum_i (R_i - u_r)(S_i - u_s)}{\sqrt{\sum_i (R_i - u_r)^2} \sqrt{\sum_i (S_i - u_s)^2}} \quad (3.14)$$

As with the Pearson correlation, the values of the Spearman coefficient range from  $-1$  to  $1$ . A value close to either  $1$  or  $-1$  indicates a strong correlation. The Spearman ranking is used to create pie charts to show the relative influence of tolerances in input variables on the scatter (quality) in a particular functionality (output). A target output behavior is selected from the output available in FEM. The values of the design variables in this first set of 15 runs scatter around the nominal values for those variables contained in the input FEM. Another set of 15 runs is performed using the result from the first set of runs that is closest to the target value as the new nominal value. Stochastic design improvement surpasses classical optimization techniques in terms of performance and computational cost. The required inputs for the SDI analysis process are shown in Figure 3.6.

The three input information are descriptions of the material properties, loading histories and geometry. Figure 3.7 shows the flows of steps that are perform in the SDI for the lower arm suspension design. The FE modeling and analysis are discussed in this chapter.

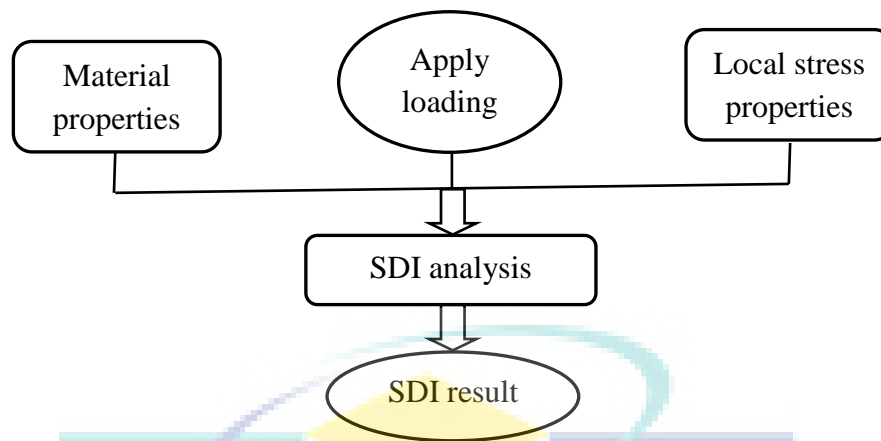


**Figure 3.6:** Schematic diagram of the SDI

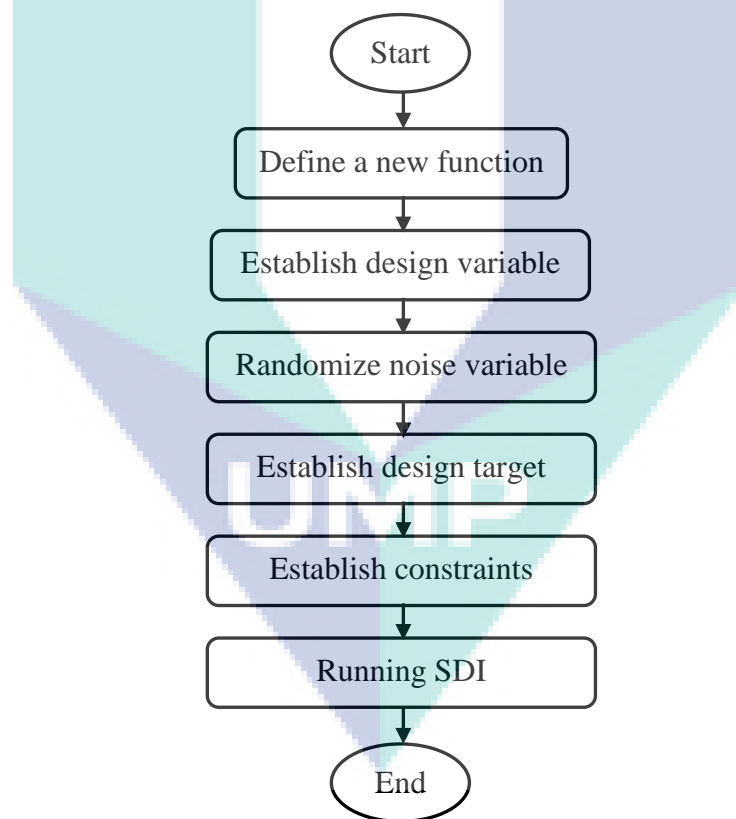
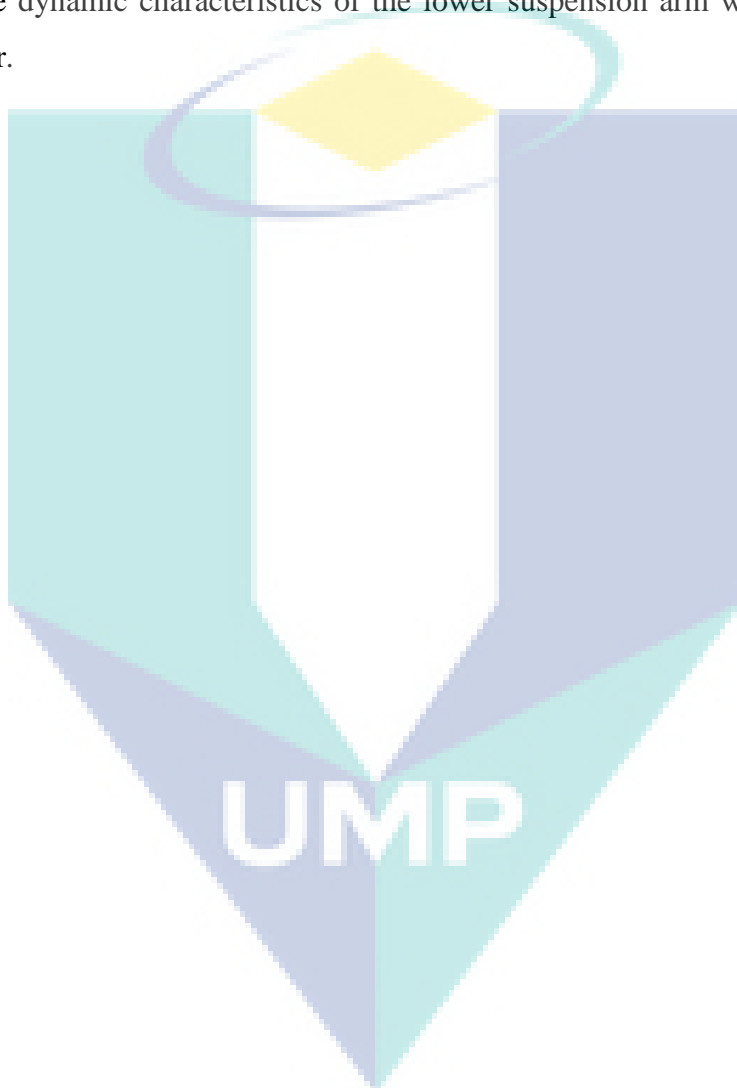


**Figure 3.7:** Flow chart of steps in SDI

### 3.7 CONCLUSION

The mechanical properties of suspension lower arm, finite element method and real eigenvalue extraction are presented in this chapter. The three techniques including the radial basis function neural network, stochastic design improvement and response surface method were also covered. The finite element modeling and analysis of lower arm and the dynamic characteristics of the lower suspension arm will be discussed in next chapter.



## CHAPTER 4

### RESULTS AND DISCUSSION

#### 4.1 INTRODUCTION

This chapter discusses the geometry of lower arm used for the FEA. The mesh generation and its convergence are also presented. In addition, the validation of the finite element model will be presented and details of the FEA addressed in this chapter. The linear elastic finite element stress analysis method is performed. The frequency response analysis for the loading conditions is presented. A new approach to investigate the influencing factors of the lower suspension arm by integrating finite element analysis results with the central composite design approach and radial basis function neural network techniques has been presented. The stochastic optimization method including SDI will be presented.

#### 4.2 FINITE ELEMENT MODELING AND ANALYSIS

The suspension arms are important parts in a vehicle. It provides ride comfort to the driver by isolating irregular vibrations from a road surface effectively and secures the maneuverability. The three dimensional structure model of suspension arm was developed using solidworks software. A 10 node tetrahedral element (TET10) was used for the solid mesh. Sensitivity analysis was performed to determine the optimum element size. Stress analyses considering the ultimate load condition applied to the parts during the driving were performed. The stress analysis was performed with NASTRAN commercial software. The mesh global length of 5.3 mm was considered and the force ( $x = -549.7\text{N}$ ,  $y = 12218.3\text{N}$ ,  $z = 845.9\text{N}$ ) was applied one end of the bushing that connected to the tire (Figure 4.1). The other two bushing that connected to the body of

the vehicle are constraints. These loads are based on Seo et al. (2007). The three dimensional finite element model, loading and constraints of suspension arm are shown in Figure 4.1.

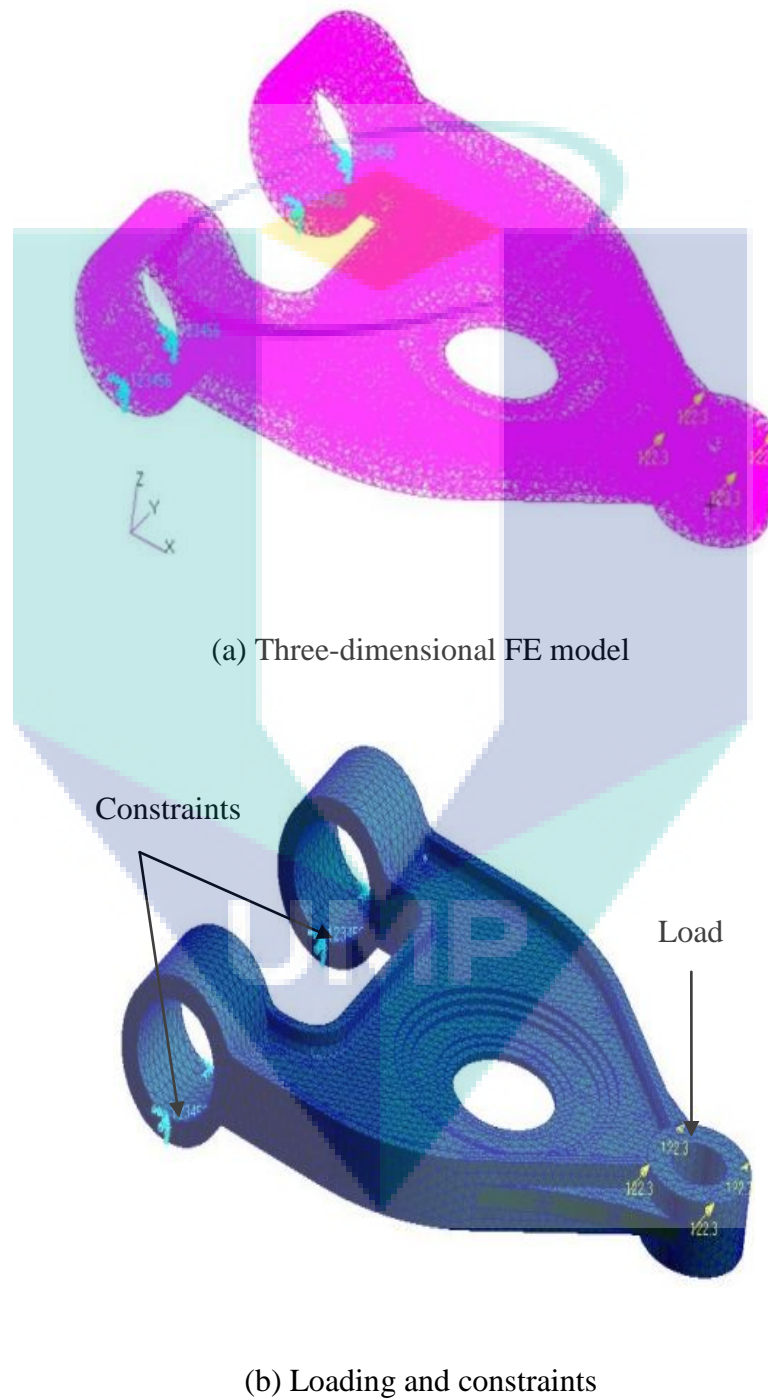
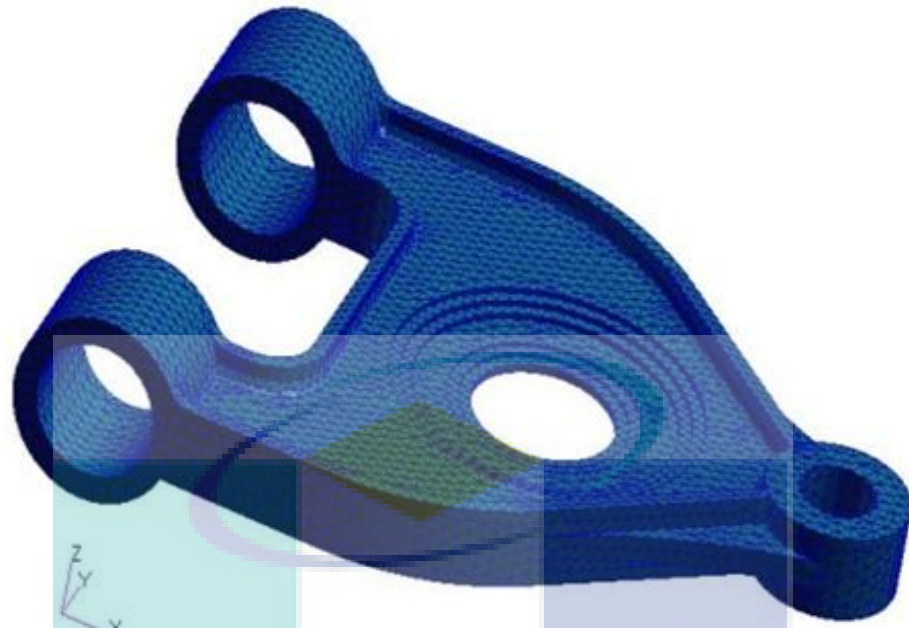


**Figure 4.1:** Three-dimensional FE model and (loading and constraints)

### 4.2.1 Meshing Technique

Mesh generation is one of the most critical aspects of engineering simulation and selecting the right techniques of meshing are based on the geometry, model topology, analysis objectives and engineering judgment. Tetrahedral meshing produce high quality meshing for boundary representation of a solids model. Three-dimensional linear tetrahedron elements with 10 nodes (TET10) and tetrahedral elements with 4 nodes (TET4) are used for the initial analysis (Figure 4.2). Convergence of stress and strain energy was considered as the criteria to select the mesh size. Too much refinement at the critical points would result in extremely lengthy analysis time and was therefore, avoided. The finite element model was using TET4 and TET10 types of elements are shown in Figure 4.2. Figure 4.3 represents von Mises stress contour for TET4 and TET10 elements. It is to analyze the influence for TET10 mesh at highest levels von Mises stress than TET4 mesh of various mesh global length. The result shows that the TET10 mesh predicted higher von Mises stresses than that the TET4 mesh. Whereas, TET10 maximum von Mises stress 561 MPa appeared on the model and 116 MPa maximum von Mises stress occurred for TET4 (Figure 4.3).

Variation of maximum principal stresses and displacement against the global mesh length are shown in Figure 4.4 and Figure 4.5 respectively. It can be seen that TET10 gives the higher stress and displacement throughout the global mesh length. As shown in Figure 4.3, there is quite a difference between the two elements, but the TET4 mesh is still capable of identifying critical areas. The TET10 mesh is presumed to represent a more accurate solution since TET4 meshes are known to be dreadfully stiff (Felippa 2001). Both meshes have some distorted elements cause an error to the modeling in areas of elevated stress. In the design stage, these areas should be remeshed and further refined to check for solution convergence. Further analysis is confined to the region with the highest von Mises stresses using the TET10 mesh. The TET4 simulation is compared to the same simulation using the TET10 mesh. Figure 4.3 shows that the TET10 mesh predicts higher von Mises stresses than the TET4 mesh. Specifically, the TET10 mesh predicts the maximum von Mises stress of 561 MPa whereas TET4 predicts 116 MPa.



(a) TET4 (46464 elements and 11319 nodes)



(b) TET10 (46469 elements and 76035 nodes)

**Figure 4.2:** Finite element model was using TET4 and TET10 elements

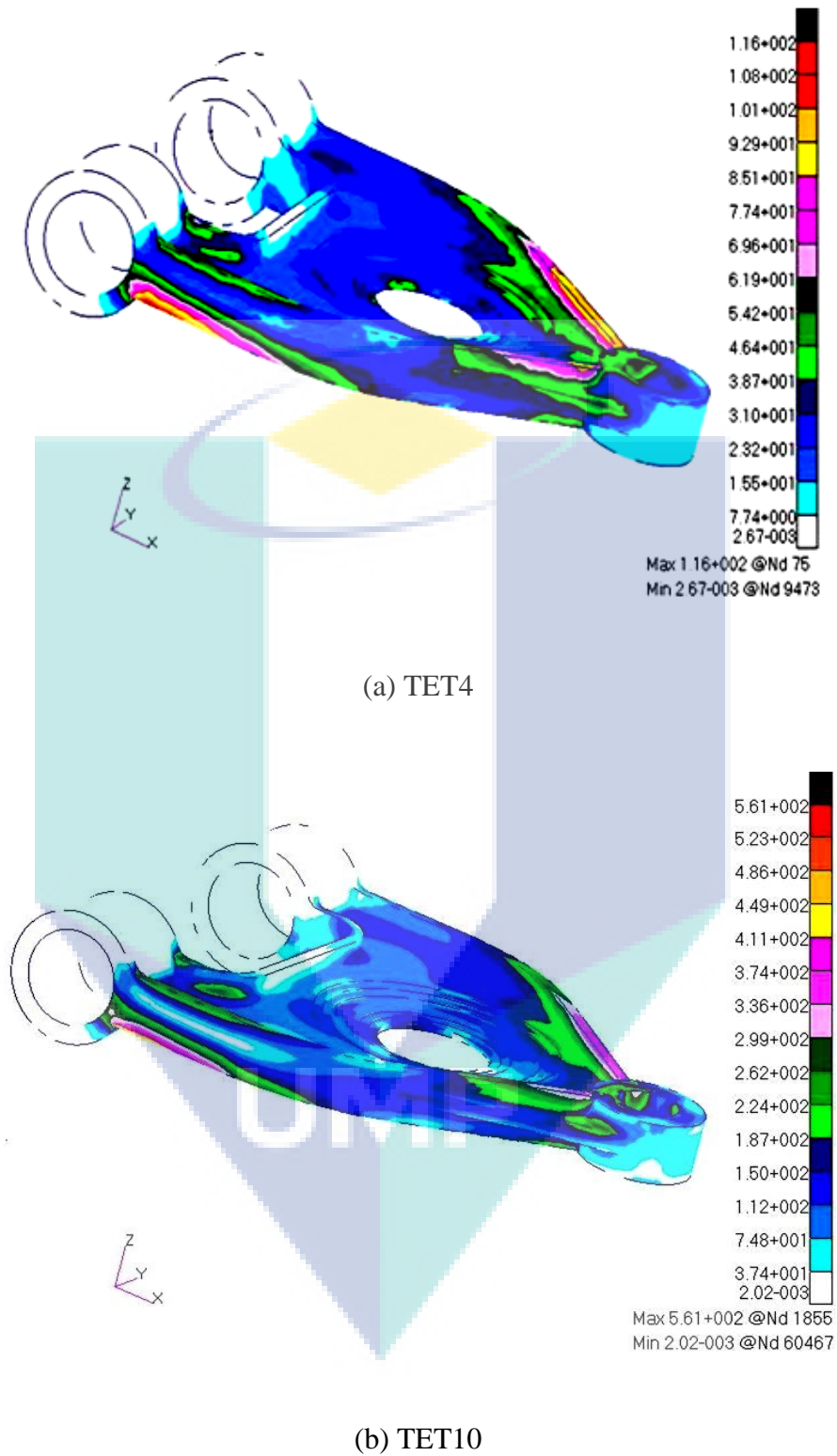


**Figure 4.3:** von Mises stresses contours

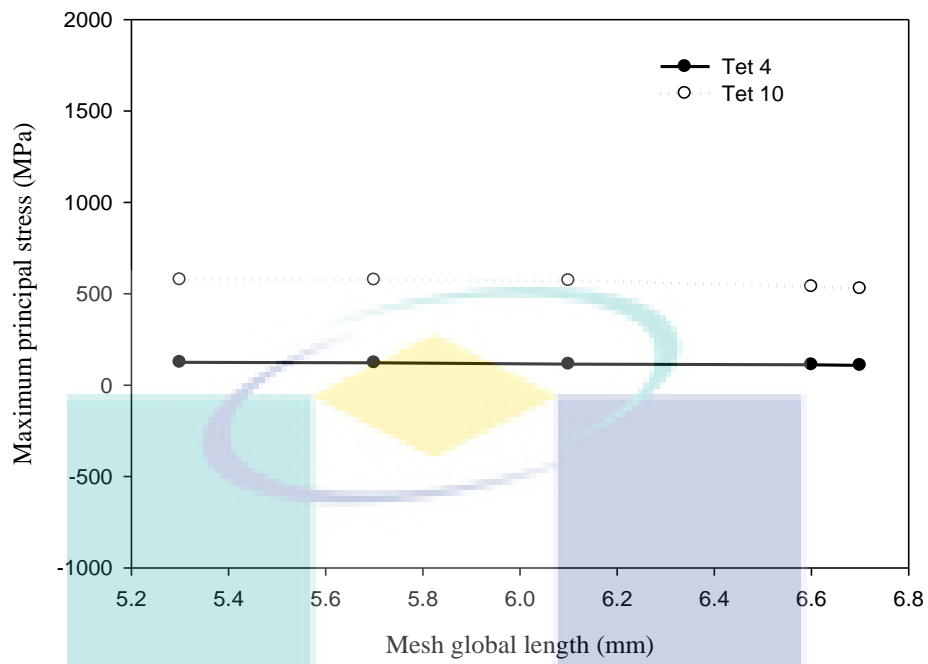


**Figure 4.4:** Variation of maximum principal stress for different element types

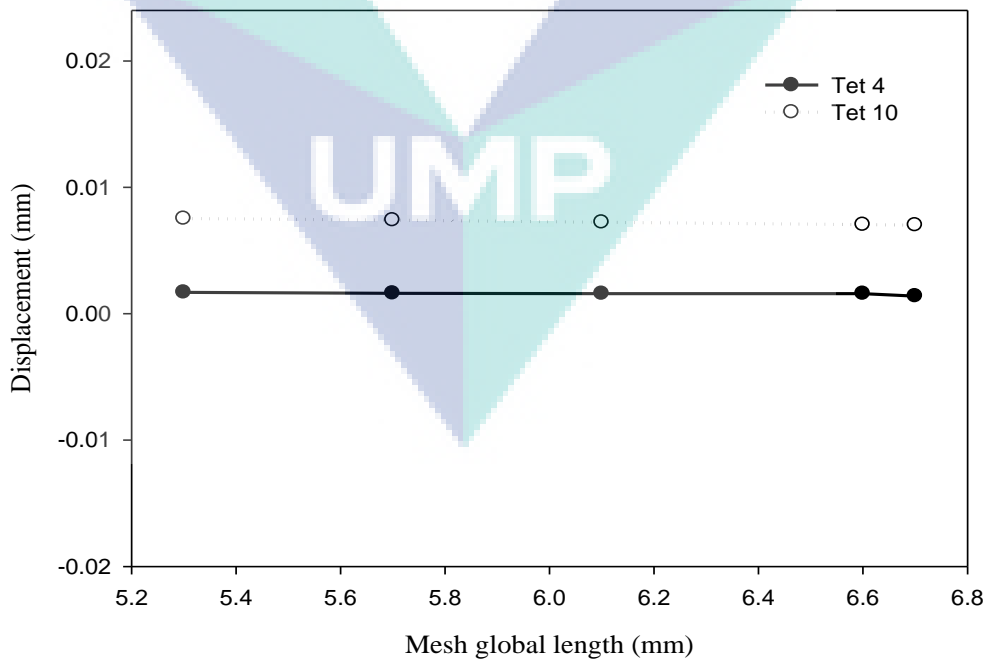


**Figure 4.5:** Variation of maximum displacement for different element type

#### 4.2.2 Identification of Mesh Convergence

The finite element modeling and analysis were carried out using MSC.PATRAN and MSC.NASTRAN finite element analysis codes respectively. The geometry model consists of lower suspension arm, modeled with 10 nodes tetrahedral elements over the model volume. The model consists of a total of 76035 nodes and 46469 elements.

The convergence of the stress was considered as the main criteria to select the mesh type. The finite element mesh was generated using TET10 for various meshes global length 6.7 mm (33532 elements), 6.6 mm (34253 elements), 6.1 mm (36353 element), 5.7 mm (39545 elements), and 5.3mm (46469 elements). It can be seen that the smaller the mesh size capture the higher predicted stresses (Figure 4.6). It is also observed that mesh size of 5.3 mm (46469 elements) has obtained the maximum stresses, which is almost flattening in nature. The maximum stress obtained of 561, 574 and 577 MPa for von Mises stress, Tresca and Maximum principal stress method respectively. Figure 4.7 shows the predicted results of stresses at the critical location of the suspension arm. The maximum principal stress method occurred highest stresses through the global length range. Thus TET10 and maximum principal stress method are selected for linear static and dynamic analyses of the suspension arm.

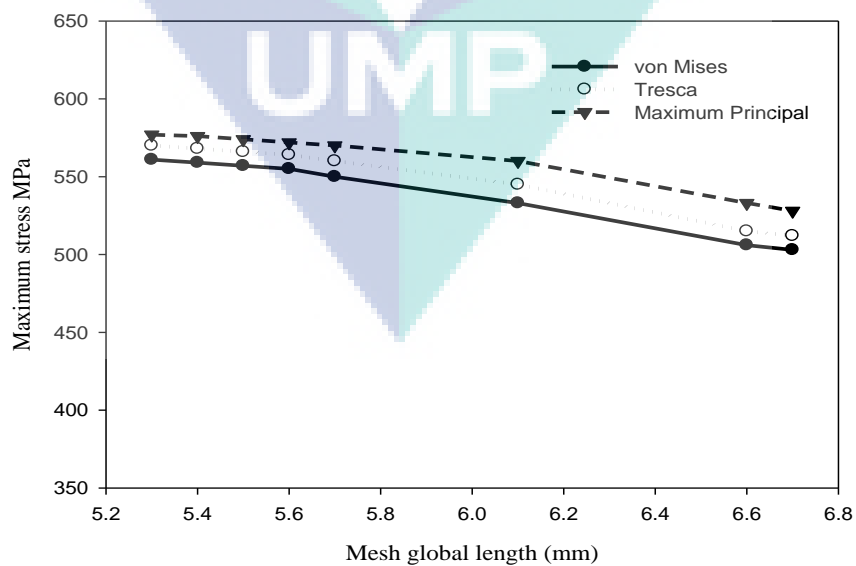


**Figure 4.6:** Maximum stresses versus mesh size at critical location for TET10 of lower suspension arm to check mesh convergence

### 4.2.3 Linear Static Analysis

The stress histories calculated using the linear static analysis method are usually the most accurate and commonly used. The linear static stress analysis was performed utilizing MSC NASTRAN to determine the stresses and strains result from the finite element model. The material models utilized of elastic and isotropic material. The convergence of the finite element model of the structure was tested for two types of elements, including TET4 and TET10 and 5 different mesh sizes. The maximum principal stresses distributions of the suspension arm for the linear static stress analysis is shown in Figure 4.7. From the results, the maximum principal stresses of 577 MPa was obtained at node 151.

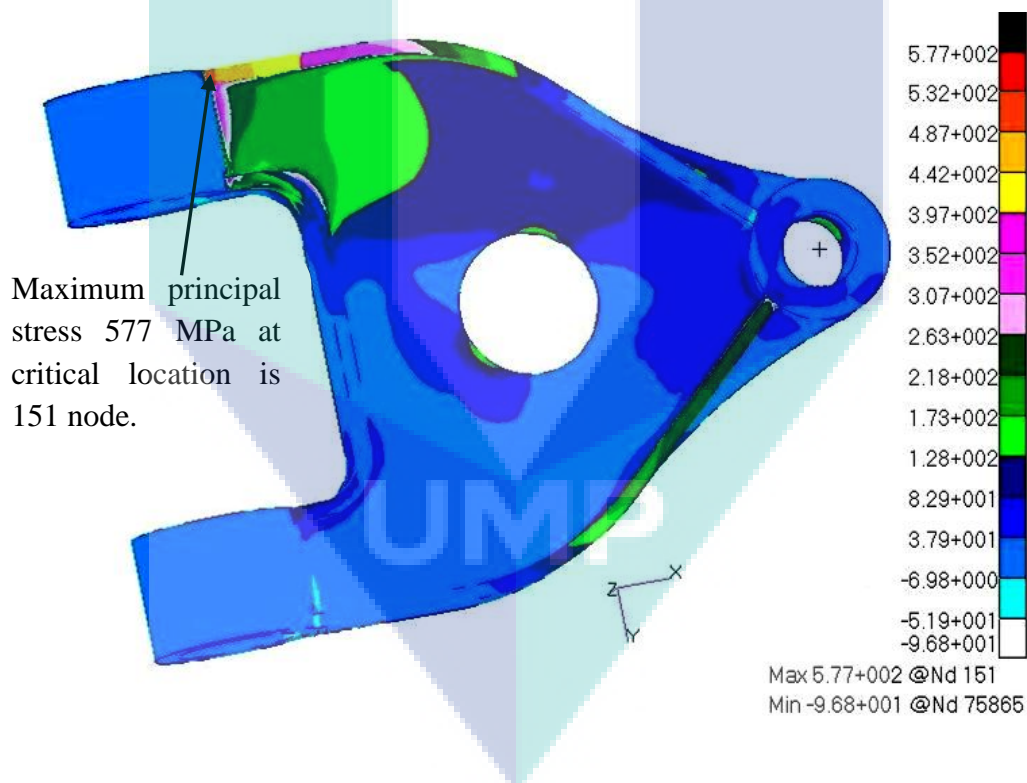


**Figure 4.7:** Stresses versus mesh size at critical location for TET10 to check mesh convergence

### 4.2.4 Dynamic Analysis of Lower Suspension Arm

Dynamic analysis is focused on the eigen-frequencies and mode shapes. From a physical point of view, an initial excitation of an undamped system causes to vibrate

and the system response is a combination of eigenmodes, where each eigenmode oscillates at its associated eigen-frequency. Modal analysis is usually used to determine the natural frequencies and mode shapes of a component. It can be used as the starting point for dynamic analysis. The finite element analysis usually used several mode extraction methods. The Lanczos mode extraction method is used in this study (Rahman et al., 2007). Lanczos is the recommended method for the medium to large models. In addition to its reliability and efficiency, the Lanczos method supports sparse matrix methods that significantly increase computational speed and reduce the storage space. This method computes precisely the eigenvalues and eigenvectors. The number of modes was extracted and used to obtain the suspension arm stress histories, which is the most important factor in this analysis (Table 4.1).

**Table 4.1:** Natural frequency of lower arm

No. of Mode	Natural Frequency (hz)
1	205.26
2	879.23
3	997.58
4	1900.1
5	1948.5
6	2349.2
7	2524
8	3079.3
9	3619.4
10	4187.4

Using Lanczos method to obtain the first 10 modes of the suspension arm, which are presented in Table 4.1 and the shape of the mode are shown in Figure 4.8. It can be seen that the working frequency (80Hz) is far away from the natural frequency (205.26 Hz) of the first mode. The maximum displacement from the model analysis is presented in Table 4.2.

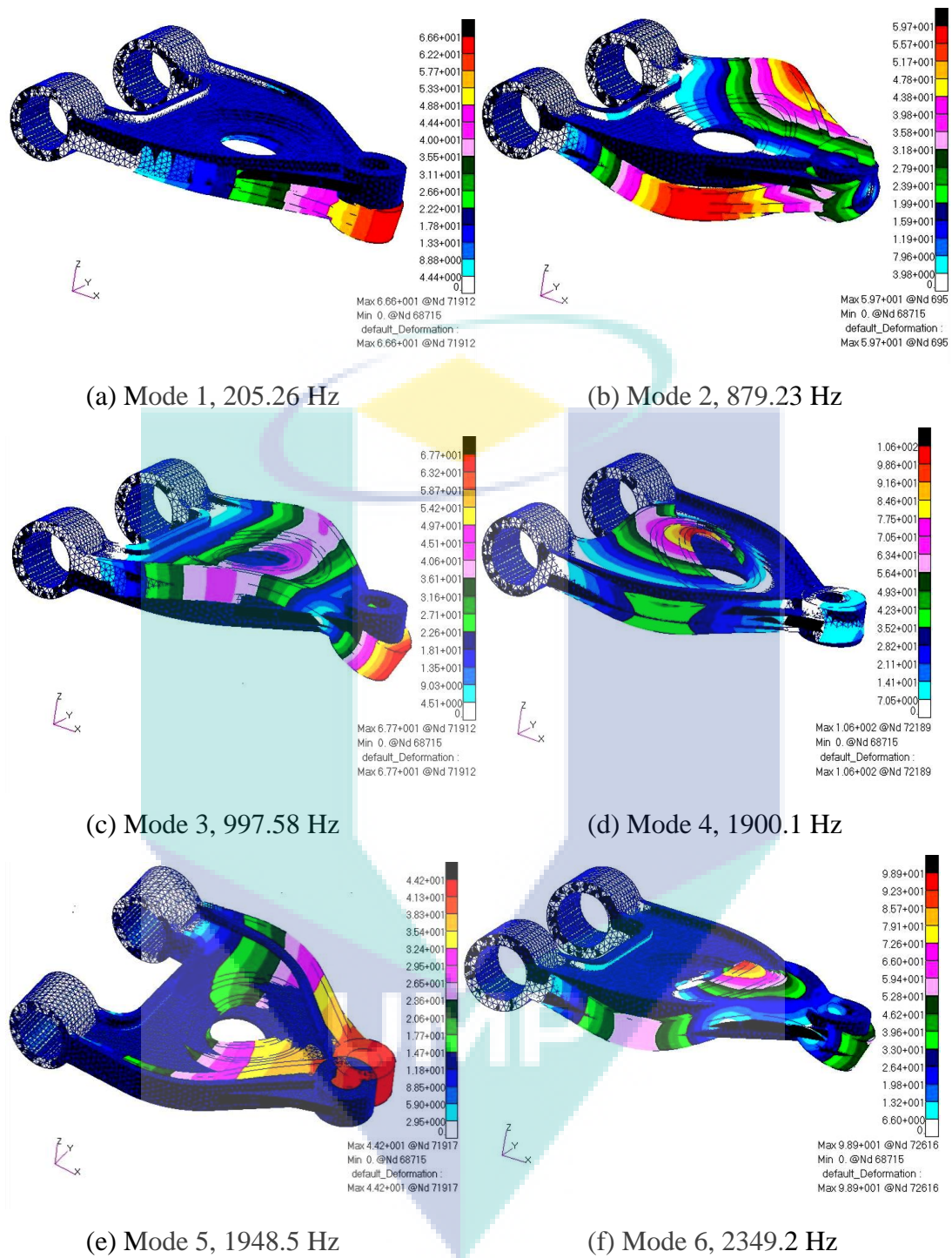


**Figure 4.8: Mode contour and mode shape**

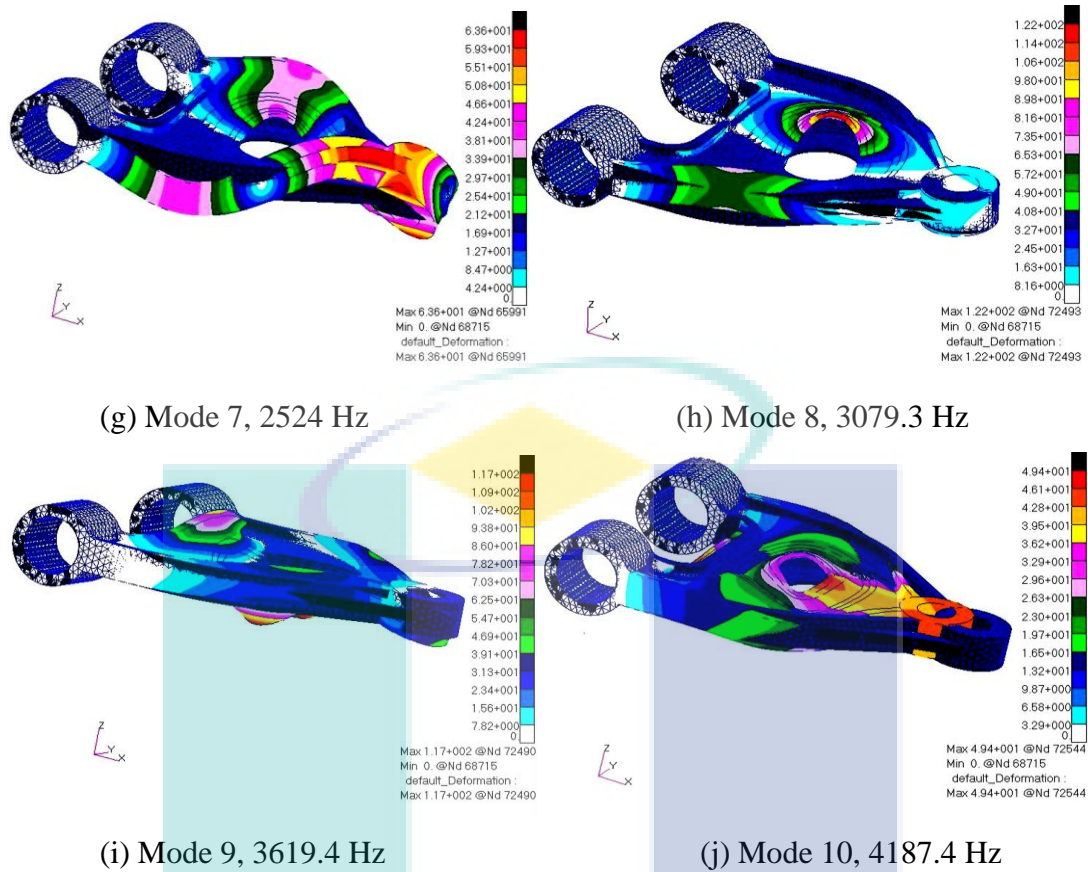


**Figure 4.8:** Continued

**Table 4.2:** Maximum displacements from modal analysis

Mode No	x-axis displacement ( $\mu\text{m}$ )	y-axis displacement ( $\mu\text{m}$ )	z-axis displacement ( $\mu\text{m}$ )
1	5.9362769	1.1423386	66.325012
2	9.1471920	18.259533	58.596310
3	18.282864	24.353616	65.195534
4	10.549701	18.638037	10.567502
5	8.2864723	44.226292	10.115671
6	20.041723	20.648651	98.877060
7	20.919615	36.880108	62.914886
8	12.581594	34.364082	122.16453
9	35.766823	21.469292	116.34058
10	45.454102	14.030432	34.420017

## 4.3 OPTIMIZATION TECHNIQUES

### 4.3.1 Response Surface Methodology

Suspension system produces unwanted outputs namely squeal for a set of input parameters. The present study was aimed to develop the input-output relationships for prediction of lower suspension arm response. In order to arrive at the most influential variables and its effects a phase strategy were proposed. RSM based on CCD was utilized to develop a linear model for prediction of lower arm response. RSM are used to estimate the transfer functions at the optimal region. Hence CCD approach was selected for the present study (Montgomery, 2005 and Wu and Hamad, 2000). The use of statistical design of experiment (DOE) techniques combined with FEA provides the engineering community with valuable tools for forecasting the behavior of a system or process. Aluminum alloys (AA7079-T6) are selected as suspension arm materials. The finite element analysis was performed utilizing the finite element analysis code. The finite element model is correlated with design of experiments modal test. Tetrahedral 10 nodes are used for constructing the finite element model. The convergence analysis has been carried out for selecting the optimum mesh size and global edge length. The linear static analysis is considered for stress analyses with applied ultimate load conditions to the parts during the driving. Table 4.3 shows the five ultimate load conditions of the lower arm. In light of the screening experiments, a decision was taken to study the effects of the top four factors namely the mesh size and load of directions. The variables and their levels are listed in Table 4.4. The strength analysis results under the five ultimate load conditions and each constraint were presented with the strain distributions are shown in Figure 4.9.

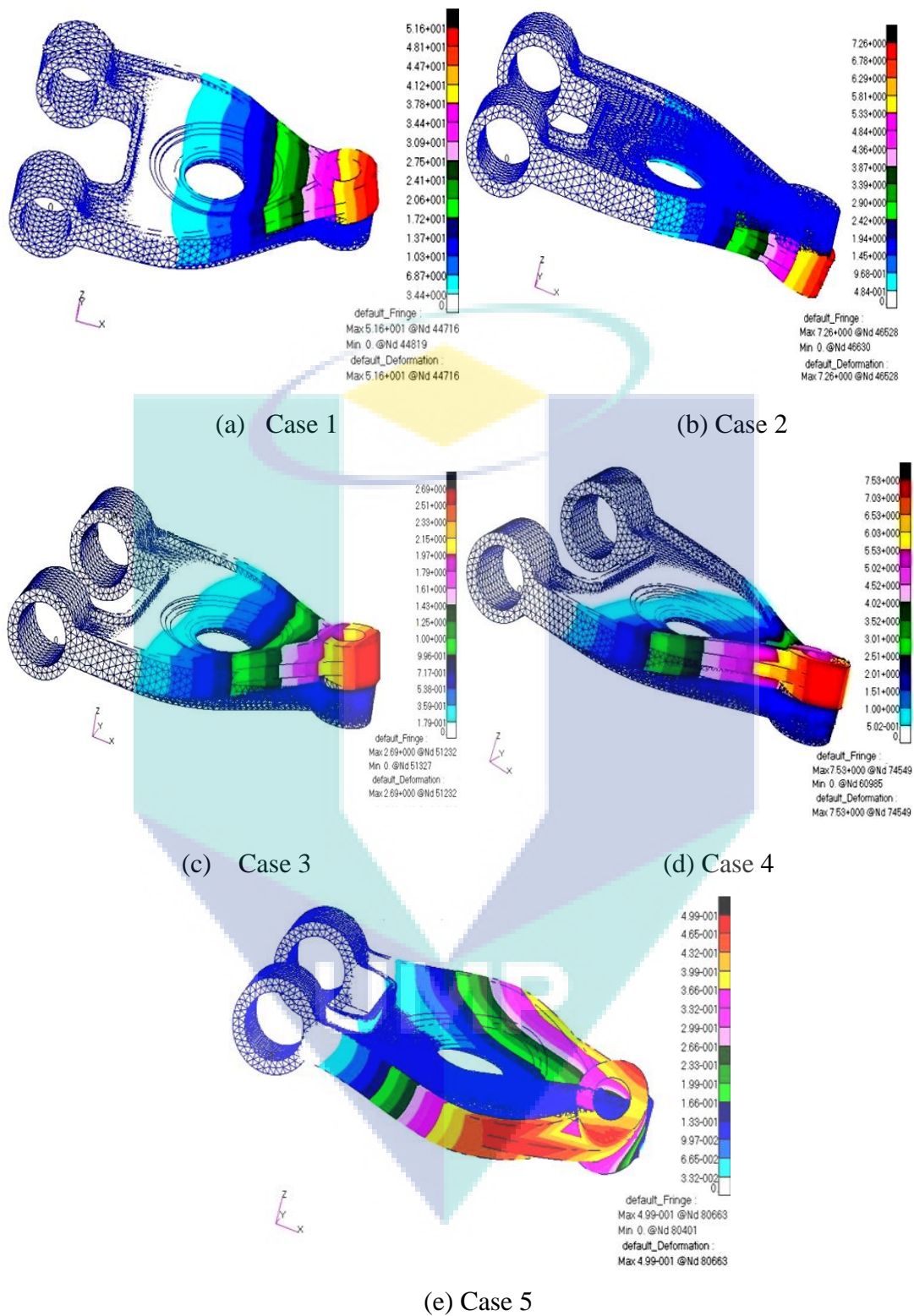


**Figure 4.9:** XY-directional strain distribution for various cases.

**Table 4.3:** Load conditions of lower arm

Case	Conditions	Load (N)		
		X	Y	Z
1	Pothole brake limit load	-5688.2	-4801.2	-60.4
2	Oblique kerb limit load	9579.7	2382.1	238.3
3	Pothole corner limit load	-1107.0	1108.3	197.6
4	Lateral kerb strike limit load	-549.7	12218.3	845.9
5	Ultimate vertical limit load	-573.7	-3408.9	-66.7

**Table 4.4:** Coded levels of variable and actual values for CCD

Factor			Level		
Coded	Uncoded	Units	Low	Center	High
A	Mesh size		5	6	7
B	Load X	N	-5688.2	7633.95	9579.7
C	Load Y	N	-4801.2	8509.75	12218.3
D	Load Z	N	-66.7	456.3	845.9

The analysis of variance (ANOVA) results are presented in Table 4.5. It can be seen that the model  $F$ -value of 8.29 implies the model is significant. There is only a 0.80% chance that a model could occur due to noise. Values of probability less than 0.0500 indicates model terms are significant. The significance model factors ( $C$ ,  $AC$ ,  $AD$ ,  $BC$  and  $CD$ ) are indicated in the Table 4.5. Values greater than 0.1000 indicate the model terms are not significant. Moreover, the design showed in significant lack of fit ( $F$ -value =3.83), which is desirable related to the pure error and this means there is a 11.78 % chance that lake of fit could have occurred due to noise. A mathematical prediction model has been developed based on the most influencing factors, and the validation simulation analysis proved its adequacy. The result aimed towards prediction of optimal lower arm design through the various factors of the suspension arm geometrical construction.

The response equation for von Mises and displacement in the coded form are developed based on the response surface method. The mathematical equation von Mises and displacement can be expressed in Eq. (4.1) and Eq. (4.2) respectively. The positive sign in front of the terms indicates the synergistic effect while the negative sign indicates the antagonistic effect.

**Table 4.5:** Analysis of variance (ANOVA) results

Source	DF	Sum of Square	F value	Prob > F	
Model	14	7546000	8.29	0.0080 *	significant
Mesh size, A	1	50	0.00076	0.9788	
Load x, B	1	53464.50	0.82	0.3996	
Load y, C	1	1322000	20.32	0.0041*	
Load z, D	1	840.50	0.013	0.9132	
AB	1	149000	2.29	0.181	
AC	1	747300	11.49	0.0147*	
AD	1	419600	6.45	0.0441*	
BC	1	713400	10.97	0.0162*	
BD	1	149900	2.30	0.1798	
CD	1	696800	10.71	0.0170*	
A <sup>2</sup>	1	10928.93	0.17	0.6961	
B <sup>2</sup>	1	261500	4.02	0.0918	
C <sup>2</sup>	1	364900	5.61	0.0556	
D <sup>2</sup>	1	2768.26	0.043	0.8434	
Residual Error	6	390300			
Lack-of-Fit	2	256400	3.83	0.1178	not significant
Pure Error	4	134000			

\* $p < 0.05$  indicate the term is significant

$$\begin{aligned}
 \text{von} \cdot \text{Mises} = & 296.96 - 5A - 163.5B + 363.6C + 20.5D + 305.12AB \\
 & + 305.62AC - 512.13AD + 298.63BC - 306.12BD - \\
 & 295.12CD - 65.43A^2 + 320.07B^2 + 378.07C^2 - 32.93D^2
 \end{aligned} \tag{4.1}$$

$$\begin{aligned} \text{Displacement} = & 0.012 - 0.00004A - 0.007B + 0.0077C + 0.0012D + \\ & 0.011AB + 0.009AC - 0.015AD + 0.009BC - 0.013BD - 0.009CD \end{aligned} \quad (4.2)$$

where  $A$  is mesh size  
 $B$  is load in  $X$  direction  
 $C$  is load in  $Y$  direction  
 $D$  is load in  $Z$  direction

Figure 4.10 presents the surface plot of von Mises stress with various load combinations. Figure 4.10 (a) shows that von Mises stress decreases with reduction of mesh size as well as increases of load  $X$ . It is observed Figure 4.10 (b) that, as the load  $Y$  increased the von Mises reduces on the other hand as the mesh size in combination decreasing. It is also noted that the near significance of  $A$  and  $C$  interaction. Figure 4.10 (c) shows that, as the mesh size is closer with decreases Load  $Z$  increased the von Mises and interaction of  $A$  and  $D$  confirms its significance on von Mises. Figure 4.10 (d) is observed that von Mises stress have significant interaction with load  $X$  and  $Y$  combinations. Figure 4.10 (e) shows that von Mises stress decreases with increases of load  $X$  in combination with Load  $D$  and interaction of  $B$  and  $D$  confirms that it is not significance on the von Mises output. Figure 4.10 (f) observed that increase in the load  $Z$  reduces the von Mises and it is much influence in  $C$  and  $D$  interaction.

Figure 4.11 presents the surface plot of displacement with various load combinations. Figure 4.11 (a) observed that decreased mesh size with increase load  $Z$  reduced the displacement. Surface plot of  $A$  and  $B$  interaction confirms its significance on the output. It is observed from the Figure 4.11 (b) that, increase in the mesh size in combination with increased load  $C$  reduces the displacement. Surface plot of  $A$  and  $C$  interaction confirms it's not significance on the output. From the Figure 4.11 (c) and 4.11 (e) it is observed that decrease in the mesh size with increase load  $Z$  increased the displacement and decrease load  $X$  with increase load  $Z$  increased displacement. Figure 4.11 (d) shows displacement reduced with increase load  $X$  combination with increase load  $Y$ . Surface plot of  $B$  and  $C$  interaction confirms its significance on the output. It is observed Figure 4.11 (f) that, as the load  $Y$  is closer with decreases load  $Z$

reduced the displacement. Surface plot of *C* and *D* interaction confirms its significance on the output.

The  $R^2$  analysis result is tabulated in Table 4.6. The Predict  $R$ -Squared of 6.5308 is in reasonable agreement with the Adjusted  $R$ -Squared of 0.8361. Adequate Precision measures the signal to noise ratio. A ratio greater than 4 is desirable; Model's ratio of 13.303 indicates an adequate signal. In fact, when the value of correlation coefficient  $R$  is close to 1, it means the response correlation FEA result and predicted values are good agreements with each other. Predicted residual sum of squares (PRESS) is a measure of how model fits each point in the design then the model estimate and calculate the residual.

**Table 4.6:**  $R^2$  analysis results

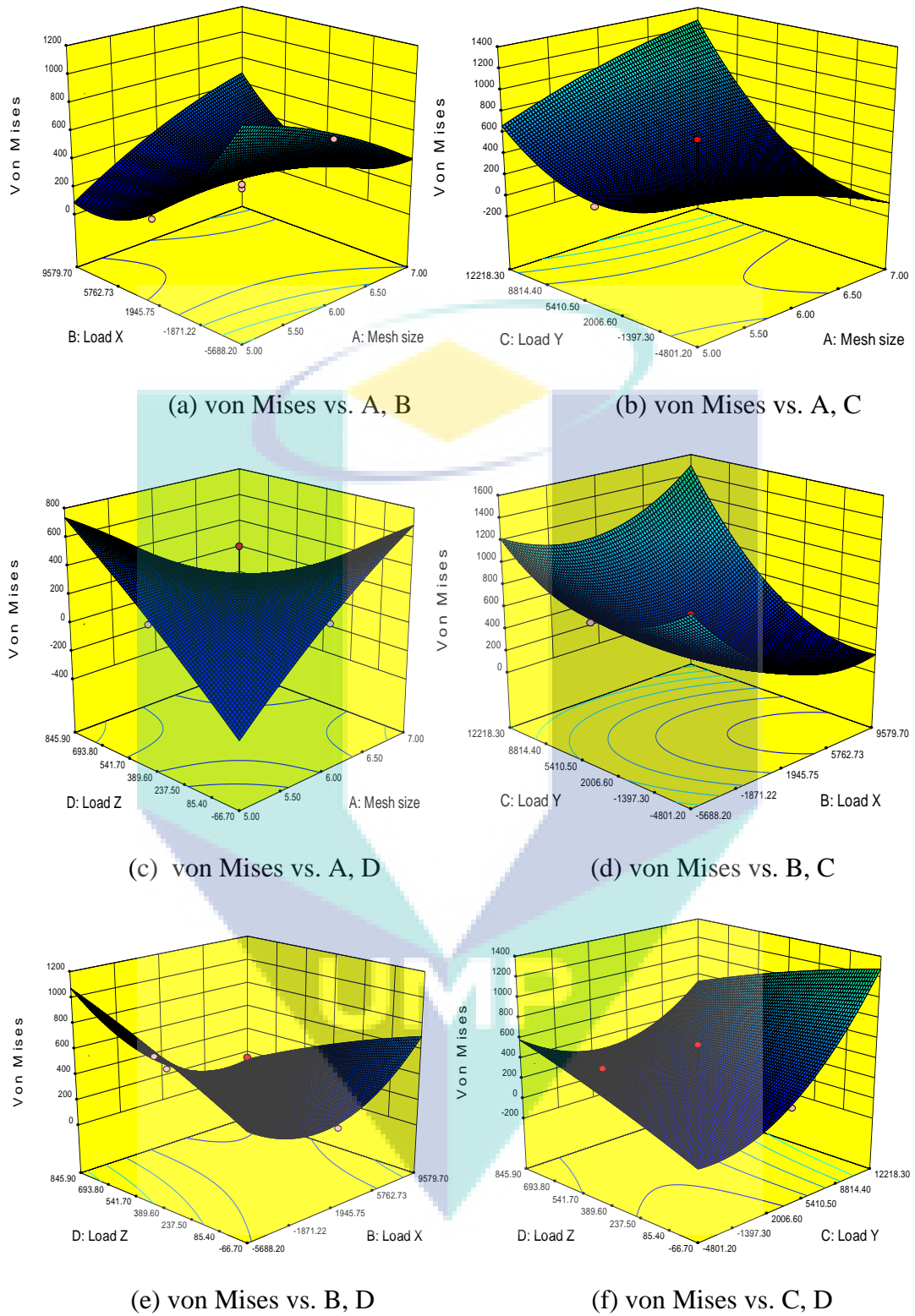
<b>Parameter</b>	<b>Value</b>	<b>Parameter</b>	<b>Value</b>
Std. Dev.	255.06	$R$ -Squared	0.9508
Mean	582.57	Adj $R$ -Squared	0.8361
C.V.%	43.78	Pred $R$ -Squared	6.5308
PRESS	5.977E+007	Adeq Precision	13.303

Table 4.7 lists the comparison between predicted versus FEA results. A total number of twenty one trials were conducted and a set of data was collected as per the structure of CCD of experiments and the table occurred the predicted responses from RSM shows good agreement with actual results also shows the deviation percentage and residual by response surface method versus the run number. Randomization provides insurance against autocorrelation and trends.

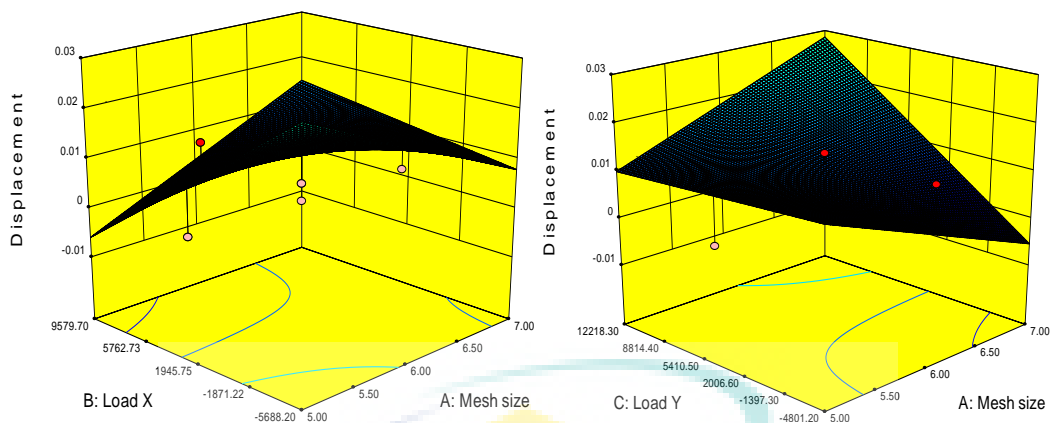
**Table 4.7:** Comparison between predicted versus FEA results

Run	A (N)	B (N)	C (N)	D (N)	FEA results (MPa)	Predicted RSM by DOE (MPa)	Residuals	% Deviation
1	5	-5688.20	-4801.20	-66.70	3180	3094	85.91	0.03
2	6	1945.75	3708.55	389.60	501	568.14	-67.14	13.4
3	7	1945.75	3708.55	389.60	726	640.09	85.91	11.83
4	7	-5688.20	12218.30	845.90	531	598.14	-67.14	12.6
5	6	1945.75	3708.55	845.90	422	489.14	-67.14	15.9
6	6	1945.75	3708.55	-389.60	672	586.09	85.91	12.7
7	6	1945.75	3708.55	-66.70	807	721.09	85.91	10.6
8	6	1945.75	3708.55	-389.60	410	477.14	-67.14	16.3
9	7	9579.70	-4801.20	-66.70	199	236.53	-37.53	18.6
10	7	-5688.20	-4801.20	845.90	189	226.53	-37.53	19.5
11	5	9579.70	12218.30	845.90	743	780.53	-37.53	4.9
12	7	9579.70	12218.30	-66.70	416	453.53	-37.53	8.89
13	6	1945.75	12218.30	389.60	580	311.43	268.57	46
14	6	1945.75	3708.55	389.60	695	1038.63	-343.63	49
15	6	1945.75	-4801.20	389.60	206	243.53	-37.53	17.9
16	6	1945.75	3708.55	389.60	247	284.53	-37.53	14.9
17	5	9579.70	-4801.20	845.90	542	500.24	245.04	7.7
18	5	1945.75	3708.55	389.60	188	296.96	-108.96	57
19	6	9579.70	3708.55	389.60	219	296.96	-77.96	35
20	6	-5688.20	3708.55	389.60	542	515.05	245.04	4.98
21	5	-5688.20	12218.30	-66.70	219	296.96	-77.96	35

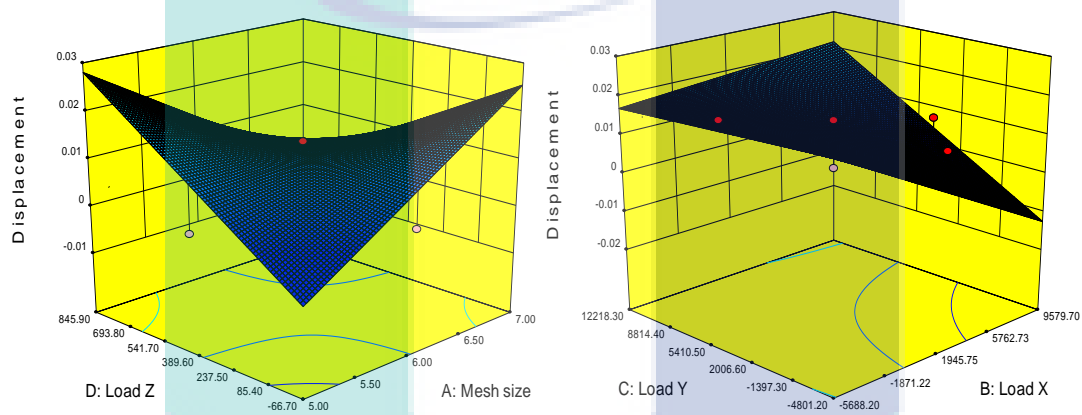
% of deviation = [(actual value – predicted value)/ actual value] × 100%



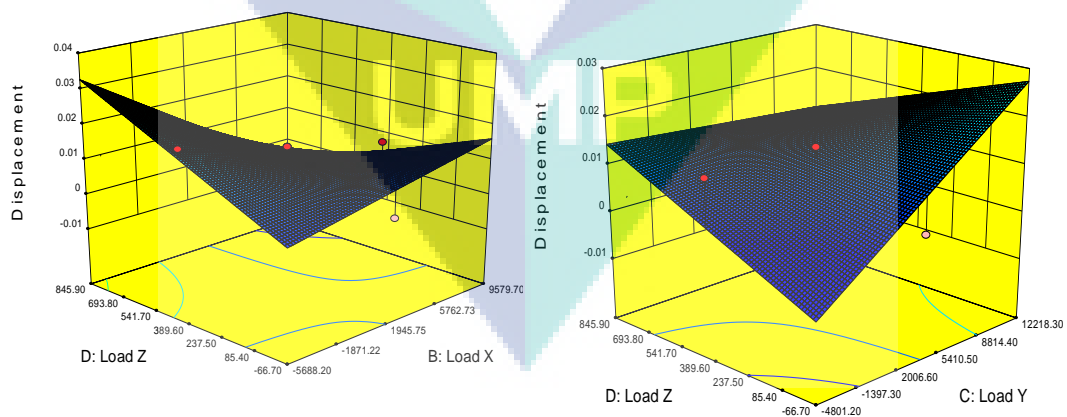
**Figure 4.10:** 3D Surface plots for the response of von Mises against load and mesh size



(a) Displacement for loading A and B      (b) Displacement for loading A and C



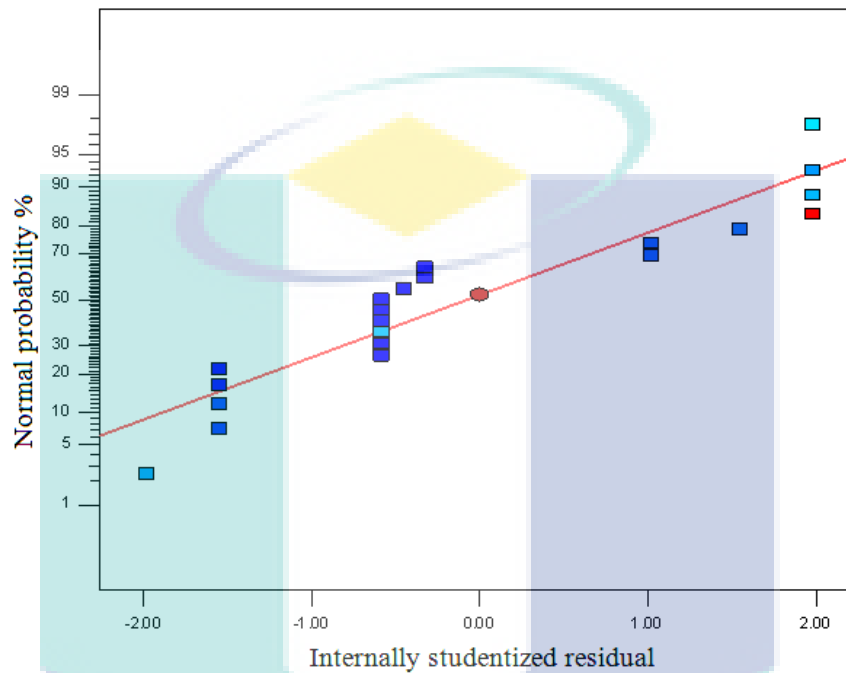
(c) Displacement for loading A and D      (d) Displacement for loading B and C



(e) Displacement for loading B and D      (f) Displacement for loading C and D

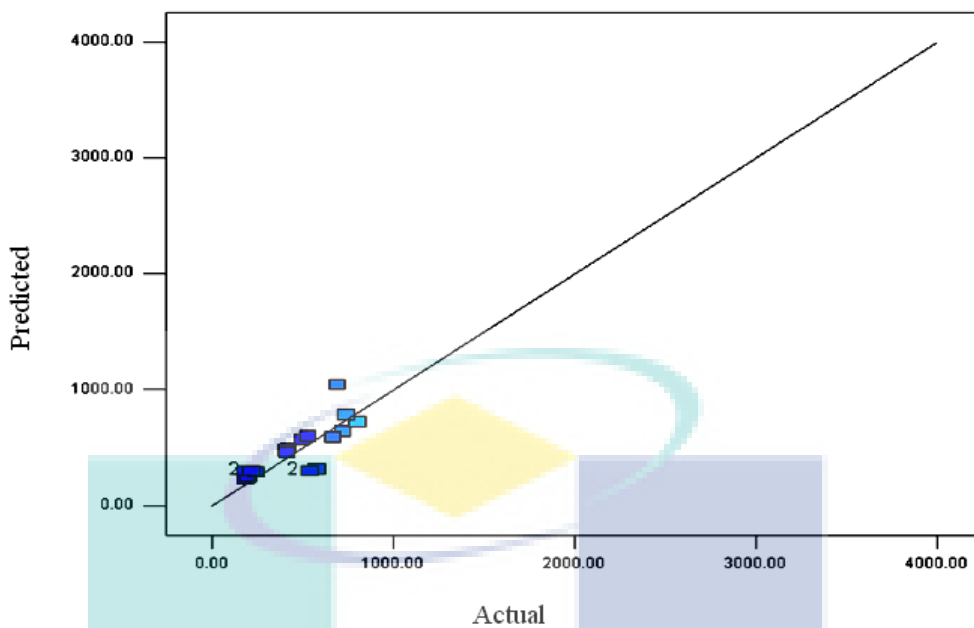
**Figure 4.11:** 3D Surface plots for the response of displacement against load and mesh size

Figure 4.12 shows the normal probability plot of residuals. It shows that there is no abnormality in the methodology adopted ( $R^2 = 0.9508$ ). The statistical analysis shows that, the developed linear model based on central composite design is statistically adequate and can be used to navigate the design space.

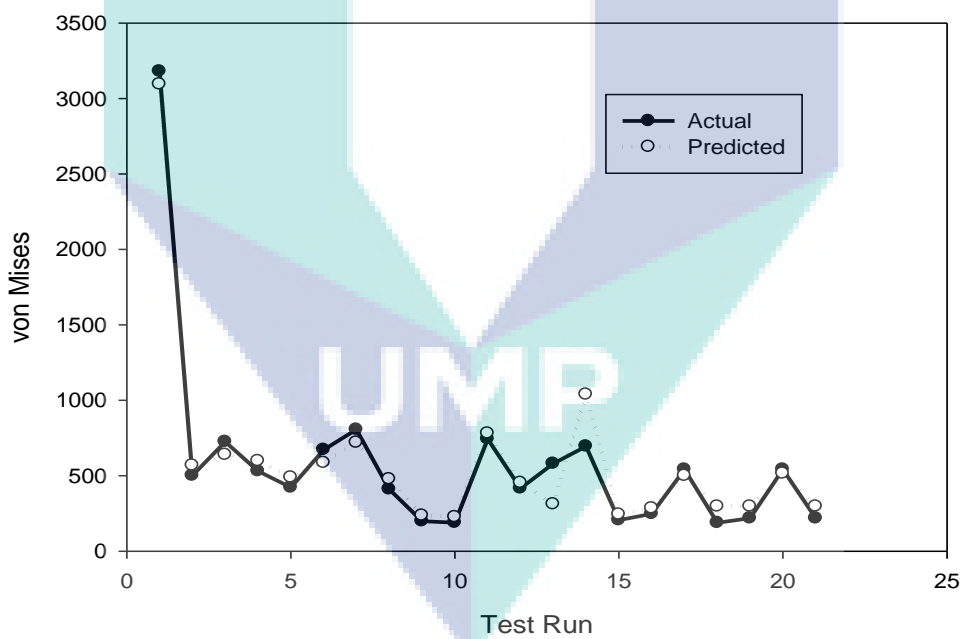


**Figure 4.12:** Normal probability plot of residuals

Figure 4.13 shows the predicted versus actual plot how the model predicts over the range of data. The best fit line plot (Figure 4.13) of the 21 points (Table 4.7) is found to be close to the ideal line ( $Y = X$ ). The predicted responses show the good agreement with actual results. The scatter shows the bowling scores can be predicted very precisely. The graphical presentation of predicted versus FEA results is presents in Figure 4.14. The average absolute residuals were found to be 194.978 and actual results varied between 268.57 and -343.63 from predicted responses. Distinct patterns indicating autocorrelation.



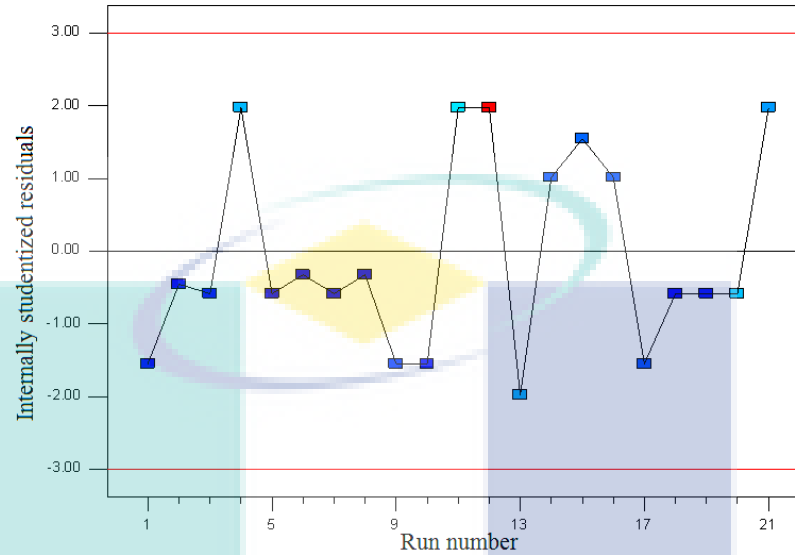
**Figure 4.13:** The best fit line plot



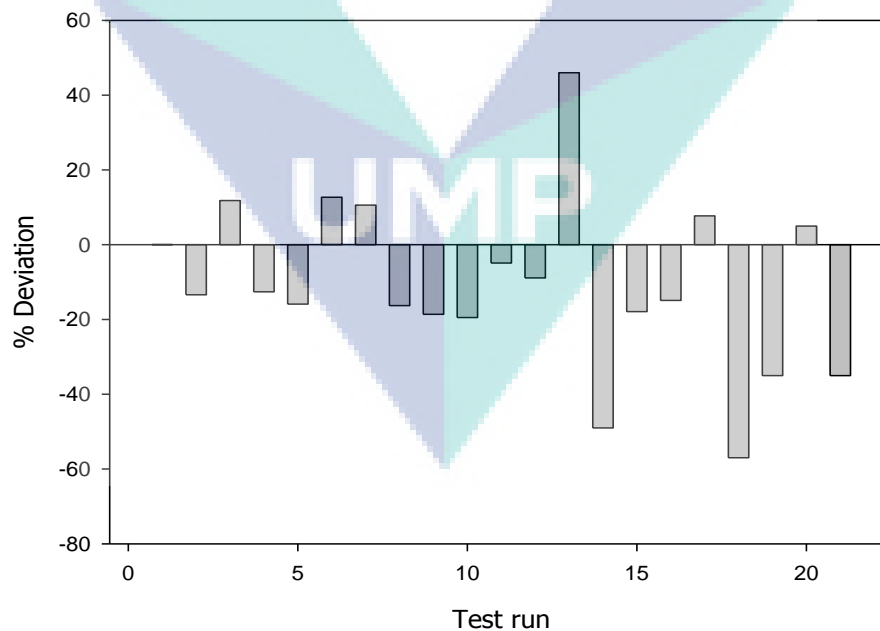
**Figure 4.14:** Predicted versus actual simulation

Figure 4.15 shows the residuals versus the run number. Randomization provides insurance against autocorrelation and trends. This indicates that designed model space can be navigated for prediction. Figure 4.16 shows the percentage of the deviation plot of FEA results. The average absolute percentage deviation is found to be 19.65.

However, predicted responses varied between -57 and 46. This indicates that designed model space can be navigated for prediction.



**Figure 4.15: Residuals versus Run**



**Figure 4.16: Percentage deviation of FEA results**

The use of statistical design of experiment techniques combined with FEA provides the engineering community with valuable tools for forecasting the behavior of a system or process. A new approach to investigate the influencing factors of the lower suspension arm by integrating finite element analysis results with the central composite design approach has been presented. This combined approach is useful in the design stage of the suspension arm. The combined approach of modeling lower suspension arm using FEM and RSM is found to be statistically adequate through verification trials.

#### 4.3.2 Artificial Neural Network

Neural network investigated and presented influences of the artificial intelligent on the response suspension lower arm. The finite element analysis and RBFNN technique are used to predict the response of suspension arm. Finite element techniques have been used as a tool to model the suspension arm in conjugation with RBFNN modeling. Figure 4.17 shows the model of RBFNN approach for stress analysis. In the present study, inputs are selected as load and mesh size. The NN outputs have been termed as the maximum displacement, maximum principal stress, von Mises and Tresca. Figure 4.18 and 4.19 show the comparison between the FEM and RBFNN result for displacement and stress respectively. Table 4.8 shows the output from FEM and the RBFNN and the Error of RBFNN with respect to FEM method is presented in Table 4.9

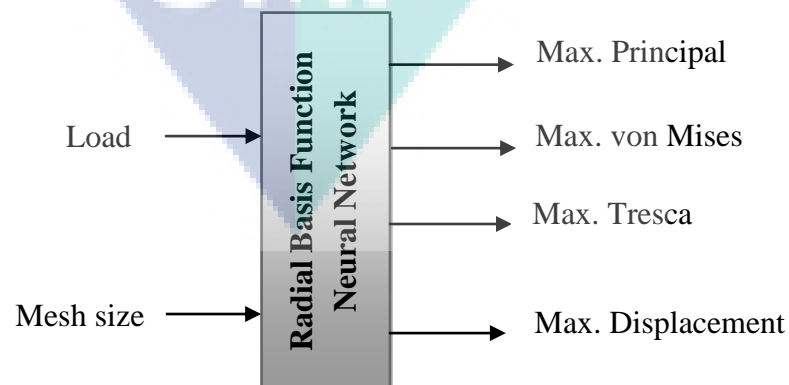


**Figure 4.17:** Model of RBFNN approach for stress analysis

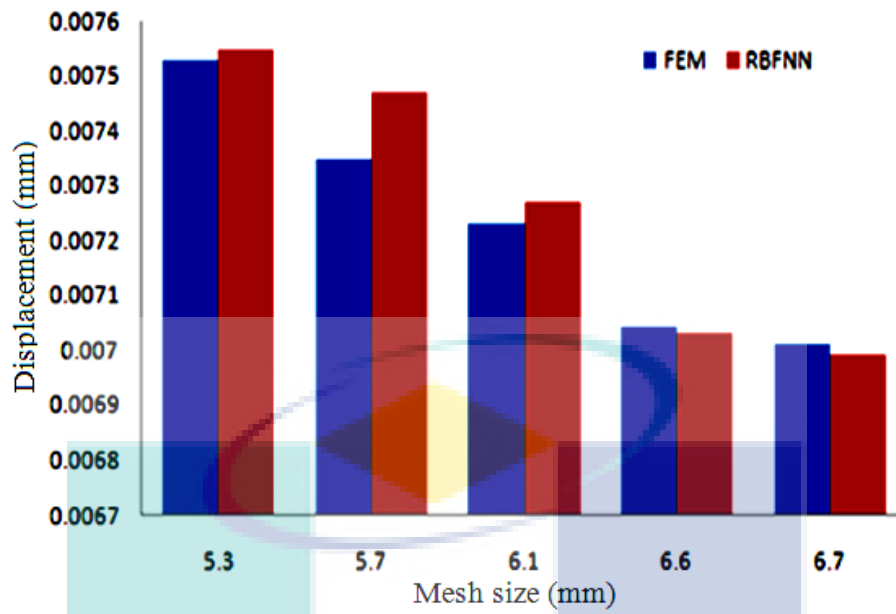


Figure 4.18: FEM and RBFNN displacement

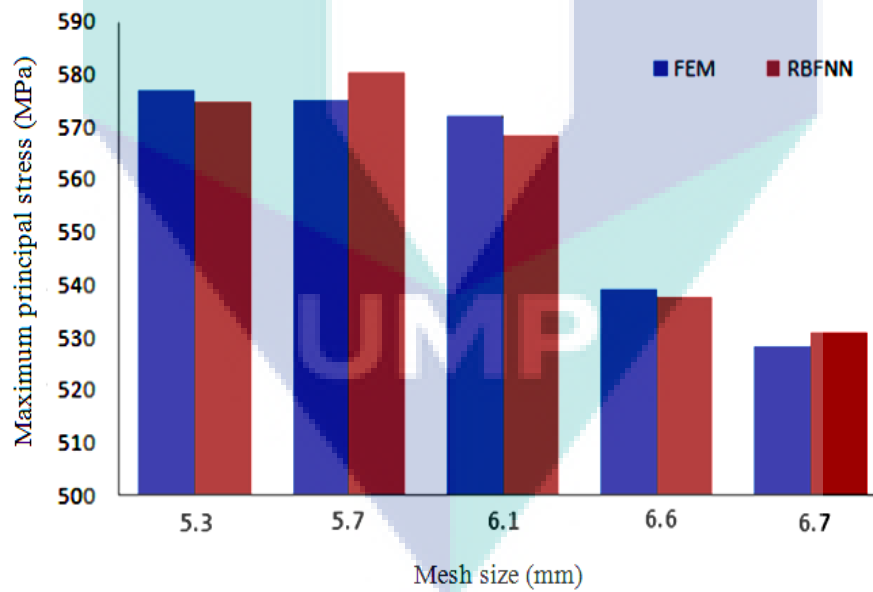


Figure 4.19: FEM and RBFNN maximum principal stress

**Table 4.8:** Output from FEM and RBFNN techniques

Mesh Size (mm)	FEM				RBFNN			
	Disp. $\times 10^{-3}$ (mm)	max. principal stress (MPa)	Tresca (Mpa)	Von Mises (MPa)	Disp. $\times 10^{-3}$ (mm)	max. principal stress (MPa)	Tresca (MPa)	Von Mises (MPa)
5.3	7.53	577	574	561	7.55	574.6	572.8	560.8
5.5*	-----	-----	-----	-----	7.532	579.7	565.7	554.0
5.7	7.35	575	553	544	7.47	580.2	555.6	544.4
5.9*	-----	-----	-----	-----	7.382	576.2	544.2	533.5
6.1	7.23	572	535	523	7.27	568.2	533	522.9
6.4*	-----	-----	-----	-----	7.124	550.8	519.9	510.3
6.6	7.04	539	515	506	7.03	537	514.6	505.2
6.7	7.01	528	512	503	6.99	530.6	513	503.7

**Table 4.9:** Error RBFNN

Mesh size	Displacement ( $\mu\text{m}$ )		Error in percentage		
	based on FEM		Max. principal stress	Tresca	von Mises
5.3	0.02		2.4	1.2	0.2
5.7	0.12		5.2	2.6	0.4
6.1	0.04		3.8	2	0.1
6.6	0.01		1.6	0.4	0.8
6.7	0.02		2.6	1	0.7

This study includes investigating influences of the artificial intelligent on the response suspension lower arm by using RBFNN to predict dynamic analysis. Figure 4.20 shows the model of RBFNN for dynamic analysis. NN inputs are selected as load and natural frequency. The NN outputs have been termed as the maximum displacement in the direction  $x$  ( $T_1$ ), maximum displacement in the direction  $y$  ( $T_2$ ) and maximum displacement in the direction  $z$  ( $T_3$ ). Comparison results between FEM and RBFNN technique are tabulated in Table 4.10. It can be seen that the RBFNN technique was found to be highly effective with least error and Table 4.10 in identification of stress

and dynamic-displacement of suspension arm (Abdullah, 2009; Wannas and Abd, 2008; Wannas, 2008).

By comparing the results from Table 4.8 and 4.10 (asterisk value) it can be observed the efficiency of NN very successively used for the enhanced navigational performance, error reduction and time required predicting the stress-displacement and dynamic-displacement response of suspension arm with few workloads of processing (test and training).

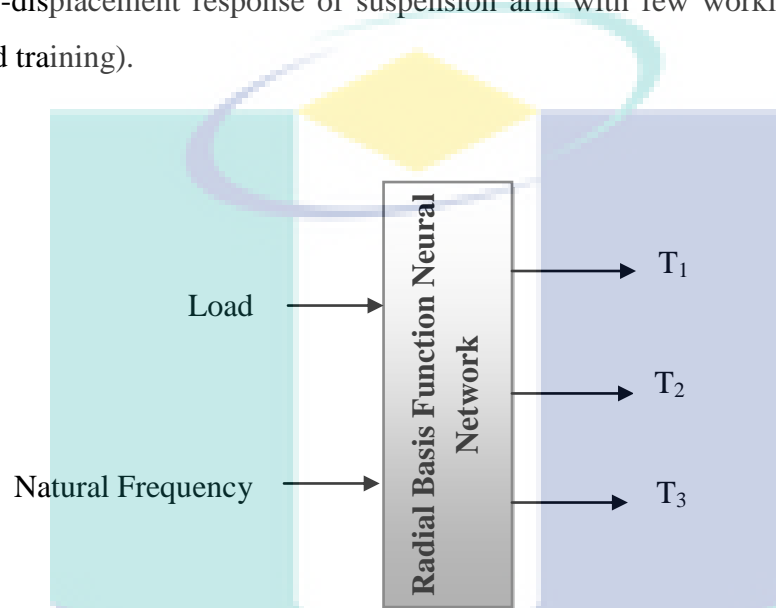


**Figure 4.20:** Model of RBFNN approach for suspension arm

This approach found to be highly effective in identification of linear response of suspension arm and it has been used of more realistic linear and nonlinear problems in order to obtained quickly solutions and with few workloads of processing. Finally, this technique shows highly effective depends upon its accuracy, speed and memory requirements in identification of stress-displacement of suspension arm.

**Table 4.10:** Output from dynamic analysis and RBFNN techniques

Mode No	Natural Frequency (hz)	Dynamic analysis (FEM)			RBFNN		
		$T_1(\mu\text{m})$	$T_2(\mu\text{m})$	$T_3(\mu\text{m})$	$T_1(\mu\text{m})$	$T_2(\mu\text{m})$	$T_3(\mu\text{m})$
1	205.26	5.9362769	1.1423386	66.325012	5.94	1.14	66.33
	500*	-----	-----	-----	3.58	14.51	54.60
2	879.23	9.1471920	18.259533	58.59631	9.15	18.26	58.6
3	997.58	18.282864	24.353616	65.195534	18.28	24.35	65.2
	1500*	-----	-----	-----	3.58	14.54	54.57
4	1900.1	10.549701	18.638037	10.567502	10.55	18.64	10.57
5	1948.5	8.2864723	44.226292	10.115671	8.29	44.23	10.12
6	2349.2	20.041723	20.648651	98.877060	20.04	20.65	98.88
7	2524*	20.919615	36.880108	62.914886	20.92	36.88	62.91
	2800*	-----	-----	-----	3.70	14.74	54.89
8	3079.3	12.581594	34.364082	122.16453	12.58	34.36	122.16
9	3619.4	35.766823	21.469292	116.34058	35.77	21.47	116.34
	3800*	-----	-----	-----	6.94	15.27	61.01
10	4187.4	45.454102	14.030432	34.420017	45.45	14.03	34.42

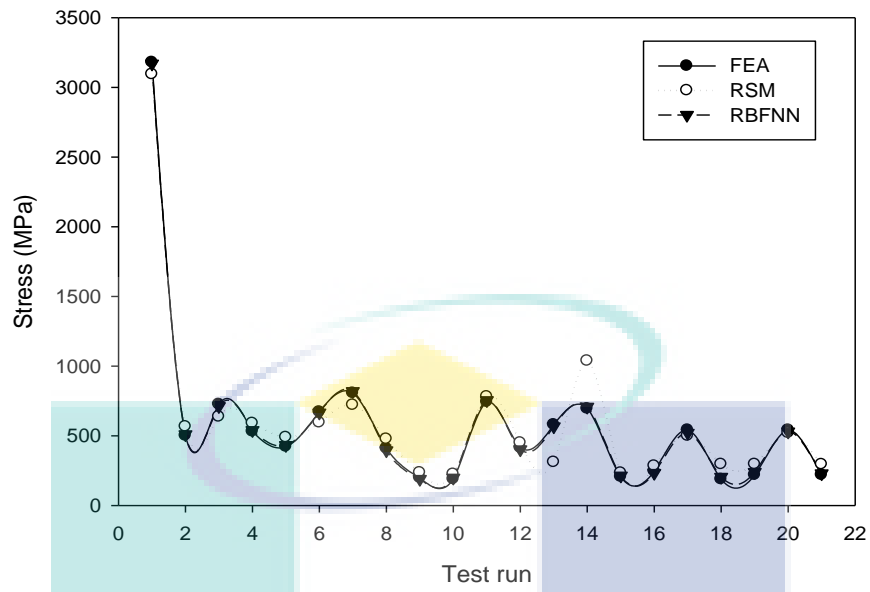
### ***Comparison between RBFNN and RSM Techniques***

After determining the surface response method equations of all the response variables and also neural network program, the prediction by both techniques was compared. Table 4.11 lists the comparison between predicted versus FEA results. The predicted responses show the good agreement with actual FEA results. Figure 4.21(a, b) shows the stress-displacement comparison between the predicted values for RSM, RBFNN and FEA result. All the three methods are in closely agreement with each other; Figure 4.22 shows the deviation percentage by neural network and response surface method. Figure 4.23 shows the residuals by neural network and response surface method versus the run number. Randomization provides insurance against autocorrelation and trends. From these Figures (4.21, 4.22, 4.23) clearly the response surface method is quite close to the prediction value of the neural network. Neural network predicted more accurate compared with RSM. The error for both techniques

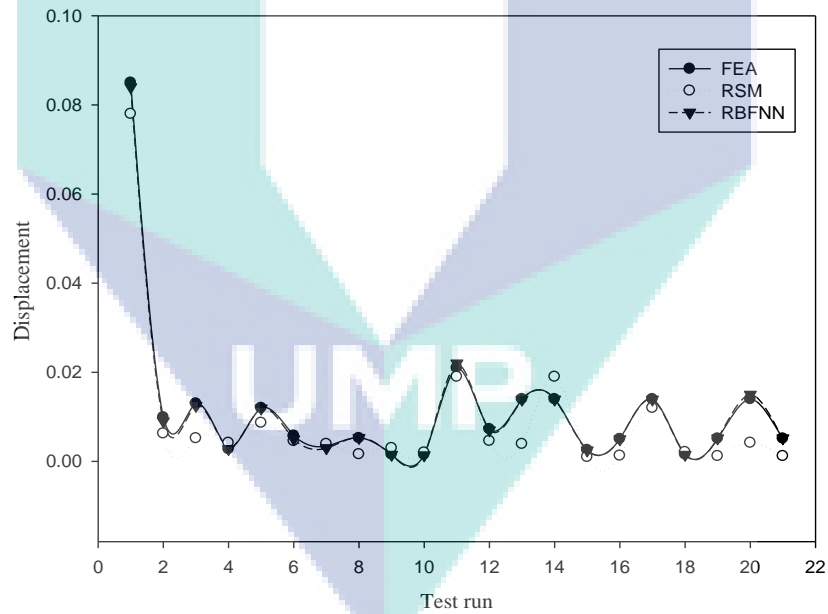
can be accepted and the model of the response surface method indicates that designed model space can be navigated for prediction.

**Table 4.11:** RSM and RBFNN techniques prediction stress-strain for suspension arm

No	A	B	C	D	Stress			Displacement		
					FEA results	Predicted by RSM	Predicted by RBFNN	FEA results	Predicted by RSM	Predicted by RBFNN
1	5	-5688	-4801	-66	3180	3094	3170	0.085	0.078	0.084
2	6	1945	3708	389	501	566	510	0.00991	0.006282	0.009
3	7	1945	3708	389	726	637	712	0.013	0.005199	0.0125
4	7	-5688	12218	845	531	590	540	0.00276	0.00417	0.0028
5	6	1945	3708	845	422	489	433	0.012	0.008672	0.0119
6	6	1945	3708	-389	672	595	666	0.00581	0.00459	0.005
7	6	1945	3708	-66	807	721	820	0.00347	0.003931	0.003
8	6	1945	3708	-389	410	477	395	0.00524	0.001612	0.0053
9	7	9579	-4801	-66	199	236	190	0.00158	0.003	0.0015
10	7	-5688	-4801	845	189	225	199	0.0015	0.002	0.0014
11	5	9579	12218	845	743	781	755	0.021	0.019	0.022
12	7	9579	12218	-66	416	450	402	0.00725	0.004597	0.007
13	6	1945	12218	389	580	311	567	0.014	0.003925	0.0139
14	6	1945	3708	389	695	1038	708	0.014	0.019	0.0139
15	6	1945	-4801	389	206	234	214	0.00258	0.0010	0.0025
16	6	1945	3708	389	247	284	233	0.00504	0.0013	0.005
17	5	9579	-4801	845	542	500	521	0.014	0.012	0.0139
18	5	1945	3708	389	188	296	205	0.00156	0.0021	0.0015
19	6	9579	3708	389	219	296	240	0.00513	0.0012	0.0052
20	6	-5688	3708	389	542	520	530	0.014	0.0042	0.015
21	5	-5688	12218	-66	219	295	230	0.00513	0.0012	0.0052

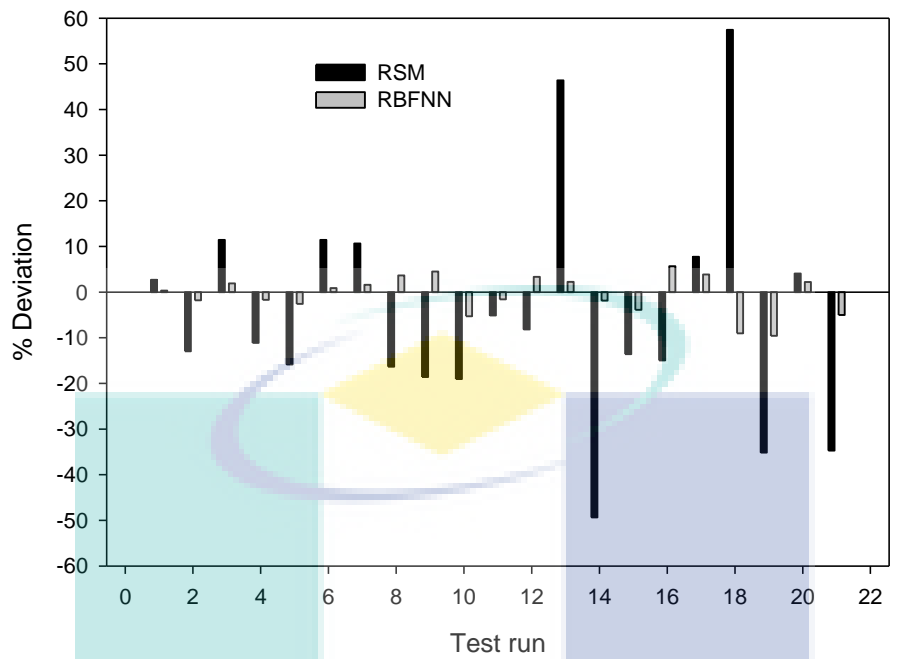


(a) Stress value

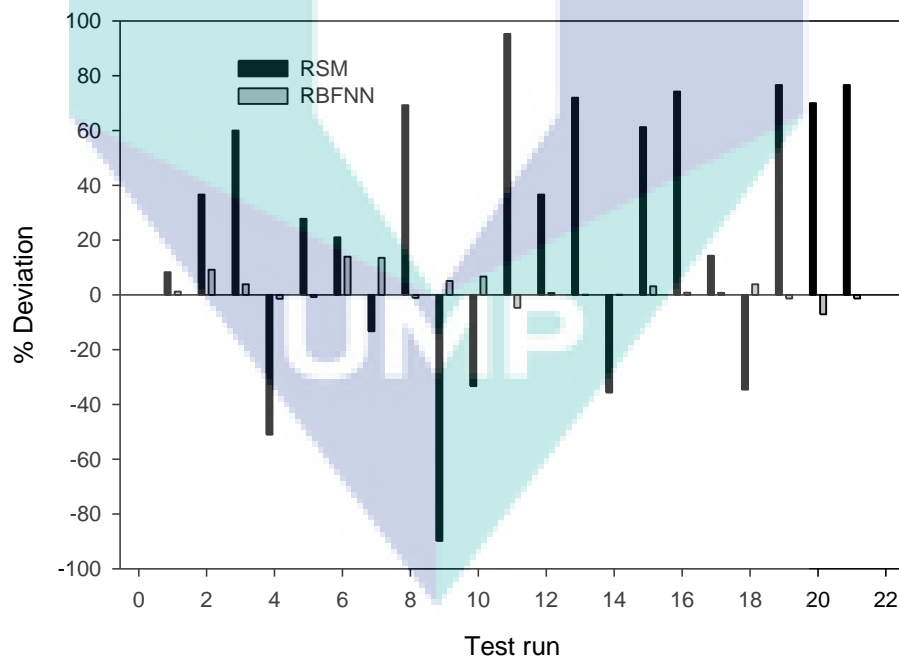


(b) Displacement value

**Figure 4.21:** Comparison of RSM models and RBFNN against experimental values (FEA)

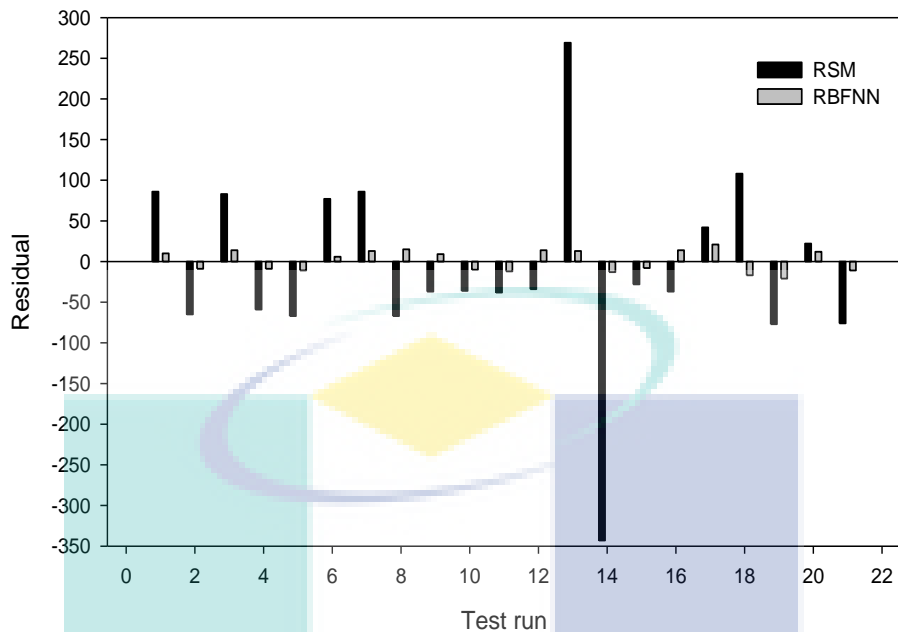


(a) Stress percentage deviation

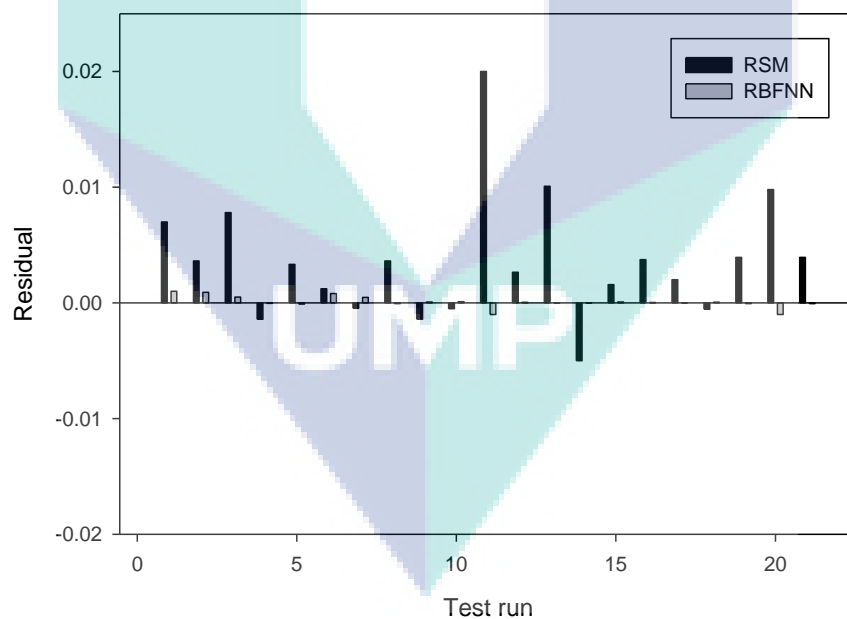


(b) Displacement percentage deviation

**Figure 4.22:** Percentage deviation by neural network and response surface method



(a) Stress residual



(b) Displacement residual

**Figure 4.23:** Residual by neural network and response surface method

Statistical techniques together with good engineering knowledge usually lead to sound conclusions. The response surface method and neural network have been proven to be a successful technique to perform the trend analysis of lower suspension arm,

statistically adequate and can be used to navigate the design space. Radial basis function neural network has very attractive properties and can be used for the enhanced navigational performance and error reduction of the effort and time required to determine the stress-displacement response of lower suspension. By applying central composite design while designing the suspension system, corrective and iterative design steps can be initiated and implemented for betterment of component design. Both RSM and neural network models reveal that power requirement is the most significant design variable in determining the stress-strain response as compared to other parameters. With the model equations obtained, a designer can subsequently select the best combination of design variables for achieving optimum lower suspension arm. Continued research in this direction can bring about more comprehensive and appropriate guide lines for designers and able to solve many problems that have mathematical and time difficulties.

#### **4.3.3 Robust Design using SDI**

A stochastic simulation generates multiple scenarios of a model by repeatedly sampling values from the probability distributions for the uncertain variables. Sometimes, very small changes in apparently insignificant variables can lead to collapse. Figure 4.24 shows the decision map (DM) which enabling to easily explore and gain a quick understanding on how different variables influence the functioning of the lower suspension arm and displaying the significant variables and correlations. However, DM shows concentrate an effort of the variables consisting of 4 inputs (load, modulus of elasticity, Poisson ratio, and density) on the lower suspension arm are significant. This means that only these inputs influence the outputs significantly.

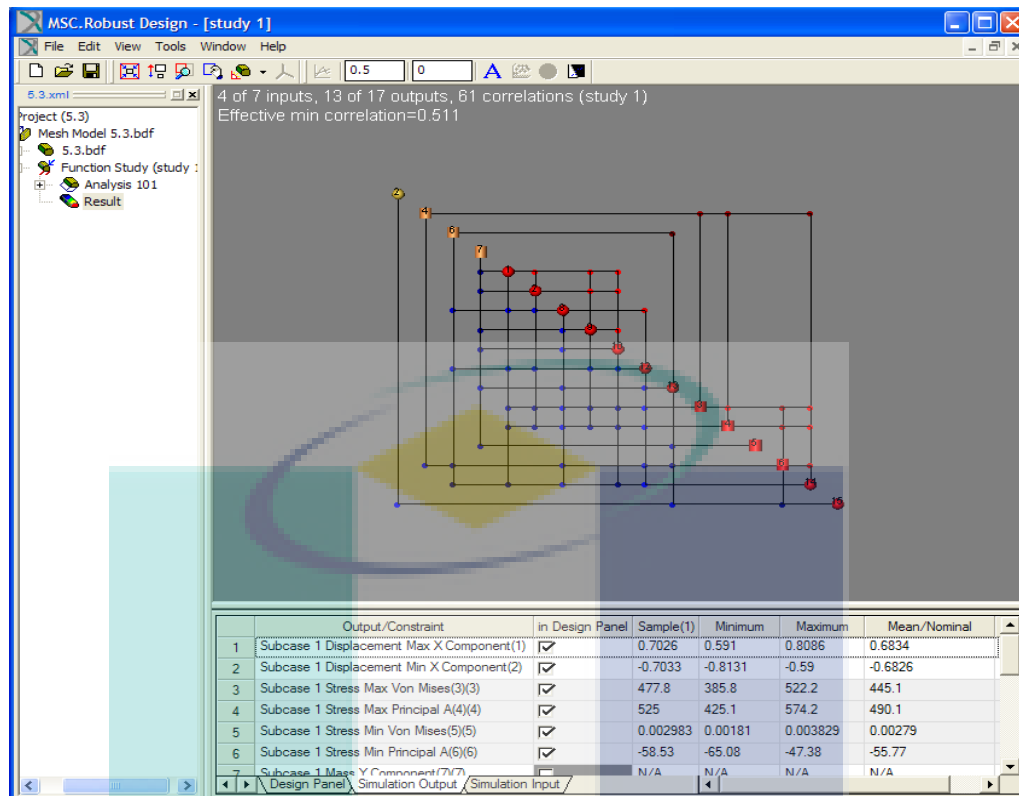
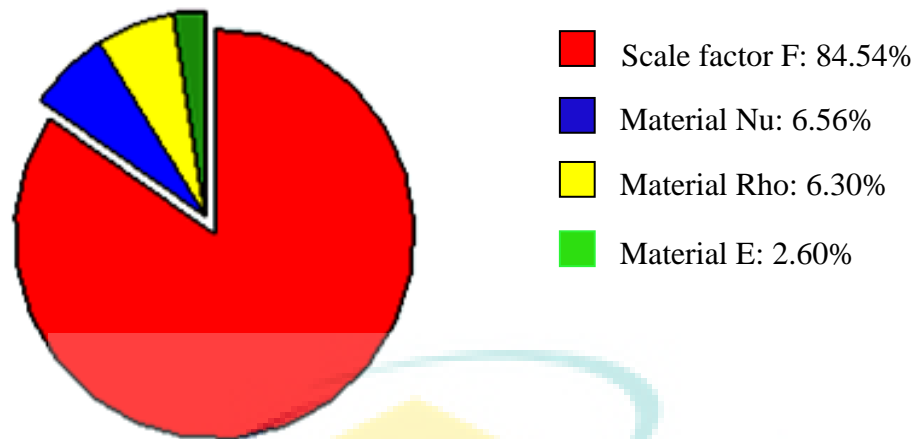


Figure 4.24: Decision map

The relative influence of tolerances in input variables on the scatter in a particular functionality (output) can be obtained. It can be seen from Figure 4.25 that the relative importance of all the variables. The pie chart shows that the load has the largest influence on the stress value followed by the Poisson ratio, density and modulus of elasticity respectively. The specific results of the influence of the variables can be seen in the ant hill scatter plots as shown in Figure 4.26-4.27. In fact, the correlation between stress and modulus of elasticity is not clear while similar relation confirms between stress and Poisson ratio.

Figure 4.26 shows ant hill scatter for stress against materials. It can be seen that there is less interaction (correlation) between them. This confirms the pie chart result that the Poisson ratio is a less factor in the stress value. Linear and non-linear correlation between them are obtained negative (linear cor. = -0.077 and non-linear cor. = -0.055).



**Figure 4.25:** Influence factors to the stress value

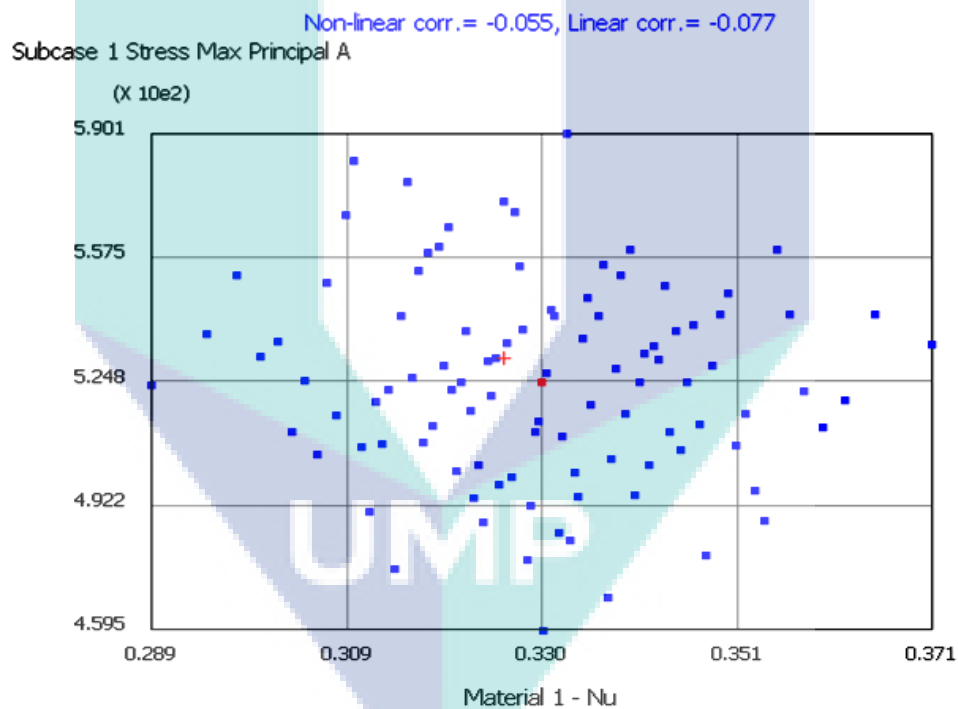


**Figure 4.26:** Ant hill scatter plot for stress versus material

Figure 4.27 shows the Ant hill correlation between the maximum principal stress and von Mises stress versus load scale factor. It can be seen that the stress and load scale factor are strongly correlation between them (linear cor. = 0.998, non-linear = 0.997 for maximum principal stress and linear cor. = 0.991, non-linear = 0.988 for von Mises stress). It is to be more dominant that's confirming the result in the pie chart Figure 4.25.

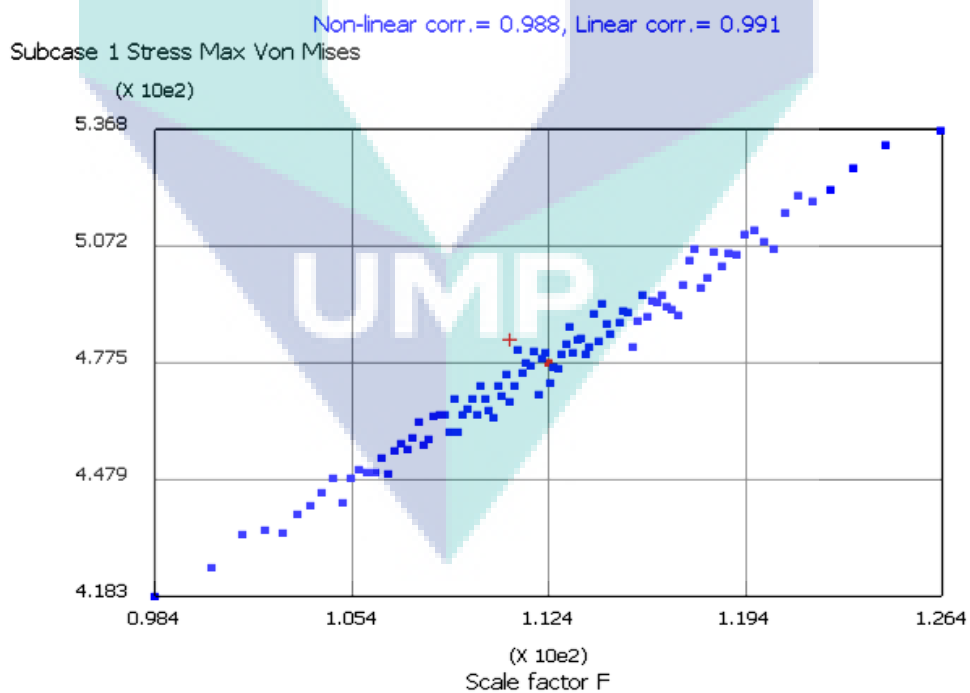
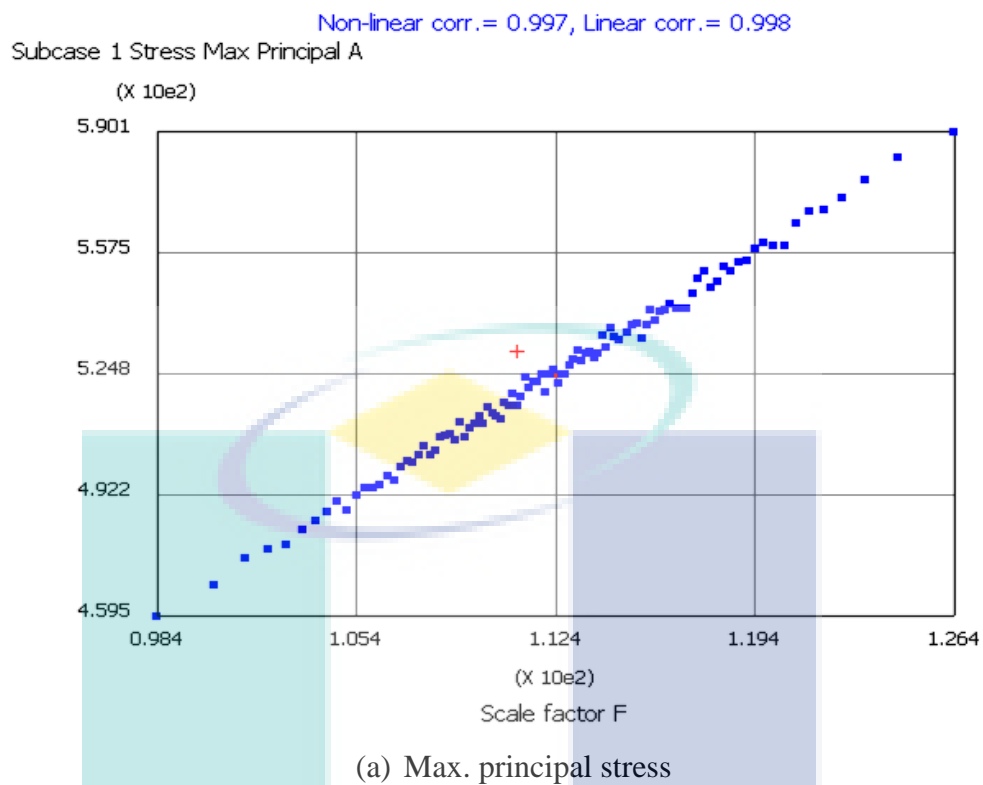


**Figure 4.27:** Ant hill scatter plot for stress versus load scale factor

These Ants Hill plots confirm the results from the variable ranking pie chart and convey much about the correlation between the variables that there is a positive correlation for the force magnitude and max principal stress in the model structure. As expected, the stress increases as the force increases. Essentially no correlation is seen between Poisson ratio and the max principal stress in the model structure. Conclude to obtain of stochastic simulation to reduce the complexity in modeling reality by addresses uncertainty and variation that establishes credibility in modeling and simulation, focuses on robustness instead of optimization through no assumptions of continuity and takes all inputs into account instead of needing initial assumptions.

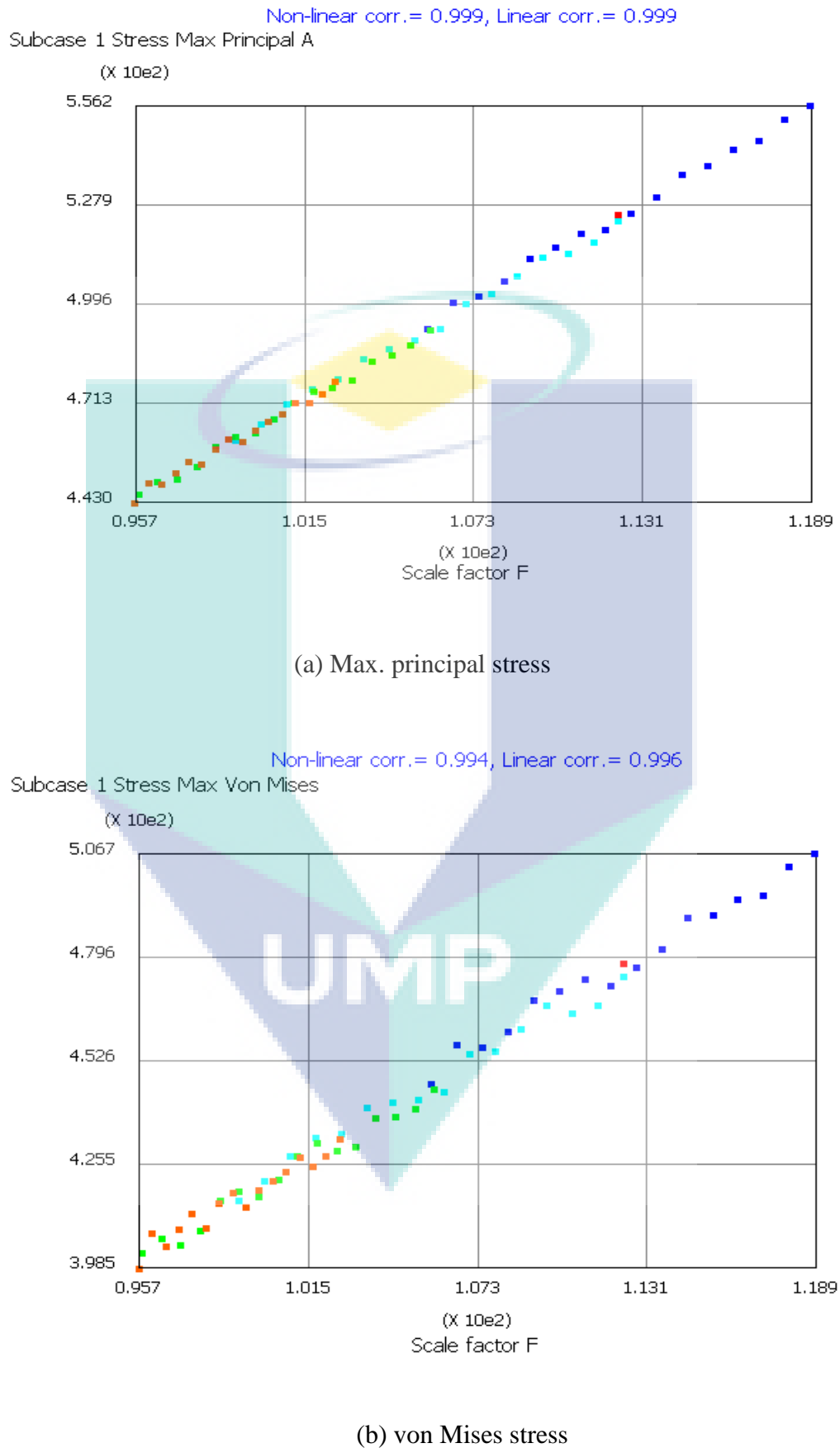
Stochastic design improvement is one of the tools to achieve the design improvement with the influence of tolerances. The goal is to minimize the effect of the stress on the model by varying the material of suspension arm. The stochastic design improvement process is very efficient to improve a system design. Typically, 5 iterations are sufficient for reasonable targets and variables that can be controlled and specified are used as design variables. The optimization processes for the design has been set to minimize stress on the lower suspension arm as the objective function and the design variables are set as the modulus of elasticity, Poisson ratio, density and load. von Mises stress (561 MPa) and maximum principal stress (577 MPa) are selected as constraints of the lower arm. The results of SDI show that there are multiple samples from the ant hill scatter plot that give the value of the parameter to use in the optimization process. The outcome from the SDI had been selected and it is listed in Table 4.12.

Figure 4.28 shows that the lower arm design has a higher capability to stand higher factor force as 118.9 ( $x, y, z$  factor load) with the maximum principal stress (556.2 MPa) acted on the lower arm while max von Mises 506.7 MPa. Finally, the realized in the optimized design of the lower suspension arm. The ants hill plots (Figure 4.28) confirm that is a positive correlation for the force magnitude and max principal stress in the model structure also confirms force magnitude has the strong linear correlation with the max principal stress and von Mises stress of the structure, i.e., as the force increases so does the stress.

**Table 4.12:** Design parameter before and after SDI

<b>Design parameter</b>	<b>FEM</b>	<b>SDI</b>
Modulus of Elasticity (E)	70 GPa	70.656 GPa
Density (Rho)	2.74 g/cc	3.143 g/cc
Poisson Ratio (Nu)	0.33	0.3483
Scale factor force	112.36	118.9
Predict stress on the model (max Principal )	577 MPa	556.2 MPa
Predict stress on the model (max von Mises)	561 MPa	506.7 MPa

A sensitivity analysis of an opportune set of design variables on the function. The considered design variables involved in the sensitivity analysis have been chosen, besides the material of the lower suspension arm, to be the mechanical properties of the three materials constituting the main components of the substructure (modulus of elasticity, Poisson ratio, density, load, von Mises stress, and maximum principal stress). It is possible to appreciate the relationship existing between the chosen design variables and the function by considering the scatter plots between them. From these scatter plots, clearly while the relationship existing between the load and the stress and the objective variable is quite linear. The results from the sensitivity analysis are also reported quite evident that the design variables which influence the objective one are the load of lower arm.



**Figure 4.28:** Ant hill scatter plot for stress versus load scale factor using SDI

In conclusion, the classical simulations based on nominal values of the input variables are not exhaustive of the phenomenon in the case of improving the design and can bring to incorrect interpretations of the dynamic behaviour of the examined structure. On the contrary, by using an SDI approach, it is possible to have a better understanding of the influence of each input variable on the structural dynamic behaviour and to assign the most appropriate nominal values in order to have results as near as possible to the target values, also in the presence of their natural variability.

#### 4.4 CONCLUSION

The finite element modeling and analysis of lower arm has been presented. The dynamic characteristics of the lower suspension arm were discussed. The artificial intelligent technique based on RBFNN has been presented and shown very attractive properties such as localization, functional approximation, interpolation, and cluster modeling. A new approach to investigate the influencing factors of the lower suspension arm by integrating finite element analysis results with the central composite design approach has been presented. This combined approach is useful in the design stage of the suspension arm. The combined approach of modeling lower suspension arm using FEM and RSM is found to be statistically adequate through verification trials. On the other hand, the modelization and simulation with SDI method is the efficient and timesaving tool to design the mechanical components and system. It is far more economical than the traditional experimental method which is more consuming in material, cost and time. The technique is very flexible and their many parameters enable us imitate closely to real life condition and make accurate predictions based on the set.

## CHAPTER 5

### CONCLUSIONS AND RECOMMENDATION

#### 5.1 INTRODUCTION

This work has been addressed using robust design method for develop and minimizing variability of lower suspension arm and processes in order to improve their quality and reliability for the vehicle. This chapter summarizes the important finding from the work carried out in this research. It also includes some suggestions for the further work in each of the areas covered during this research.

#### 5.2 SUMMARY OF FINDINGS

The aim of this thesis was to identify the critical locations and to provide lower control part capable of enduring more loads with lower predict stress and able to designer accomplish stress reduction and shape development with the advanced method. Continued research in this direction can bring about more comprehensive and appropriate guide lines for designers.

The finite element model is computational intensive due to the complicated operation on very large matrices. Mesh generation is one of the most critical aspects of engineering simulation and selecting the right techniques of meshing are based on the geometry, model topology, analysis objectives and engineering judgment. The concept of the FE model validation has been defined in this thesis. The convergence of the stress was considered as the main criteria to select the mesh type. The finite element mesh was generated using TET10 for various meshes global length.

The response surface method has been proven to be a successful technique to perform the trend analysis of lower suspension arm, statistically adequate and can be used to navigate the design space. In order to arrive at the most influential variables and its effects a phase strategy, RSM aimed to develop the input-output relationships for prediction of lower suspension arm response. By applying central composite design, while designing a suspension system, corrective and iterative design steps can be initiated and implemented for betterment of component design. RSM is used to estimate the transfer functions at the optimal region. The use of statistical design of experiment techniques combined with FEA provides the engineering community with valuable tools for forecasting the behavior of a system or process. The DOE investigated the influencing factors of the lower suspension arm by integrating finite element analysis results with the central composite design approach. The combined approach of modeling Lower suspension Arm using FEM and DOE is found to be statistically adequate through verification trials.

Neural network investigated and presented influences of the artificial intelligent on the response suspension lower arm. Evaluated stress analysis for aluminum automobile part with the advanced method. The RBFNN found to be highly effective in identification linear response of suspension arm, and it has been used of more realistic linear and nonlinear problems in order to get quickly solutions. The finite element analysis and RBFNN techniques are used to predict the response of suspension arm. Finally, this technique shows highly effective depends upon its accuracy, speed and memory requirements in identification of stress-displacement of suspension arm. Therefore, the RBFNN can be very successively used for the enhanced navigational performance and error reduction of the effort and time required to determine the stress-displacement response of lower suspension arm.

A stochastic simulation generates multiple scenarios of a model by repeatedly sampling values from the probability distributions for the uncertain variables. Stochastic design improvement achieved the design improvement with the influence of tolerances. The simulation and modelization software with SDI method enabled us to optimize the shape of the lower arm with respect to the stress constrains in order to endure more stress on the part. SDI is a fast and efficient technique to improving the performance of

suspension arm so that it's most probable behavior coincides with specified target values.

### **5.3 CONTRIBUTION OF THE STUDY**

- i. Design of experiment (DOE) with combination neural network (NN) reveal power requirement to determine, achieve and gave a simple solution compatible for better assess linear response of lower suspension arm.
- ii. Stochastic design improvement (SDI) method provide lower control part capable of enduring more loads with lower predict stress also the technique endow with enhance performance of lower suspension arm.
- iii. This study is presented how robust design technique could be applied in the design stage of the product optimum process to maximize product reliability.

### **5.4 RECOMMENDATIONS FOR FUTURE RESEARCH**

It is recommended that the methods discuss to herein be extended into the more contemporary areas of FE capability, the need for close interaction between the CAE analyst and the designer has been highlighted. All the parameter of optimization that has been obtained from this research should be tested of the prototype components of the lower suspension arm then making as a range and guidelines during the experimental works of modifying and optimizing the control lower arm suspension, this seriously improve the reliability and confidence of the user.

## REFERENCES

- AA (Aluminum Association Inc.). 2004. Automotive aluminum the performance advantage. <http://www.autoaluminum.org> accessed on 07 August 2009.
- Abdullah, A.H. 2009. RBFNN Model for predicting nonlinear response of uniformly Loaded Paddle Cantilever. *American Journal of Applied Sciences*. **6**(1): 89-92.
- Abello, J., Butenko, S., Pardalos, P. and Resende, M. 2001. Finding independent sets in a graph using continuous multivariable polynomial formulations. *Journal of Global Optimization*. **21**: 111–137.
- Acevedo, J. and Pitsikopoulos, E.N. 1988. Stochastic optimization based algorithm for process synthesis under uncertainty. *Computers and Chemical Engineering*. 647–671.
- Asadi, M.R., Rasekh, M., Golmohammadi, A., Jafari, A., Kheiralipour, K. and Borghei, A.M. 2010. Optimization of connecting rod of MF-285 tractor. *Journal of Agricultural Technology*. **6**(4): 649-662.
- Afzal, A. and Fatemi, A. 2004. A comparative study of fatigue behavior and life predictions of forged steel and PM connecting rods. *SAE Technical Paper*, 2004-01-1529.
- Ang, H.S.A. and Lee, J.C. 2001. Cost optimal design of R/C buildings. *Reliability Engineering and System Safety*. **73**: 233–238.
- Anthony, J. 2003. *Design of experiments for engineers and scientists*. Britain: Butterworth-heinemann, Inc.
- Attia, H.A. 2002. Dynamic modeling of the double wishbone motor vehicle suspension system. *European Journal of Mechanics A/Solids*. **21**: 167-174.
- Au, S.K. 2005. Reliability-based design sensitivity by efficient simulation. *Computers and Structures*. **83**: 1048–1061.
- Bath, K-J. 1996. *Finite element procedures*. NJ: Prentice-Hall.
- Baek, W.K., Stephens, R.I. and Dopker, B. 1993. Integrated computational durability analysis. *Journal of Engineering for Industry, Transactions of the ASME*. **115**(4): 492-499.
- Beale, E. 1955. On minimizing a convex function subject to linear inequalities. *Journal of the Royal Statistical Society*. **17B**: 173–184.
- Bharatendra, R., Nanua, S. and Mustafa, A. 2004. Robust design of an interior hard trim to improve occupant safety in a vehicle crash. *Reliability Engineering and System Safety*. **89**(3): 296-304.

- Birge, J.R. and Louveaux, F.V. 1997. *Introduction to stochastic programming*. New York: Springer.
- Broomhead, D.S. and Lowe, D. 1988. Multivariable function interpolation and adaptive networks. *Complex System*. **2**: 321–355.
- Carle, D. and Blount, G. 1999. The suitability of aluminium as an alternative material for car bodies. *Materials and Design*. **20**(5):267–272.
- Chandrupatla, T.R. and Belegundu, A.D. 1997. *Beams and frames*. In *introduction to finite elements in engineering*. NY: Prentice-Hall, Inc.
- Chen, C.I., Napolitano, M.R. and Chen, C.L. 1992. A new learning algorithm for neural network estimation in active vibration control. *Smart Materials and Structures*. **1**: 250-257.
- Chiang, K., Chang, H., Li, C. and Huang, Y. 2009. An ANN embedded position and Orientation determination algorithm for low cost MEMS INS/GPS Integrated sensors. *Sensors*. **9**: 2586-2610.
- Church, R. A. 1995. *The rise and decline of the British motor industry*. Cambridge University Press.
- Coccorese, E., Martone, R. and Morabito, F.C. 1994. A neural network approach for the solution of electric and magnetic inverse problems. *IEEE Transactions on Magnetics*. **30**(5): 2829-2839.
- Conle, F.A. and Mousseau, C.W. 1991. Using vehicle dynamic simulation and finite element result to generate fatigue life contours for chassis component. *International Journal of Fatigue*. **13**(3): 195 - 205.
- Dantzig, G. 1955. Linear programming under uncertainty. *Management Science*. 197–206.
- De Alcantara, N.P., Alexandre, J. and De Carvalho, M. 2002. Computational investigation on the use of FEM and ANN in the non-destructive analysis of metallic tubes. *10th Biennial conference on electromagnetic field computation ICEFC*, Perugia, Italy.
- Diaz, J. and Hernandez, S. 2010. Uncertainty quantification and robust design of aircraft components under thermal loads. *Aerospace Science and Technology*. **14**(8): 527-534.
- Dimarogonas, A. 1996. *Vibration for engineers*. Second Edition. New York: Prentice Hall.
- Dwight, J. 1999. *Aluminium design and construction*. London: Spon press.

- Enevoldsen, I. and Sorensen, J.D. 1994. Reliability-based optimization in structural engineering. *Structural Safety*. **15**(3), 169–196.
- Erdman, A.G., Sandor, G.N. and Kota, S. 2001. *Mechanism design analysis and synthesis*. 4th Edition. New York: Prentice Hall.
- Ermoliev, Y. and Wets, R.B. 1988. *Numerical techniques for stochastic optimization*. Berlin: Springer-Verlag.
- Fanglin, C. 2007. Design and mechanical analysis of aluminum parts for automobile application. Master Thesis. University du Quebec a Chicoutimi. Canada.
- Felippa, C.A. 2001. Advanced finite element methods. Department of Aerospace Engineering Sciences, University of Colorado.
- Fleuren, P.W. 2009. Independent front suspension on trucks ride comfort analysis and improvements. Master Thesis. Department of Mechanical Engineering. Eindhoven University of Technology. Netherland.
- Floudas, C. and Pardalos, P.M. 2002. *Encyclopedia of optimization*. Dordrecht, Netherlands: Kluwer Academic Publishers.
- Frimpong, S. and Li, Y. 2007. Stress loading of the cable shovel boom under in-situ digging conditions. *Engineering Failure Analysis*. **14**: 702–715
- Frimpong, S., Yafei, H. and Awuah, O.K. 2005. Mechanics of cable shovel-formation interactions in surface mining excavations. *Journal of Terramechanics*. **42**: 15–33.
- Gass, V., Schoot, V.D. and De Rooij, N.F. 1993. Nanofluid handling by micro-flow sensor based on drag force measurement. *Proceeding MEMS*. **93**: 167-72.
- Giancarlo, G. and Lorenzo, M. 2009. *The Automotive chassis: components design*. Library of congress control. Italy.
- Gopalakrishnan, R. and Agrawal, H.N. 1993. Durability analysis of full automotive body structure. *SAE International Congress and Exposition, Detroit, MI*.
- Gupta, A., and Maranas, C.D. 2000. A two-stage modeling and solution framework for multisite midterm planning under demand uncertainty. *Industrial and Engineering Chemistry Research*. **39**: 3799–3813.
- Hartman, E.J., Keeler, J.D. and Kowalski, J.M. 1990. Layered neural networks with Gaussian hidden units as universal approximators. *Neural Computation*. **2**: 210–215.
- Haykin, S. 1998. *Neural networks: A comprehensive foundation*. 2nd Edition, Prentice Hall.

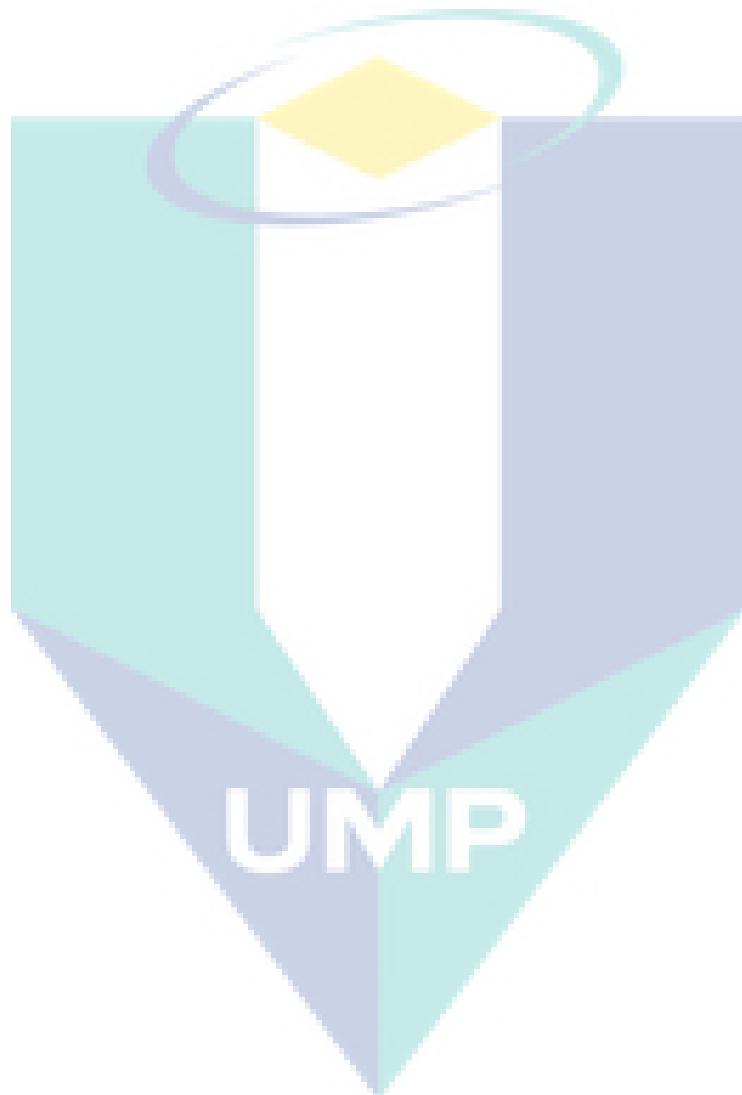
- Homeister, N.L. 2001. Vehicle emission standards around the globe. Ford Motor Company.
- Hutton, D.V. 2004. *Fundamentals of finite element analysis*. New York: McGraw Hill
- Jack, E. 2005. *Automotive technology: A systems approach*. USA: Thomson Delmar.
- Jensrud, O., Osthus, R. and Solerod, H. 2006. New improved forging technology and high volume serial production of aluminium wheel suspension arms. *Steel Grips*. 4- 26
- Johnson, J.D. 1997. *Driving America*. Press AEI.
- Kall, P. and Wallace, S.W. 1994. *Stochastic programming*. NY: Wiley John, Inc.
- Kim, H.S., Yim, H.J. and Kim, C.M. 2002. Computational durability prediction of body structure in prototype vehicles. *International Journal of Automotive Technology*. **3**(4): 129-136.
- KM (Key to Metals). 2011. Stress corrosion cracking of aluminum alloys. <http://www.keymetals.com/Article17.htm> accessed on 01 May 2011.
- Knowles, D. 2010. *Automotive suspension and steering system: Classroom manual*. USA: Cengage Learning, Inc.
- Kong, J.S. and Frangopol, D.M. 2003. Life-cycle reliability-based maintenance cost optimization of deteriorating structures with emphasis on bridges. *Journal of Structural Engineering*. **129**(6): 818–828.
- Kouwenberg, R. and Zenios, S.A. 2001. Stochastic programming models for asset liability management, HERMES Center of Excellence on Computational Finance and Economics, University of Cyprus, Nicosia, Cyprus.
- Krishna, M.M.R. 1998. Chassis cross-member design using shapes optimization-a case study. *SAE*, technical paper No.981011.
- Krishna, M.M.R. and Carifo, J. 2000. Optimization of an engine cradle in frequency domain. *SAE*, technical paper No. 2000-01-0599.
- Kumar, S. 2005. *Neural networks: A class room approach*. India: McGraw-Hill.Inc.
- Kurban, T. and Besdok, E. 2009. A comparison of RBF neural network training algorithms for inertial sensor based terrain classification. *Sensors*. **9**: 6312-6329.
- Laguna, M. 1998. Applying robust optimization to capacity expansion of one location in telecommunications with demand uncertainty. *Management Science*. **44**(11-2): S101 S110.

- Lanczos, C. 1950. An iteration method for the solution of the eigenvalue problem of linear differential and integral operators. *Journal of the Research of the National Bureau of Standards*. **45**: 255-282.
- LDA (Light-duty automotive). 2009. Light-duty automotive technology and fuel economy trends: 1975 through 2009. *United States Environmental Protection Agency*. Number EPA420-S-06-003.
- Lucor, D., Meyers, J. and Sagaut, P. 2007. Sensitivity analysis of LES t subgrid-scale-model parametric uncertainty using polynomial chaos. *Journal of Fluid Mechanics*. **585**: 255-279.
- Ma, Z.D., Kikuchi, N. and Cheng, H.C. 1995. Topological design for vibrating structures. *Computer Methods in Applied Mechanics and Engineering*. **121**: 259–80.
- May, B. and Beck, J. 1998. Probabilistic control for the active mass driver benchmark structural model. *Earthquake Engineering and Structural Dynamics*. **27**(11): 1331–1346.
- Medepalli, S. and Rao, R. 2000. Prediction of road loads for fatigue design—a sensitivity study. *International Journal of Vehicle Design*. **23**(1-2): 161-175.
- Miller, W.S., Zhuang, L., Bottema, J., Wittebrood, A.J., De Smet, P., Haszler, A. and Vieregge, A. 2000. Recent development in aluminium alloys for the automotive industry. *Materials Science and Engineering*. **A280**(1):37–49.
- Milliken, F. 2002. Chassis design: principles and analysis. Society of Automotive engineers Inc. USA
- Milliken, F. and Milliken, D. L. 2002. Race car vehicle dynamics. USA: Society of Automotive Engineering, Inc. USA
- Montgomery, D.C. 2005. Design and analysis of experiments. 5th Edition. Singapore: Wiley John.
- Morton, D.P. 1996. An enhanced decomposition algorithm for multistage stochastic hydroelectric scheduling. *Annals of Operations Research*. **64**: 211–235.
- Mulvey, J.M., Vanderbei, R.J. and Zenios, S.A. 1995. Robust optimization of large-scale systems. *Operations Research*. **43**: 264–281.
- Musavi, M.T., Ahmed, W., Chan, K.H., Faris, K.B. and Hummels, D.M. 1992. On the training algorithm for radial basis function classifiers. *Neural Networks*. **5**: 595-603.
- Pandya, A.S. 1995. *Pattern recognition with neural networks in C++*. USA.

- Park, J. and Sandberg, I.W. 1993. Universal approximation and radial basis-function networks. *Neural Computation*. **5**: 305–316.
- Park, J. and Sandberg, W. 1991. Universal approximation using radial-basis-function networks. *Neural Computation*. **3**: 246–257.
- Praya, P. and Jamel, E.B. 2004. *Vehicle crashworthiness and occupant protection*. USA
- Rahman, M.M. 2007. Finite element based durability assessment for a new free piston linear engine. PhD Thesis. Universiti Kebangsaan Malaysia, Malaysia
- Rahman, M.M., Ariffin, A.K., Abdullah, S. and Jamaludin, N. 2007. Finite element based durability assessment of a free piston linear engine component. *SDHM*, **3** (1): 1-13
- Rahman, M.M., Kadirgama, K., Noor, M.M., Rejab, M.R.M. and Kesulai, S.A. 2009. Fatigue life of lower suspension arm using strain-life approach. *European Journal of Scientific Research*. **30**(3): 437-450.
- Rakesh, M., Tong, L.H., Zhijie, L. and Ibrahim, Y. 2002. Robust design of a spindle motor: a case study. *Reliability Engineering and System Safety*. **75**(3): 313-319
- Raymond, H.M. and Douglas, C.M. 2002. *Response surface methodology: Process and product optimization using designed experiments*. 2nd Edition, USA: John Wiley and Sons, Inc.
- Rowlands, H. and Antony, J. 2003. Application of design of experiments to a spot welding process. *Assembly Automation*. **23**(3): 273 – 279
- Sahinidis, N.V. 2004. Optimization under uncertainty: state-of-the-art and opportunities. *Computers and Chemical Engineering*. **28**: 971–983.
- Sakawa, M., Nishizaki, I. and Uemura, Y. 2002. A decentralized two-level transportation problem in a housing material manufacturer: Interactive fuzzy programming. *European Journal of Operational Research*. **141**: 167–185.
- Sandro, R. 2006. Iterative application of the ainet algorithm in the construction of a radial basis function neural network. *Learning and Nonlinear Models*. 1: 24-31.
- SCC (Suncoast Car Care). 2011. Suspension System - How does it work. <http://www.suncoastcarcare.com.au/suspension.htm> accessed on 01 May 2011.
- Schultz, R., Sougie, L. and van der, V.M. 1998. Solving stochastic programs with complete integer recourse by enumeration: A framework using Grobner basis reductions. *Mathematical Programming*. **83**: 229–252.
- Seo, P.K., Kim, H.C. and Kang, C.G. 2007. Numerical integration design process to development of suspension parts by semi-solid die casting process. *Journal of Materials Processing Technology*. **183**: 18–32

- Sigmund, K.A. 2006. Fatigue life prediction of an aluminium alloy automotive component using finite element analysis of surface topography. Phd Thesis. Norwegian University of Science and Technology, Norway.
- Simon, D. 2002. Training radial basis neural networks with the extended Kalman filter. *Neurocomputing*. **48**: 455–475.
- Srikantan, S., Yerrapalli, S. and Keshtkaqr, H. 2000. Durability design process for truck body structures. *International Journal of Vehicle Design*. **23**(1-2): 94-108.
- Staley, J.T. and Lege, D.J. 1993. Advances in aluminum-alloy products for structural applications in transportation. *Journal De Physique*. **3**(4):179–190.
- Sreeram, P. 1994. Robust design of an automotive suspension system. Master Thesis. Michigan Technological University, USA.
- Szewczyk, Z.P. and Hajela, P. 1993. Neural network based selection of dynamic system parameters. *Transactions of the Canadian Society of Mechanical Engineers*. **17**(4A): 567-584
- Takriti, S. and Birge, J. 2000. Lagrangian solution techniques and bounds for loosely coupled mixed-integer stochastic programs. *Operations Research*. **48**(1): 91–98.
- Vietor, T. 1997. Stochastic optimization for mechanical structures. *Mathematical Methods of Operations Research*. **46**: 377–408.
- Wang, F. 2001. Passive suspensions. in design and synthesis of active and passive vehicle suspensions. PhD Thesis, Department of Engineering, University of Cambridge, UK
- Wang, Q. and Stengel, R.F. 2002. Robust control of nonlinear systems with parametric uncertainty. *Automatica*. **38**: 1591–1599.
- Wannas, A.A. 2008 .RBFNN model for prediction recognition of tool wear in hard turing. *Journal of Engineering and Applied Sciences*. **3**(10): 780-785.
- Wannas, A.A. and Abd, M.K. 2008. Nonlinear response of uniformly loaded paddle cantilever based upon intelligent techniques. *Research Journal of Applied Science*. **3**(8): 566-571.
- Wu, C.F. and Hamad, M. 2000. *Experiments: Planning, analysis, and parameter design optimization*. New York: John Wiley and Sons, Inc.
- Yim, H.J. and Lee, S.B. 1996. An integrated CAE system for dynamic stress and fatigue life prediction of mechanical systems. *KSME International Journal*. **10**(2): 158-168.
- Yuan, J. 2004. Robust vibration control based on identified models. *Journal of Sound and Vibration*. **269**: 3–17.

Zang, C., Friswell, M.I. and Mottershead, J.E. 2004. A review of robust optimal design and its application in dynamics. *Computers and Structures*. **83**(4-5): 315-326.



## LIST OF PUBLICATION

1. Hemin M. Mohyaldeen, M.M. Rahman and Ahmed N. Abdalla. 2001. Radial Basis Function in conjunction with Response Surface Model for Design of Lower Suspension Arm. 3rd International Conference on Mechanical and Electrical Technology (published by ASME press and Thomason ISI indexed) (accepted)
2. M. M. Rahman, Hemin M. Mohyaldeen, M. M. Noor and Rosli A. Bakar. 2010. Robust Design of Suspension Arm based on Stochastic Design Improvement. 2010 2nd International Conference on Mechanical and Electronics Engineering (ICMEE 2010), Kyoto, Japan. (Scopus, IEEE Proceedings, ISI proceedings indexing)
3. M. M. Rahman, Hemin M. Mohyaldeen, M. M. Noor, K. Kadirgama and Rosli A. Bakar. 2011. Linear Static Response of Suspension Arm based on Artificial Neural Network Technique. Advanced Materials Research. (Accepted)
4. Hemin M. Mohyaldeen, M. M. Rahman, M. M. Noor and K. Kadirgama. 2010. New Approach to Design of Suspension Arm using Central Composite Design of Experiment in Conjunction with FEA. In Proceedings of 2nd National Conference in Mechanical Engineering for Research and Postgraduate Studies (2nd NCMER), pp. 236-247.
5. Hemin M. Mohyaldeen, M. M. Rahman, M. M. Noor and K. Kadirgama. 2010. Suspension Arm Design Based on Stochastic Optimization Approach. In Proceedings of 1st National Conference in Mechanical Engineering for Research and Postgraduate Students (NCMER), pp. 261-273.
6. Hemin M. Mohyaldeen, M. M. Rahman, M. M. Noor and K. Kadirgama. 2009. Dynamic analysis of suspension arm based on finite element Method. National Conference on Postgraduate Research (NCON-PGR). Malaysia, pp. 251- 264.